OHIO STATE
UNIVERSITY
AUG 14 1961
LIBRARY

MONTHLY NOTICES

OF THE ROYAL ASTRONOMICAL SOCIETY

VOLUME 122 1961

XUM

ROYAL ASTRONOMICAL SOCIETY

Subscribers to *Monthly Notices* may like to note that the Royal Astronomical Society of

The Earth Today

A collection of papers dedicated to Sir Harold Jeffreys by some of his students and colleagues on the occasion of his 80th birthday.

This is an extra volume of the Society's publications which is now made available to the general public, suitably bound in cloth boards. The Geophysical Journal co-operation of many of Sir Harold's distinguished colleagues in the preparation of this volume and they believe that it will be advanced work in a number of fields in which they are interested.

Price £4 (US$ 12)

Orders should be sent to the Publications Secretary, Royal Astronomical Society, Burlington House, London W1V 0NL, England.

Messrs. Oliver & Boyd, Tweeddale Court, 14 High Street, Edinburgh EH1 1YL, Scotland.

SPECIAL OFFER TO FELLOWS

Fellows of the Society may purchase copies of *The Earth Today* at the special price of £1 net. (US$ 3) plus postage. Fellows who wish to receive a copy should send their order and remittance to the Assistant Secretary, Royal Astronomical Society, Burlington House, London W1V 0NL, England.

MONTHLY NOTICES
OF THE
ROYAL ASTRONOMICAL SOCIETY
Vol. 122 No. 5

AN INVESTIGATION OF THE CLUSTERING OF RADIO STARS

Patricia R. R. Leslie

(Communicated by M. Ryle)

(Received 1960 December 28)

Summary

An examination has been made of the results of two recent surveys of radio sources at Cambridge, in order to investigate the clustering of sources. Two methods of analysis have been used, which allowed the study of associations of sources having angular separations in the range 3′·5 to 200′ arc.

No evidence for clustering was found, and over most of this range an upper limit of about 10 per cent could be set to the percentage of sources which occur in clusters.

During the observations a number of intense sources, hitherto believed to be extended, were found to be close double or multiple systems; they represent only a small fraction of the total, however, and the number found is not inconsistent with the upper limits of clustering which have been derived.

1. *Introduction.*—A number of surveys of radio sources have been examined statistically in order to find whether the sources are distributed randomly in position or whether there is any evidence for clustering (Shakeshaft *et al.*, 1955; Mills, Slee and Hill, 1958; Edge *et al.*, 1959). Owing to the limited resolution of these surveys, the analyses were restricted to associations having angular dimensions greater than a few degrees. Apart from the well-known excess of radio sources at low galactic latitudes and a smaller increase in source density in the area of the "spur" of galactic background radiation at $l^{\text{II}}=30°$, no conclusive evidence for clustering has been found.

From the present knowledge of the nature of radio sources, it appears unlikely that clustering on so large a scale as that previously investigated (3°–30°) will occur. A new investigation to detect clustering on a smaller scale than this has been completed, using two sets of observations made at a frequency of 178 Mc/s with the large interferometric radio telescope at the Mullard Radio Astronomy Observatory (Ryle, 1960). Details of the observations are given in Section 3. In the course of this work, a number of intense close double and multiple sources have been found; these are described in Section 4 together with the optical evidence where it exists. In some cases this evidence suggests a definite physical relationship between the components.

The analysis carried out on all the new observational material is given in Section 5; no evidence for clustering is found and upper limits are computed for the percentage of sources which could occur in clusters without producing a detectable effect.

2. *The probable scale of clustering.*—(*a*) If collisions between galaxies are responsible for an appreciable fraction of the sources, it might be thought that the sources would occur mainly in the dense clusters of galaxies and that associations of radio sources with a scale of a few degrees might therefore be

XUM

expected. Apart from the lack of correlation between radio sources and clusters of galaxies, it can easily be shown that the probability of such encounters is remote and the simultaneous occurrence of more than one in a given cluster can probably be ignored.

(*b*) Cygnus A is itself a double source, having components of almost equal flux density separated by about 1′·4 arc (Jennison and Latham 1959) and disposed on either side of the optical object. The dynamics of such encounters are not fully understood (Spitzer and Baade, 1951; Shklovsky, 1955; Ambartsumian, 1960) but it seems probable that other sources related to interacting galaxies might also appear as double or multiple systems. Other objects physically similar to the Cygnus A source would have smaller angular separations, but collisions producing less radio emission than Cygnus A might occur at smaller distances with angular separations of several minutes of arc. There is some evidence that the radio sources in Perseus and Hercules are such objects (Leslie and Elsmore, 1961; Williams, Dewhirst and Leslie, 1961).

(*c*) A number of radio sources have been related to nebulosities which probably represent the remains of supernovae (SN 1054, 1572, 1604, Cygnus Loop and IC 443). In some sources (IC 443, 3C 392) the radio emission may originate in a thin shell (Baldwin and Dewhirst, 1954; Leslie, 1960). In the latter case, the shell, which produces effectively the whole of the radio emission, appears to be remarkably uniform. In the case of a gaseous shell expanding in a region of non-uniform density, the shape of the emitting region would be less regular and might take the form of a number of relatively isolated sources within a region which could extend up to several degrees. Examples of such associations which have been observed at low galactic latitudes are given in Section 4.

On the basis of these observations, associations of extragalactic sources having angular dimensions of a few minutes of arc might be expected, whilst at low galactic latitudes associations having dimensions up to 2° might also occur. The new observations have permitted the study of clustering in this range of angular separations.

3. *The method of analysis.*—The analysis was based on two recent surveys of sources:

(*a*) Observations over an area of sky between $\delta = -05°$ and $+61°$, using both a total power system and a 465 λ interferometer (Leslie, 1961); the primary resolution of both systems was about 14′ arc in α and 4°·6 in δ and sources with $S \geqslant 6 \times 10^{-26}$ w.m.$^{-2}$ (c/s)$^{-1}$ could be observed.

(*b*) Areas of sky from declination 16° 30′ to 21°, 40° to 44° and 48° to 54° have been observed with an interferometer having a primary resolution of 25′·0 in α and 35′ in δ (Scott, Ryle and Hewish, 1961). In these observations sources having $S \geqslant 2 \times 10^{-26}$ w.m.$^{-2}$ (c/s)$^{-1}$ could be observed.

Two different types of analysis have been employed:

(i) *Counts of sources.*—The distribution of the sources observed in each set of observations was investigated by dividing the sky into rectangular areas, and counting the number of rectangles containing 0, 1, 2, ... etc. sources; this analysis was repeated for rectangles of different sizes. The results were in each case compared with the Poisson distribution expected if the sources were distributed randomly. For the smaller rectangles a correction was applied to the observed distribution to take account of the impossibility of recognizing double sources with an angular separation less than the limit of resolution.

This method allowed the investigation of sources having components separated by 15′ arc to 3°.

(ii) *Evidence provided by the measurement of apparent angular diameter.*—As has already been described (Leslie, 1961), the ratio of the recorded amplitudes observed with the interferometric and total power systems mentioned in Section 3 (*a*), enables an angular diameter to be ascribed to each source on the assumption of a particular distribution of brightness across it. In the previous paper, a Gaussian model was adopted.

It is possible to use the same observations to investigate the presence of double sources having angular separations of a few minutes of arc. The records produced by a single point source and by extended sources having diameters of 3′ and 6′ arc on the total power and interferometric systems are shown in Fig. 1 (*a*), (*b*) and (*c*); the records produced by two point sources of equal flux density and angular separations of 3′ and 6′ arc in α, are shown in Fig. 1 (*d*) and (*e*). Similar records for pairs with the same angular separations but flux densities in the ratio 2 : 1 are shown in Fig. 1 (*f*) and (*g*).

A comparison of these traces shows that, provided the flux densities of the two components of a double source differ by less than 2 : 1 and the angular separation exceeds 5′ arc, it is possible to recognize them as such and distinguish them from an extended source. In practice it has been found possible to use the method for sources having a combined flux density greater than 10×10^{-26} w.m.$^{-2}$ (c/s)$^{-1}$; below this level the discrimination is limited by the errors due to noise and confusion with weak adjacent sources. Associations of three or more sources cannot usually be distinguished from a single extended source.

Although it is not possible to make a distinction between a double source in which the components have an angular separation of less than 5′ arc and an extended source, it is evident that both double and multiple sources can be distinguished from a single point source by the ratio, γ, of the amplitudes observed with the two systems of 3 (*a*). Angular separations of 2′·5 to 5′·0 arc will give rise to values of γ between 0·7 and 0·1, figures which would correspond to Gaussian sources having widths to half intensity of 2′·5–7′·0 arc.

The number of sources having values of γ in this range is small, and the observations are therefore valuable in deriving upper limits to the number of multiple sources with separations of 2′·5 to 5′·0 arc.

4. *Examples of double and multiple sources.*—Before describing the results of carrying out the analysis outlined in the previous section, it may be valuable to list a number of double and multiple sources having $S > 20 \times 10^{-26}$ w.m.$^{-2}$ (c/s)$^{-1}$ which were found during the observations. In most of these cases previous surveys had indicated the presence of an extended source.

The positions and intensities of the components observed in the present survey are listed in Table I. The apparent flux densities measured by the two systems described in Section 3 (*a*) represent two values of the Fourier transform of the brightness distribution across the source. A unique solution for the extent of the source is therefore not possible unless a specific model is adopted. In all but the most exceptional cases a Gaussian distribution had previously been assumed (Leslie, 1961). However where the source is clearly non-Gaussian (e.g. 3C 392) the positions and flux densities obtained with both systems 3 (*a*) (i) (total power) and 3 (*a*) (ii) (interferometer) are given. Improved

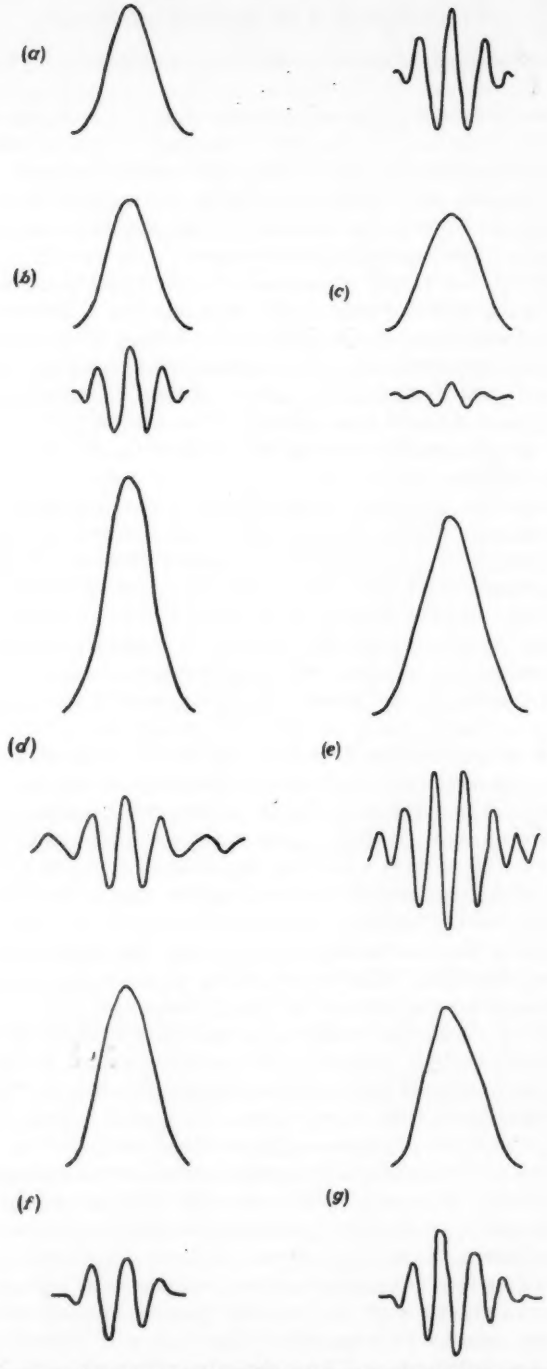

FIG. 1.—*Responses of total power and interferometer systems for: (a) point source; (b) Gaussian source of 3′ arc diameter; (c) Gaussian source of 6′ arc diameter; (d) two point sources of equal flux density separated by 3′ arc; (e) two point sources of equal flux density separated by 6′ arc; (f) two point sources whose fluxes differ by 2 : 1, separated by 3′ arc; (g) two point sources whose fluxes differ by 2 : 1 separated by 6′ arc.*

TABLE I

3C	Survey	α h	m	s	±s	δ °	′	±′	$S(\times 10^{26}$ w.m.$^{-2}$ (c/s)$^{-1})$	Angular diameter	±	
10	3(a)(i)	00	22	42	9	64	00	30	135			Possibly an incomplete shell of diameter 9′·0 arc similar to 3C 392.
	3(a)(ii)	00	21	33	9	64	00	30	18			
	3(a)(ii)	00	24	21	9	64	00	30	25			
15	3(a)	00	34	21	9	−01	18	30	20·5	<3′·0		Slight clustering of faint galaxies.
17	3(a)	00	35	33	9	−02	15	30	27·0	3′·5	1′·0	
66	3(b)	02	20	08·3	1·5	42	49	1·5	25·0	3′·5	1′·0	14^m and 15^m galaxies surrounded by several 16^m galaxies.
	3(b)	02	20	36·2	1·5	39	46·8	1·5	34·0	3′·5	1′·0	
84	3(b)	03	14	54·2	1·5	41	44·1	1·5	15·5	2′·0	1′·0	Leslie and Elsmore (in preparation).
	3(b)	03	16	28·6	1·5	41	20·4	1·5	41·0	1′·0	1′·0	
	3(a)	03	15	54·0	20·0	41	00	30·0	40	26′·0	4′·0	
264	ERL	11	40	49·1	1·5	22	26·1	2·0	19·0	<1′·5		Dense cluster of galaxies 13^m upwards*.
	ERL	11	42	32·1	1·5	19	51·6	2·0	26·0	3′·0	2′·0	
327	3(a)	15	59	33	9	03	00	30	43	3′·5	1′·5	14^m spiral 15′p, 10′s.
	3(a)	16	01	45	9	00	54	30	27	<1′·5		
	3(a)	16	02	33	18	00	42	45	10	<1′·5		
348	ERL	16	48	36·2	1·0	05	05·2	1·5	162			Williams, Dewhirst and Leslie (in preparation).
	3(b)	16	48	44·2	1·0	05	04·6	1·5	162			
392	3(a)(i)	18	53	37	5	01	18	30	390			Leslie 1960.
	ERL	18	52	52·3	2	01	16·2	1·0	32			
	ERL	18	54	16·9	2	01	12·3	1·0	30			

* Recent observations made with the full resolution of the instrument (Scott *et al.* 1961) have shown an error in the interpretation of the ERL observations, which were incomplete for this double source, and led to the selection of the wrong lobes.

positions of some of the sources of small angular size have been obtained from the observations of high resolving power (3 (*b*)), and from a previous survey designed to give good positional accuracy (Elsmore, Ryle and Leslie, 1959).

5. *The results obtained.*

(*a*) *Poisson test of clustering.*—In the observations of intermediate resolving power described in Section 3 (*a*), a total of 330 sources with $S > 10 \times 10^{-26}$ w.m.$^{-2}$ (c/s)$^{-1}$ were observed between $\delta = -05°$ and $+61°$ (an area of 5·5 steradians). The sky was divided into strips 2° wide in declination with boxes whose extent in right ascension was (1) 15′ arc and (2) 60′ arc; the counts of boxes containing different numbers of sources were then compared with the distribution predicted for a random distribution of sources. The observed distribution was corrected to take account of the instrumental limitation that sources separated by less than 5′ arc cannot be distinguished. The results are shown in Table II.

TABLE II

Number of sources in box	0	1	2	3
(1) *Area of box :* 15′ × 2°				
Number of times observed	37668	325	4	0
Number of times predicted	37690	329	1·5	0·01
(2) *Area of box :* 1° × 2°				
Number of times observed	8168	314	9	0
Number of times predicted	8180	319	6·2	0·08

It can be seen that there is no evidence for a non-random distribution of sources. The limits set by the statistical uncertainty were established by computing the maximum number of true double sources which could exist before the probability of finding the observed distribution was reduced below 10 per cent. On this basis it was found that not more than 2·4 per cent of the sources occur in pairs with separations between 5′ and 15′ arc in α and not more than 4·5 per cent occur with separations between 5′ arc and 1°·0.

A similar type of analysis was performed using the observations of higher resolution described in Section 3 (*b*). In this case, all sources down to about 2×10^{-26} w.m.$^{-2}$ (c/s)$^{-1}$ were included in the three areas of sky bounded by $\delta = 16° 30'$ to 21°, $\delta = 40°$ to 44° and $\delta = 48°$ to 54°. The total area was 1·2 steradians.

Separate investigations were made of the regions with $|b| > 20°$ and $|b| < 20°$. The total number of sources in the two regions were 341 and 306 respectively. Since high resolution in both coordinates is available, the counts were made in boxes (1) 37′ in $\alpha \times 58'$ in δ, (2) 74′ × 114′ and (3) 148′ × 228′. The results are shown in Table III.

For all three areas of box, there is no significant departure from a random distribution for either of the two regions. For either region the statistical fluctuations would allow (on the basis of a probability of occurrence of 10 per cent) a maximum of 5 per cent of sources occurring in pairs with separations of less than 45′ arc and 6 per cent with separations less than 90′ arc.

A special investigation was also made of that part of the area between $\delta = 16° 30'$ and $\delta = 21°$ which falls within the "spur" of emission at $l^{II} = 0°$ ($\alpha = 12^h 00$ to $17^h 00$). Earlier observations (Edge *et al.*, 1959) have reported

TABLE III

Number of sources in box		0	1	2	3	4	5	6	7	8
$\|b\| > 20°$										
Area of box	Number of times									
$37' \times 57'$	observed	2762	313	14	0	0				
	expected	2763	307	17	0·6					
$74' \times 114'$	observed	499	208	58	5	0				
	expected	496	218	48	7	0·9				
$148' \times 228'$	observed	30	46	49	18	30	3	3	0	1
	expected	24·3	48·6	48·6	32·4	16·2	6·7	2·2	0·6	0·15
$\|b\| < 20°$										
Area of box										
$37' \times 57'$	observed	2114	287	9	1	0				
	expected	2126	268	17	1·1	0·4				
$74' \times 114'$	observed	358	194	42	10	0				
	expected	349	196	57	10·6	1·5				
$148' \times 228'$	observed	15	36	27	21	19	5	4	0	
	expected	13·0	30	34	26	14·5	6·6	2·5	0·8	

additional point sources in this area. Because of the great interest to different theories of this feature (Tunmer, 1958; Hanbury Brown, Davies and Hazard, 1960) a detailed survey is now being made. An analysis made of the small area of the "spur" already available provided no evidence for clustering.

(*b*) *Evidence on clustering with smaller angular spacing.*—The analysis described above was carried out to investigate double sources having separations greater than 5′·0 arc. In order to derive upper limits to the number of multiple sources with angular separations $< 5'$ arc, an analysis has also been made of the distribution of γ, the ratio of the record amplitudes observed with the 465λ interferometer and the total power system of 3 (*a*). This analysis follows that used earlier (Leslie, 1961) to derive an upper limit to the number of extended sources. A histogram is given in Fig. 2 which shows the observed distribution in γ for all sources with $S > 10 \times 10^{-26}$ w.m.$^{-2}$ (c/s)$^{-1}$ in the area $|b| > 20°$. The effects of noise and weak confused sources on the amplitude of a particular source recorded on the two systems of measurement may be computed from a knowledge of the observed distribution of record amplitude (Ryle, 1958). The expected distribution of γ for a random distribution of sources of negligible angular size can then be derived and is also shown in Fig. 2.

It can be seen that the observations show some evidence for an excess of sources having $\gamma < 0{\cdot}6$. This may indicate the presence of a small proportion of extended sources as discussed earlier (Leslie, 1961); alternatively it might indicate that a proportion of sources occur in pairs with angular separations of the order of 3′ arc. If the latter interpretation were correct, then not more than 15 per cent of all sources with $S \geqslant 5 \times 10^{-26}$ w.m.$^{-2}$ (c/s)$^{-1}$ occur in double or multiple systems with separations in α of 2′·5–5′·0 arc.

From more detailed observations of the more intense sources and from the available optical data it is believed that more than half of the observed excess of sources having $\gamma < 0{\cdot}6$ must be due to extended sources. It may therefore be concluded that less than 7·5 per cent of all sources with $S \geqslant 5 \times 10^{-26}$ w.m.$^{-2}$ (c/s)$^{-1}$ occur in clusters with separations of 2′·5–5′·0 arc in α.

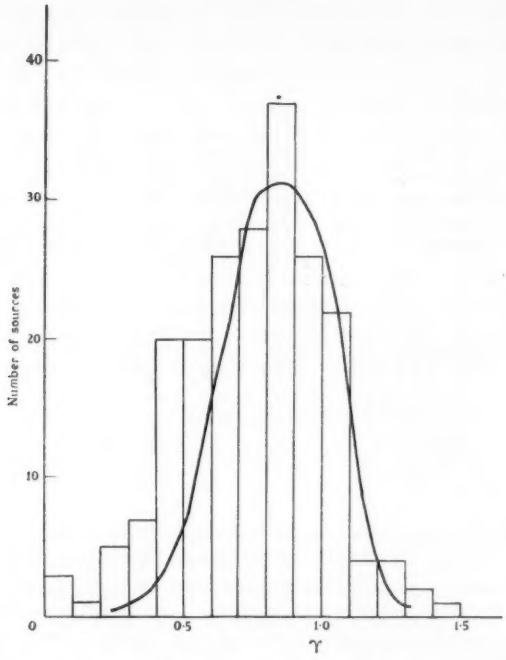

FIG. 2.—*Histogram of the number of sources, in areas having* $|b| > 20°$, *with different values of* γ, *the ratio of the amplitudes observed with the* 465λ *interferometer and with the total power system. The full line is the theoretical curve for a model in which all sources are of negligible angular diameter and are randomly distributed.*

A similar analysis for the area $|b| < 20°$ also gives a figure of 15 per cent, but in these areas, the presence of sources known to be extended allows an interpretation of the observed histogram mainly in terms of these extended sources. The number of sources occurring in close associations is again less than 7·5 per cent.

6. *Discussion.*—The results given in Section 5 show that none of the observations provides evidence for clustering of the sources.

Although a number of remarkable associations of intense sources have been noted (some of which are listed in Table I), they only represent a small percentage of the total number of sources of this flux density. Thus it is found that 8·5 per cent of sources having $S > 25 \times 10^{-26}$ w.m.$^{-2}$ (c/s)$^{-1}$ lie within 1° and 14 per cent within 3° of another such source. Objects of similar physical size occurring at larger distances would give rise to associations of less intense sources at smaller angular separations; the percentages found do not differ significantly from the statistically more accurate limits derived from the observations of the weaker sources.

It is convenient to combine in a single figure the results derived by the different methods for the maximum percentage of sources which can occur with different angular separations. For this purpose the quoted angular measures are scaled to bring the limiting flux density of the different surveys to a common value (5×10^{-26} w.m.$^{-2}$ (c/s)$^{-1}$), on the assumption that objects of similar physical

extent are distributed uniformly in space. At the same time the projected separation of the sources measured in some of the surveys, has been corrected to give a true angular separation, assuming a random distribution of position angle.

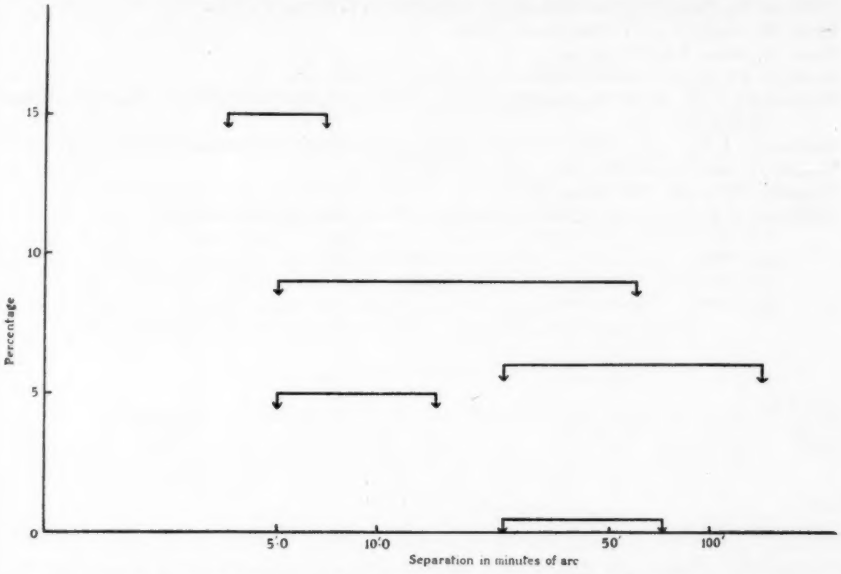

FIG. 3.—*Diagram showing, for sources having* $S \geqslant 5 \times 10^{-26}$ *w.m.*$^{-2}$ $(c/s)^{-1}$, *the maximum percentage of sources occurring in clusters with different ranges of angular separation.*

The results are combined in Fig. 3, which shows, for sources having $S \geqslant 5 \times 10^{-26}$ w.m.$^{-2}$ $(c/s)^{-1}$, the maximum percentage which can occur in double or multiple systems with any angular separation between 3′·5 and 140′ arc. As can be seen from Table III the results obtained for the largest angular separations (box area 148′ × 228′) also show no evidence for clustering, but the statistical limits are more difficult to establish and have not been included in Fig. 3.

The author wishes to thank Mr P. F. Scott for allowing her to make use of unpublished results and Professor M. Ryle for continual help and encouragement. She also wishes to thank the Trustees of the Robert Cormack Bequest for a Fellowship during the tenure of which this work was carried out.

Mullard Radio Astronomy Observatory,
Cavendish Laboratory,
Cambridge:

1960 *December* 20.

References

Ambartsumian, V. A., 1960, *Observatory*, **80**, 126.
Baldwin, J. E. and Dewhirst, D. W., 1954, *Nature*, **173**, 164.
Brown, R. Hanbury, Davies, R. D. and Hazard, C., 1960, *Observatory*, **80**, 191.
Edge, D. O., Shakeshaft, J. R., McAdam, W. B., Baldwin, J. E. and Archer, S., 1959, *Mem. R.A.S.*, **68**, 37.
Elsmore, B., Ryle, M. and Leslie, P. R. R., 1959, *Mem. R.A.S.*, **68**, 61.

XUM

Jennison, R. C. and Latham, V., 1959, *M.N.*, **119**, 174.
Leslie, P. R. R., 1960, *Observatory*, **80**, 23.
Leslie, P. R. R., 1961, *M.N.*, **122**, 51.
Leslie, P. R. R. and Elsmore, B., 1961 (in preparation).
Mills, B. Y., Slee, O. B. and Hill, E. R., 1958, *Austr. J. Phys.*, **11**, 360.
Ryle, M., 1958, *I.A.U. Symposium, Paris.*
Ryle, M., 1960, *J.I.E.E.*, **6**, 14.
Scott, P. F., Ryle, M. and Hewish, A., 1961, *M.N.*, **122**, 95.
Shakeshaft, J. R., Ryle, M., Baldwin, J. E., Elsmore, B. and Thomson, J. H., 1955, *Mem. R.A.S.*, **67**, 106.
Shklovsky, I. S., 1955, *Fifth Conference on Cosmology* (*Radio Astronomy*) *Moscow*, 395.
Spitzer, L. and Baade, W., 1951, *Ap. J.*, **113**, 413.
Tunmer, H., 1958, *Phil. Mag.*, **3**, 370.
Williams, P. J., Dewhirst, D. W. and Leslie, P. R. R., 1961 (in preparation).

HOYLE'S COVARIANT FORMULATION OF THE LAW OF CREATION OF MATTER

W. B. Bonnor and G. C. McVittie

(Received 1961 January 19)

Summary

Some solutions are obtained of the field equations recently proposed by Hoyle (1960) as a basis for the steady-state cosmology.

In the cases studied it appears that Hoyle's theory is weaker than general relativity in that its solutions are more numerous. It is shown also that, for a model containing dust, prescription of both the metric and the density does not uniquely determine the motion of the matter present. Moreover, this motion does not necessarily follow geodesics of the space-time.

---

1. *Introduction.*—This paper is concerned with the latest attempt of Hoyle (1960) to provide the steady-state cosmology with field equations. Hoyle introduces a scalar field ϕ by means of an inhomogeneous wave equation

$$g^{ik}\phi_{;ik}=K\rho, \tag{1.1}$$

where ; means covariant differentiation, ρ is the proper density of matter present, and g^{ik} is the contravariant metric tensor of space-time*. He goes on to show, however, that the steady-state theory is deducible from his field equations only if $K=3$ and we shall therefore adopt this value throughout. The field equations are

$$R_{ik}-\tfrac{1}{2}g_{ik}R=-8\pi(T_{ik}+C_{ik}), \tag{1.2}$$

where

$$C_{ik}=\phi_{;ik}, \tag{1.3}$$

where R_{ik} is the Ricci tensor and T_{ik} is the energy tensor, which for a perfect fluid is given by

$$T^{ik}=(p+\rho)v^iv^k-g^{ik}p, \tag{1.4}$$

p being the proper pressure. Hoyle shows that the steady-state universe is a solution of (1.1) to (1.4), with $p=0$.

It is clear that ϕ is not uniquely determined by (1.1), since to any solution of (1.1) one may add a solution of the homogeneous wave equation

$$g^{ik}\phi_{;ik}=0.$$

This arbitrariness in ϕ (and therefore in C_{ik}) might be expected to show up in the solutions of the field equations (1.2) in the following way. In general relativity T^{ik} must satisfy

$$T^{i\,k}_{;\,k}=0,$$

whereas the corresponding equation in Hoyle's theory is

$$T^{i\,k}_{;\,k}=-C^{i\,k}_{;\,k},$$

---

* Relativistic units will be used, so that the velocity of light and the Newtonian constant of gravitation are unity.

which is weaker because of the arbitrariness of C^{ik}. From this one might guess that, for a field of given symmetry, the class of solutions in Hoyle's theory contains more members than the corresponding class in general relativity. This possibility is investigated in Section 3, and it is shown that the class of metrics which are spatially isotropic, homogeneous and flat is indeed much more numerous in Hoyle's theory.

A further possibility to be considered is that the metric and the field equations together do not in all cases uniquely determine the energy tensor T_{ik}. This too is shown to be so by an example in Section 4, where it is found that, given the metric *and* the proper density of matter appropriate to the steady-state universe, the motion of matter is not uniquely determined.

The effect of these results on the theory is briefly discussed in Section 5.

2. *The field equations.*—We are interested in solutions of Hoyle's equations for which the metric is spatially isotropic, homogeneous, and flat, so that it may be taken as

$$ds^2 = -e^{g(t)}(dr^2 + r^2\,d\theta^2 + r^2\sin^2\theta\,d\psi^2) + dt^2.$$

We shall also require that the density ρ be a function of the time only, that the pressure p vanish, and that matter present shall move in the radial direction relative to the origin of coordinates. Regarding the function ϕ, we shall suppose in Section 3 that this is a function of the time only, but in Section 4 we shall allow it to be a function also of the radial coordinate r.

If the coordinates are labelled as follows:

$$x^1 = r, \qquad x^2 = \theta, \qquad x^3 = \psi, \qquad x^4 = t,$$

one finds that the non-zero components of C^i_k are

$$C^1_1 = -e^{-g}\phi'' + \tfrac{1}{2}\dot{g}\dot{\phi},$$
$$C^2_2 = C^3_3 = -e^{-g}r^{-1}\phi' + \tfrac{1}{2}\dot{g}\dot{\phi},$$
$$C^4_4 = \ddot{\phi},$$
$$C^4_1 = -e^{+g}C^1_4 = \dot{\phi}' - \tfrac{1}{2}\dot{g}\phi',$$

where $'$ and $\cdot$ mean partial differentiation with respect to r and t respectively.

The field equations (1.2) become

$$-G^1_1 = \ddot{g} + \tfrac{3}{4}\dot{g}^2 = 8\pi(T^1_1 - e^{-g}\phi'' + \tfrac{1}{2}\dot{g}\dot{\phi}), \tag{2.1}$$
$$-G^2_2 = \ddot{g} + \tfrac{3}{4}\dot{g}^2 = 8\pi(T^2_2 - e^{-g}r^{-1}\phi' + \tfrac{1}{2}\dot{g}\dot{\phi}), \tag{2.2}$$
$$-G^3_3 = \ddot{g} + \tfrac{3}{4}\dot{g}^2 = 8\pi(T^3_3 - e^{-g}r^{-1}\phi' + \tfrac{1}{2}\dot{g}\dot{\phi}), \tag{2.3}$$
$$-G^4_4 = \tfrac{3}{4}\dot{g}^2 = 8\pi(T^4_4 + \ddot{\phi}), \tag{2.4}$$
$$-G^4_1 = 0 = 8\pi(T^4_1 + \dot{\phi}' - \tfrac{1}{2}\dot{g}\phi'), \tag{2.5}$$

where

$$G^i_k = R^i_k - \tfrac{1}{2}\delta^i_k R$$

and T^i_k is the energy tensor given by (1.4) with $p = 0$.

The inhomogeneous wave equation (1.1) becomes

$$-e^{-g}(\phi'' + 2r^{-1}\phi' - \tfrac{3}{2}e^{g}\dot{g}\dot{\phi}) + \ddot{\phi} = 3\rho. \tag{2.6}$$

A solution of Hoyle's equations will be given by a set of functions $g(t)$, $\rho(t)$, $\phi(r, t)$, T^i_k satisfying (2.1) to (2.6).

3. *The general purely time-dependent solution.*—In this section we consider solutions in which the conditions of Section 2 are fulfilled, and which also satisfy

$$\phi = \phi(t). \tag{3.1}$$

One solution of this type was given by Hoyle, and others were implicitly considered by him in the approximation procedure used to study stability.

Using (3.1) in (2.1) to (2.3) we find

$$T_1^1 = T_2^2 = T_3^3,$$

and since the assumptions of radial motion and vanishing pressure require $T_2^2 = T_3^3 = 0$, we have also $T_1^1 = 0$. Hence the only non-zero component of T_k^i is

$$T_4^4 = \rho,$$

which is consistent with (2.5). The fluid is at rest in the coordinate system so that $v^1 = v^2 = v^3 = 0$, $v^4 = 1$.

Equations (2.1) to (2.6) now reduce to

$$\ddot{g} + \tfrac{3}{4}\dot{g}^2 = 4\pi\dot{g}\dot{\phi}, \tag{3.2}$$

$$\tfrac{3}{4}\dot{g}^2 = 8\pi(\rho + \ddot{\phi}), \tag{3.3}$$

$$\ddot{\phi} + \tfrac{3}{2}\dot{g}\dot{\phi} = 3\rho, \tag{3.4}$$

which are equivalent to equations (13) to (15) of Hoyle's paper with $K = 3$, $c = 1$, $\kappa = 8\pi$.

From (3.3) and (3.4) we can obtain the linear combination

$$32\pi\ddot{\phi} + 12\pi\dot{g}\dot{\phi} = \tfrac{9}{4}\dot{g}^2,$$

and substituting for $\dot{g}^2$ from (3.2) we obtain

$$32\pi\ddot{\phi} + 3\ddot{g} = 0.$$

Integrating this equation once, we have

$$4\pi\dot{\phi} = -\tfrac{3}{8}\dot{g} + \tfrac{9}{4}H, \tag{3.5}$$

where H is a constant of integration. Equations (3.2) and (3.5) give

$$\ddot{g} + \tfrac{9}{8}\dot{g}^2 = \tfrac{9}{4}\dot{g}H,$$

and after two integrations we find

$$e^g = \alpha^2 e^{2Ht}(1 + \beta e^{-9Ht/4})^{8/9}, \tag{3.6}$$

where α and β are further constants of integration. From (3.5) we easily find ϕ, and thence ρ from (3.3):

$$\left.\begin{aligned} 8\pi\phi &= 3Ht - \tfrac{8}{3}\log(1 + \beta e^{-9Ht/4}) + \gamma, \\ 8\pi\rho &= 3H^2(1 + \tfrac{9}{8}\beta e^{-9Ht/4})(1 + \beta e^{-9Ht/4})^{-2}; \end{aligned}\right\} \tag{3.7}$$

γ is another constant of integration which, however, seems to have no physical significance in the theory, and will hereafter be ignored.

The constant α in (3.6) can be removed by the coordinate transformation

$$r^* = \alpha r$$

without (3.7) being affected, so we may write the solution as

$$\left.\begin{aligned} e^g &= e^{2Ht}(1 + \beta e^{-9Ht/4})^{8/9}, \\ 8\pi\phi &= 3Ht - \tfrac{8}{3}\log(1 + \beta e^{-9Ht/4}), \\ 8\pi\rho &= 3H^2(1 + \tfrac{9}{8}\beta e^{-9Ht/4})(1 + \beta e^{-9Ht/4})^{-2}; \end{aligned}\right\} \tag{3.8}$$

XUM

This is the general solution of equations (2.1) to (2.6) under the conditions stated in Section 2, together with the extra condition (3.1).

The solution corresponding to the steady-state theory is obtained by putting $\beta=0$ in (3.8), and may be written

$$e^{\vartheta}=e^{2H_0t}, \qquad 8\pi\phi=3H_0t, \qquad 8\pi\rho=3H_0^2, \tag{3.9}$$

where H_0 is a constant. The perturbed universe considered by Hoyle is a member of (3.8) in which β is small, and in which H differs from H_0 by another small constant. If $H>0$, the general solution (3.8) approaches the steady-state solution as $t\to\infty$ whatever the value of β. If $\beta<0$, a singularity will occur for some finite value of t.

If the constant β in (3.8) is non-zero, it can be removed by the coordinate transformation

$$t=t^*+\frac{4}{9H}\log|\beta|, \qquad r^*=|\beta|^{4/9}\alpha r$$

which is equivalent to changing the origin of t and altering the scale of r. We may drop the asterisks after these transformations are made so that the metric still has the form shown at the beginning of Section 2. Then the general solution becomes

$$\left.\begin{aligned} e^{\vartheta}&=e^{2Ht}(1+\epsilon e^{-9Ht/4})^{8/9},\\ 8\pi\phi&=3Ht-\tfrac{8}{3}\log(1+\epsilon e^{-9Ht/4}),\\ 8\pi\rho&=3H^2(1+\tfrac{9}{8}\epsilon e^{-9Ht/4})(1+\epsilon e^{-9Ht/4})^{-2},\end{aligned}\right\} \tag{3.10}$$

where $\epsilon=0$, $+1$ or -1 and where once again the additive constant in the expression for ϕ has been ignored.

For an observer at $r=0$, making his observations at time $t=T$, the Hubble "constant" and the acceleration parameter† are respectively,

$$h_1=\left(e^{-\vartheta/2}\frac{de^{\vartheta/2}}{dt}\right)_{t=T}=H(1+\epsilon e^{-9Ht/4})^{-1}; \tag{3.11}$$

$$h_2=\left(e^{-\vartheta/2}\frac{d^2e^{\vartheta/2}}{dt^2}\right)_{t=T}=(1+\tfrac{9}{4}\epsilon e^{-9HT/4})h_1^2.$$

As has already been mentioned, the steady-state theory solution occurs for $\epsilon=0$ and then the density ρ and the Hubble "constant" h_1 are both constants. The acceleration parameter is positive and equal to the square of h_1. However, there is no prescription in Hoyle's theory for choosing this particular value of ϵ. In all other cases, the solution gives rise to model universes in an unsteady state in which ρ, h_1 and h_2 are all functions of the time, a situation similar to that of general relativity.

The purely time-dependent solution of Hoyle's field equations which is spatially isotropic, homogeneous and flat, consists indeed of three one-parameter families of model universes of which one only is in a steady state. The corresponding case in general relativity (with the cosmical constant equal to zero) is the Einstein–de Sitter universe, which is unique: that is to say, it contains no arbitrary constants which cannot be removed by coordinate transformations. This suggests, as stated in the introduction, that Hoyle's theory may be weaker than general relativity.

† See e.g. McVittie (1956). The scale-factor R is, in our present notation, $e^{\vartheta/2}$.

At present, observations of the red-shifts of remote galaxies indicate that the acceleration parameter is a negative multiple of h_1^2 (Humason, Mayall and Sandage 1956; McVittie 1959, Baum 1958). The family of model universes (3.10) in which $\epsilon = -1$ permits of this possibility for a period in the history of the universe. If $\epsilon = -1$, the singular state occurs at $t = 0$ and the density is then negatively infinite. It vanishes when $e^{9Ht/4} = 9/8$ and is positive thereafter. However during the interval in which

$$9/4 > e^{9Ht/4} > 9/8, \tag{3.12}$$

the density is positive and the acceleration parameter negative. Whether such a model universe can have physical significance at all is doubtful. In any case, supposing that the acceleration parameter is at present negative, it follows from (3.12) that the time T which has elapsed since the singular state must satisfy

$$T < \frac{4}{9H} \log \frac{9}{4}; \tag{3.13}$$

now from (3.11) we have, approximately

$$H = \frac{9}{2} T h_1^2 - 2h_1,$$

and inserting this into (3.13) we find

$$T < \frac{2}{9h_1} \left(1 + \sqrt{1 + 2 \log \frac{9}{4}} \right) \sim 0{\cdot}6 h_1^{-1}.$$

It is somewhat doubtful whether this period is sufficient to allow for the observed evolutionary data.

4. *A non-homogeneous solution.*—It will now be shown by an example that, given the metric and the density of matter present, the motion of the latter is not uniquely determined by Hoyle's field equations.

We take the metric of space-time, and the proper density of matter, to be those of the steady-state universe

$$ds^2 = -e^{2Ht}(dr^2 + r^2 d\theta^2 + r^2 \sin^2 \theta \, d\phi^2) + dt^2, \tag{4.1}$$

$$8\pi\rho = 3H^2, \tag{4.2}$$

where H is a constant. The energy tensor is assumed to have the form

$$T^{ik} = \rho v^i v^k, \tag{4.3}$$

and the motion of matter is supposed to be radial from the origin of coordinates, so that

$$T^{22} = T^{33} = 0. \tag{4.4}$$

The function ϕ is allowed to depend on r and t.

The field equations are (2.1) to (2.6) with $g = 2Ht$. Using (4.4) we find that (2.2) (or (2.3)) gives

$$\phi = \frac{3Ht}{8} + \eta(u), \qquad u = r^2 - H^{-2} e^{-2Ht}, \tag{4.5}$$

where $\eta(u)$ is for the present an arbitrary function of u.

Substituting (4.5) in (2.6) and using (4.2), we find after a calculation

$$\eta(u) = P \log u + Q \tag{4.6}$$

where P, Q are constants of integration.

It remains to show that there exists a v^1 and a v^4 such that (2.1), (2.4) and (2.5) are satisfied with ρ (which occurs in T^i_k) given by (4.2). The conditions for this are

$$T^{11}T^{44} = (T^{14})^2, \tag{4.7}$$

$$T^{44} - e^{2Ht}T^{11} = 3H^2/8\pi; \tag{4.8}$$

in deriving these relations we have used (4.3), and the fact that v^i is a unit vector.

The values of T^{11}, T^{44} and T^{14} are found from (2.1), (2.4) and (2.5), using (4.5), (4.6) and $g = 2Ht$; they are

$$\begin{aligned} T^{11} &= 4Pr^2e^{-4Ht}u^{-2}, \\ T^{44} &= 4Pr^2e^{-2Ht}u^{-2} + 3H^2/8\pi, \\ T^{14} &= -2PrH^{-1}e^{-2Ht}u^{-2}(H^2r^2 + e^{-2Ht}). \end{aligned}$$

These are found to satisfy (4.7) and (4.8) if

$$P = 0 \quad \text{or} \quad P = 3/8\pi.$$

The case $P = 0$ corresponds to the steady-state solution (3.9) (with $H = H_0$). The case $P = 3/8\pi$ is different, and the solution for this value of P is given by

$$\left.\begin{aligned} ds^2 &= -e^{2Ht}(dr^2 + r^2\,d\theta^2 + r^2\sin^2\theta\,d\psi^2) + dt^2, \\ 8\pi\rho &= 3H^2, \\ 8\pi\phi &= 3Ht + 3\log(r^2 - H^{-2}e^{-2Ht}) + 8\pi Q, \\ v^1 &= \pm\frac{2rH}{H^2r^2e^{2Ht} - 1}, \\ v^4 &= \mp\frac{H^2r^2e^{2Ht} + 1}{H^2r^2e^{2Ht} - 1}. \end{aligned}\right\} \tag{4.9}$$

This solution is non-homogeneous in the sense that, although the metric is homogeneous and the density uniform, the velocity of matter depends on the distance from the origin. It shows that, given the metric and the density, Hoyle's field equations do not uniquely determine the motion of the matter present. Moreover, as can easily be verified, the motion in (4.9) is not represented by a geodesic in the space-time (4.1).

5. *Conclusion.*—The result of Section 3 was that, in the case considered, Hoyle's theory is weaker than general relativity in that it gives three infinite families of solutions in place of the unique solution of general relativity. This alone is perhaps not a very serious objection to Hoyle's theory, since one may be prepared to accept that, although one wishes a theory to be as determinate as possible in its predictions, certain parameters of a cosmological theory have to be determined by observation. However, it has not been possible to obtain a negative acceleration parameter in a convincing fashion from the results of Section 3.

The conclusion of Section 4 seems, however, more disturbing. From general relativity one is accustomed to expect all observable features of a given gravitational problem to be determined by the metric describing it. One also expects matter to follow geodesics in the absence of non-gravitational forces. Neither of these expectations is fulfilled in Hoyle's theory.

We can put the objection in a more definite form. What in Hoyle's theory is the physical significance of the metric (4.1)? Since it does not play the same

role as in general relativity, can one be sure that light rays travel on its null-geodesics, and that one may carry through with confidence the arguments which lead to, say, the relation of red-shift and apparent magnitude as determined in a model of general relativity?

Evidently to use the theory one would have to examine carefully the meaning of metric in it. One would also need some experimental procedure for finding the creation field ϕ, which seems to play a decisive part in distinguishing between physical situations described by the same metric tensor. Until such matters have been clarified it seems that the theory must be regarded as incomplete.

The workd escribed in this paper was done while one of us (W. B. B.) was on leave of absence at the University of Illinois Observatory.

Queen Elizabeth College,
London, W.8:
1961 *January.*

University of Illinois Observatory,
Urbana, Illinois,
U.S.A.

References

Baum, W. A., 1958, *Trans. I.A.U.*, **10**, 437.
Hoyle, F., 1960, *M.N.*, **120**, 256.
Humason, M. L., Mayall, N. U., and Sandage, A. R., 1956, *Astron. J.*, **61**, 97.
McVittie, G. C., 1956, *General Relativity and Cosmology*, Sec. 9.1 (London, Chapman and Hall).
McVittie, G. C., 1959, *Handbuch der Physik*, **53**, p. 475 *et seq* (Heidelberg, Springer).

THE NUMBER–FLUX DENSITY RELATION FOR RADIO SOURCES AWAY FROM THE GALACTIC PLANE

P. F. Scott and M. Ryle

(Received 1961 January 30)

Summary

Two new series of observations at a frequency of 178 Mc/s have been combined to derive the number-flux density (N–S) relation for radio sources situated at galactic latitudes $>20°$.

In order to investigate the possible errors which might be introduced by various instrumental selection effects, detailed investigations have been made both of the distribution in " surface brightness " of the sources, and of the extent to which radio sources occur in clusters. It is shown that neither effect introduces an important error in the observed number-flux density relation. The observations, when corrected for these effects, provide a plot of log N against log S which, over the range $100 > S > 2 \times 10^{-26}$ w.(c/s)$^{-1}$ m^{-2}, may be approximated by a straight line of slope $-1{\cdot}80$. If account is taken of the errors in the observations and uncertainties in the analysis it is concluded that the slope lies in the range $-1{\cdot}68$ to $-1{\cdot}93$.

---

1. *Introduction.*—Previous observations of radio sources have revealed an almost isotropic distribution of sources having small angular diameters; in areas near to the galactic equator there are in addition a number of extended sources, but for $|b| > 15°$–$20°$ extended sources are rare and represent only a small fraction of the total in any given range of flux density.

An analysis of the sources remote from the galactic equator showed that the number N having a flux density greater than a given value S did not vary as $N \propto S^{-1{\cdot}5}$ as would be expected for a uniform distribution of sources; observations of an area of sky of 3·2 steradians, and flux densities between 200 and 8×10^{-26} w. (c/s)$^{-1}$ m^{-2}, indicated a relation $N \propto S^{-2{\cdot}0}$ (Edge, Shakeshaft, McAdam, Baldwin and Archer 1959). It was also shown that, although the partial resolution of extended sources might give rise to an effect of this kind, the number of such sources was inadequate to account for the discrepancy. A similar result ($N \propto S^{-1{\cdot}8}$) was found by Mills, Slee and Hill (1958) but these authors considered that the difference between their value of the exponent and the expected value of $-1{\cdot}5$ could largely be accounted for by instrumental effects.

A recent examination (Bennett and Smith 1961) of both surveys in the light of new observations at Cambridge (Leslie 1961 a; Scott, Ryle and Hewish 1961) suggests however that the survey of Mills, Slee and Hill is not suitable for this analysis since it is probably incomplete in its coverage of the weaker sources and since a number of the intense extended sources listed appear to be associations of weak "point" sources. Similar reservations have been expressed by Bolton (1960).

The new Cambridge observations, which were made with the large 178 Mc/s interferometer (Ryle 1960), have now been used to derive a more accurate number–flux relation density than was possible before.

XUM

The large resolving power of the instrument has permitted observations, at the level of 1 source per 30 beam areas, of sources having $S \geqslant 2 \times 10^{-26}$ w. (c/s)$^{-1}$ m^{-2}; sources of this flux density can be recorded with a signal-to-noise ratio of 25 : 1. The observations of the more intense sources ($S \geqslant 6 \times 10^{-26}$ w. (c/s)$^{-1}$ m^{-2}) were made both with a total power system and with an interferometer so that any selection effects which might arise from partial resolution of extended sources could be eliminated; at the same time, sufficient information on the distribution of sources with different "surface brightness" could be obtained to allow corrections (which are small) to be made for this selection effect in the survey of high resolution. The survey of the more intense sources covered most of the available sky in order to minimize the statistical errors arising from the small density of intense sources.

Both surveys have been used to establish the extent to which radio sources may occur in clusters (Leslie 1961 b), since a clustering tendency would also affect the apparent number–flux density relation.

The two sets of observations are described in Section 2 and the effects of extended sources, clustering and side-lobe responses in the aerial reception pattern are examined in Section 3. The results of both sets of observations in areas having $|b| > 20°$ are combined in Section 4 to derive the N–S relation for $100 > S > 2 \times 10^{-26}$ w. (c/s)$^{-1}$ m^{-2}.

2. *The observations.*

(*a*) *The survey of sources having* $S \geqslant 6 \times 10^{-26}$ *w.* (*c/s*)$^{-1}$ *m*$^{-2}$.—The observations, which have already been described in detail (Leslie 1961), were made over the whole sky between $\delta = -05°$ and $\delta = +60°$. Two sets of measurements were made using (i) the fixed aerial of the instrument (1450 ft × 65 ft) with a total-power receiver and (ii) both aerials as a simple interferometer of 465 λ spacing.

In both systems the reception pattern to half-power was approximately 14′ in α and 4°·6 in δ.

The total-power system allowed the determination of the positions and flux densities of 910 sources having $S \geqslant 6 \times 10^{-26}$ w. (c/s)$^{-1}$ m^{-2}, 629 of which lay in areas with $|b| > 20°$; at this level there is approximately 1 source per 20 beam areas. Information on the angular diameter of the sources was derived by combining these observations with those made with the interferometer; for sources having $S \geqslant 20 \times 10^{-26}$ w. (c/s)$^{-1}$ m^{-2} angular diameters in the range 2′·5 to 40′ arc could be measured, whilst statistical information on the distribution of angular diameters of the weaker sources could also be obtained.

For sources having an angular diameter greater than 40′ arc the detection sensitivity which could be achieved decreased inversely as the diameter and sources whose "brightness temperature" (T_b) was less than 500 °K could not be detected with uniform sensitivity. Observations of the most intense sources, however, showed none with brightness temperatures in the range 200–10^4 °K, and only 2 per cent in the range 100–200 °K; the latter sources have been identified with nearby normal galaxies. The remainder had $T_b > 10\,000$ °K and 83 per cent had $T_b > 60\,000$ °K.

The omission in these observations of any sources having very low surface brightness ($T_b < 100$ °K) is of little importance, since they would be completely resolved with a 465 λ interferometer and would therefore not be observed except at distances where their flux density was less than $0{\cdot}07 \times 10^{-26}$ w. (c/s)$^{-1}$ m^{-2}.

Using the flux density provided by the total-power observations, the number–flux density relation for sources having $S \geqslant 6 \times 10^{-26}$ w. (c/s)$^{-1}$ m^{-2} and situated more than 20° from the galactic equator is shown in Fig. 1.

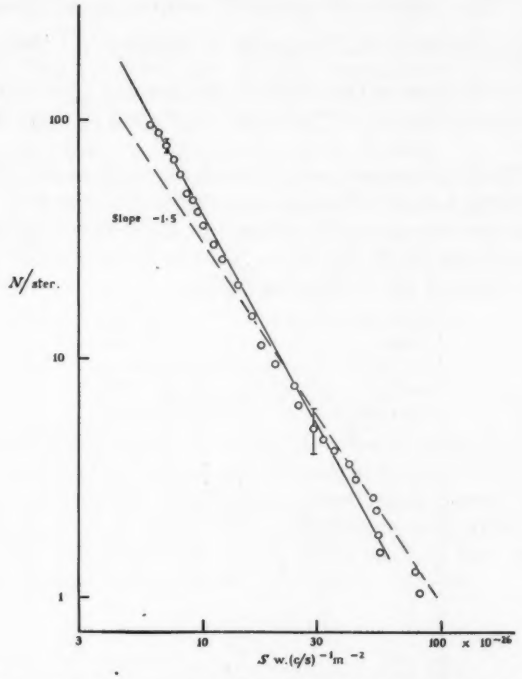

FIG. 1.—*The number of sources per steradian (N) with a flux density greater than S, derived from 3·9 steradians of sky having* $|b| > 20°$*; the observations were made with the total power system and include all sources having* $S > 6 \times 10^{-26}$ *w.* $(c/s)^{-1}$ m^{-2}. *The vertical lines indicate the statistical errors.*

(*b*) *The high resolution observations.*—The second series of observations used the method of aperture synthesis to obtain the full resolution of the instrument (Scott, Ryle and Hewish 1961). The reception pattern is that of a 465 λ interferometer with an envelope pattern 25′ arc in α and 35′ arc in δ.

The present analysis is based on observations of four areas of sky covering nearly 24 hours in α and $\delta = 50°$–$54°$, $\delta = 48°$–$52°$, $\delta = 40°$–$44°$ and $\delta = 16° 30'$–$21° 30'$; the first two areas were chosen to overlap in order to test the overall operation of the instrument. The total area observed having $|b| > 20°$ is approximately 0·6 steradian and includes a sufficiently large number of sources for the statistical errors to be small compared with those of the "whole-sky" counts of the more intense sources.

The positions and flux densities of all sources having $S > 2 \times 10^{-26}$ w. (c/s)$^{-1}$ m^{-2} were obtained, a level at which there is approximately one source per 30 beam areas. The noise level corresponded to a flux density of 8×10^{-28} w. (c/s)$^{-1}$ m^{-2}. The errors arising from the effects of confusion with weak sources may be determined from the probability distribution, $P(D)$, of the record amplitude D (Ryle 1958).

The form of the probability distribution depends on the actual N–S distribution of the sources, and it may be computed for any given model (Scheuer 1957). In the present case the observations were used to determine an approximate distribution of the sources from which the theoretical $P(D)$ curve was computed. The error in the counts of sources at any given flux density will then be represented by the departure of the curve $\int_D^\infty P(D)\,dD$ from the assumed N–S distribution. The error in the number of sources at the limit of the present survey ($S = 2 \times 10^{-26}$ w. (c/s)$^{-1}$ m^{-2}) was in this way found to be about 7 per cent.

Although this paper is concerned only with the number–flux density relation as determined from counts of individual sources, the low noise level on the records allows the use of the experimentally determined $P(D)$ distribution both to avoid this error and to extend the N–S relation to sources of smaller flux density; this analysis has been carried out by Hewish (1961).

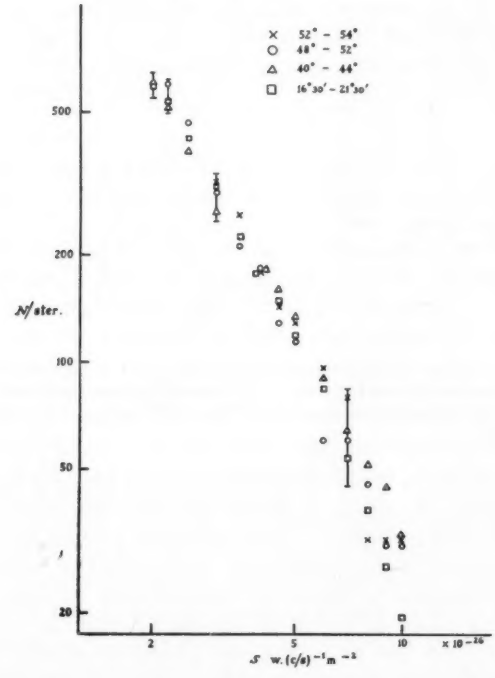

FIG. 2.—*The number of sources per steradian (N) having a flux density greater than S, derived from four area of sky observed with the system of high resolving power. The statistical errors shown are appropriate to a single set of observations.*

The results obtained for the four areas of sky are plotted separately in Fig. 2; the statistical uncertainty of any one set of observations is shown and it can be seen that there is no significant difference in the counts obtained for the different areas of sky.

In the next section consideration is given to the corrections which may have to be applied to the results on account of source clustering, the presence of extended sources and the effects of side-lobe responses of the aerial system.

3. *The effects of angular diameter and clustering of the sources, and of side-lobes of the aerial system.*

(*a*) *The presence of extended sources.*—The observations of sources having $S \geqslant 6 \times 10^{-26}$ w. (c/s)$^{-1}$ m^{-2} have provided information on their angular diameters. It is convenient to express the distribution of angular diameters in terms of an equivalent distribution of "surface brightness" so that observations in one range of flux density may easily be related to those in another.

The results obtained by Miss Leslie (1961 a) for areas of sky having $|b| > 20°$ are summarized in Table I, which gives the proportion of the sources in a given range of flux density, which have brightness temperatures (T_b) falling in different ranges.

TABLE I

T_b (°K)	Percentages of sources
100–200	2 per cent
200–10^4	None
10^4–6×10^4	> 15 per cent
$> 6 \times 10^4$	< 83 per cent

Observations of a number of sources have been made with interferometers of larger resolving power, both at Jodrell Bank and at the California Institute of Technology (Bolton 1960). Whilst these observations do not provide complete information on sources of small surface brightness, they allow closer limits to be placed on the distribution at larger values of T_b. The results show that 60 per cent of all sources have $T_b > 4 \times 10^5$ °K.

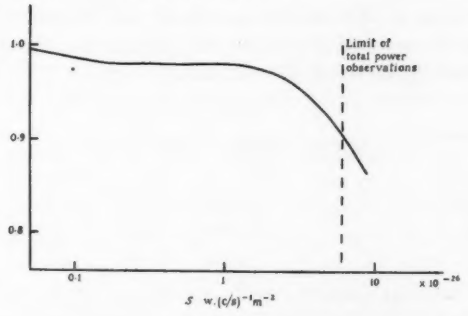

FIG. 3.—*The maximum reduction in the source counts which would occur with the system of high resolving power due to sources having the derived distribution of surface brightness.*

Using the results of all the observations it is now possible to determine the effect of this distribution on the counts of weaker sources ($S \geqslant 2 \times 10^{-26}$ w. (c/s)$^{-1}$ m^{-2}) which were made exclusively with a 465λ interferometer. Sources whose angular extent exceeds about 6′ of arc will not be observed at all, whilst those with angular diameters in the range 2′–6′ of arc will be recorded with reduced intensity. The apparent number of sources in each range of flux density will therefore be reduced and the maximum effect which would be produced by the derived distribution of T_b is shown in Fig. 3.

It can be seen that for $S = 6 \times 10^{-26}$ w. (c/s)$^{-1}$ m^{-2} the error in the apparent number of sources may be as great as 10 per cent; for smaller flux densities the error decreases to 2 per cent. The errors which would arise at $S > 6 \times 10^{-26}$ w. (c/s)$^{-1}$ m^{-2} are unimportant since measurements are here available with the total power system.

The 2 per cent reduction, which affects all sources having $S > 0{\cdot}15 \times 10^{-26}$ w. (c/s)$^{-1}$ m^{-2}, arises from the presence of a few sources of very low surface brightness ($100 < T_b < 200$ °K); it is therefore convenient to omit these sources from the analysis and to derive, with the corrections of Fig. 3, the number–flux density relation for the main class of source. Such a procedure would not be permissible if the relation were to be extended to $S < 0{\cdot}15 \times 10^{-26}$ w. (c/s)$^{-1}$ m^{-2}, although even at smaller flux densities the errors in source number would be only a few per cent.

(*b*) *Source clustering.*—If the distribution of the sources in space were not random, errors in deriving the number–flux density relation might arise. If, for example, a significant proportion of the sources occurred in close double or multiple systems they might be observed as individual sources when they were nearby, but as a single and possibly extended source when at a greater distance; it would then be necessary to examine separately the effects on observations made with the total-power system and with the interferometer.

An analysis of source clustering has been made by Miss Leslie (1961 b) in which angular separations of the components from 3′·5 to 200′ arc were investigated; these separations apply to sources having $S \sim 5 \times 10^{-26}$ w. (c/s)$^{-1}$ m^{-2}. This range of angular separation is sufficient to allow a full determination of the effects of clustering on both total-power and interferometric observations.

Three different sets of observations were made, corresponding to different angular separations in α. The results are shown in Table II which gives, for each set, the maximum percentage of sources occurring in double or multiple systems, with the corresponding limiting flux density.

TABLE II

	Maximum percentage of sources	Angular separation (min of arc)	Range of flux density (10^{-26} w. (c/s)$^{-1}$ m^{-2})
(*a*)	0·5	15–45	$S > 2$
	6	15–90	
(*b*)	15	2·5–5·0	$S > 5$
(*c*)	2·4	5–15	$S > 10$
	4·5	5–60	

It is clear that any sources falling in category (*a*) in the table will not introduce errors since they may be adequately resolved for all values of S. The possibility of close associations of sources (*b*) was derived from the measurements of angular diameter and is based on the supposition that all the sources previously recorded as being extended with $10^4 < T_b < 6 \times 10^4$ °K are in fact close multiple systems. It is likely that at least half such systems represent true extended sources (Leslie 1961 b) and the number of double or multiple sources with a separation in α of 2′·5–5′·0 of arc is therefore probably less than 7·5 per cent. It is, however, necessary to consider the alternative possibilities that the whole of the observed effect might be due to (*a*) extended sources or (*b*) close multiple sources, when

considering the limits of error in the number–flux density relation. It is any in case evident that such sources will not have an important effect, since at $S \simeq 2 \times 10^{-26}$ w. (c/s)$^{-1}$ m^{-2} the angular separation will be so small that the combined intensity will be measured, which is also the case when similar nearer systems ($S > 10 \times 10^{-26}$ w. (c/s)$^{-1}$ m^{-2}) are observed with the total-power system.

It is therefore only those sources for which limits (*c*) are given which might affect the results appreciably; such sources would be observed with reduced intensity with the interferometric system and the effects at different values of S must be computed. The total error introduced cannot, however, exceed 4·5 per cent in the observed number of sources at a given value of S.

(*c*) *The effects of aerial side-lobes.*—The observed number–flux density relation would be modified if intense sources received in subsidiary responses of the aerial system were mistaken for weak sources. It can be shown that if the number of sources can be expressed as $N \propto S^{-p}$ then the existence of unrecognized spurious responses does not affect the observed law although it increases the apparent number of sources at a given flux density. Errors may however be introduced if the relation is not a power law; this is of particular importance in the case of the intense sources Cassiopeia-A and Cygnus-A, which have flux densities some 100 times greater than that expected for a power law distribution. Special attention must therefore be paid to the unintentional reception of these sources.

The observed response of the aerial system has already been given (Scott *et al.* 1961); except near the two principal planes the response is everywhere less than 10^{-4} of that in the forward direction. At the same δ the response in α is only appreciable within 1° of the forward direction, the first order maxima having an amplitude of 4 per cent with the second and higher orders less than 1 per cent. At the same α, the response in δ includes several maxima with an r.m.s. amplitude of < 6 per cent within $2\frac{1}{2}$° of the forward direction; elsewhere the response is $< 0{\cdot}03$ per cent except for a small number (which depends on δ) of single "diffraction grating" responses each 35′ in extent and $< 0{\cdot}5$ per cent in magnitude.

From these figures it is clear that observations of sources having $S \geqslant 2 \times 10^{-26}$ w. (c/s)$^{-1}$ m^{-2} are only affected by the presence of sources having $S > 30 \times 10^{-26}$ w. (c/s)$^{-1}$ m^{-2} in the immediate proximity of the area investigated, and by sources having $S > 400 \times 10^{-26}$ w. (c/s)$^{-1}$ m^{-2} situated at nearly the same α.

In reducing the high resolution observations, an area of sky $2° \times 4°$ centred on each source having $S > 25 \times 10^{-26}$ w. (c/s)$^{-1}$ m^{-2} was therefore omitted, allowance being made for the small reduction (2 per cent) in the total area of sky involved in the observations of weak sources. Narrow strips were also omitted near the α of each of the four intense sources having $S > 400 \times 10^{-26}$ w. (c/s)$^{-1}$ m^{-2}.

In the total power observations the subsidiary responses were smaller, and since only sources having $S \geqslant 6 \times 10^{-26}$ w. (c/s)$^{-1}$ m^{-2} were recorded, it was only necessary to omit a strip near the α of each of the two most intense sources.

4. *The results.*—The figures obtained from the two sets of observations must now be combined to give the number–flux density relation for the available range of flux density $100 > S > 2 \times 10^{-26}$ w. (c/s)$^{-1}$ m^{-2}. Sources having $S \geqslant 6 \times 10^{-26}$ w. (c/s)$^{-1}$ m^{-2} were observed by a method which is independent of

angular diameter, and all instrumental effects are likely to be small for $S > 10 \times 10^{-26}$ w. (c/s)$^{-1}$ m^{-2}. Weaker sources were observed with an interferometer, and the presence of extended sources may therefore affect the apparent number of sources at a given flux density; an analysis of the distribution of surface brightness of the more intense sources allows an upper limit to be established for the effect at any given value of S. The observations have therefore been corrected on the basis of the best estimate of the distribution of surface brightness and limits have been determined, based on the presence of the maximum and minimum possible percentages of extended sources.

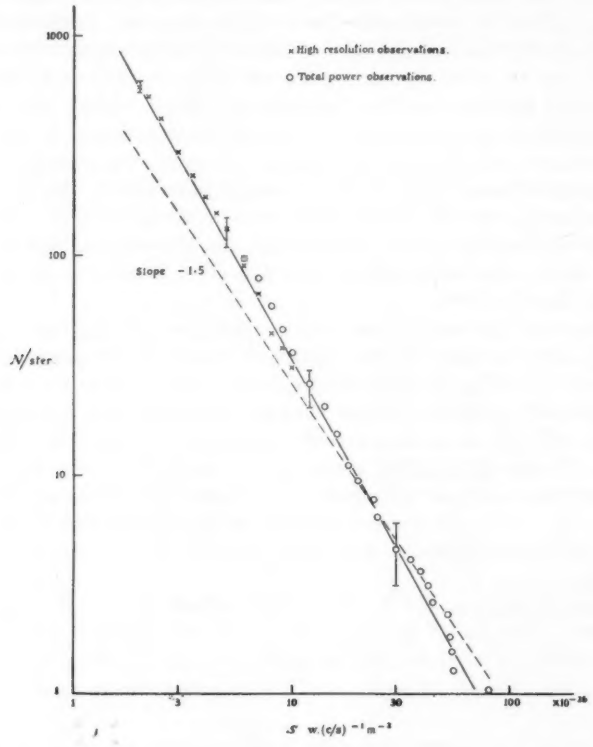

FIG. 4.—*The combined N–S distribution for* $2 < S < 100 \times 10^{-26}$ *w.* $(c/s)^{-1}$ m^{-2}. *The observed counts have been corrected for the effects of source diameter, clustering and confusion. The errors shown include the uncertainty in these effects, the statistical errors and the uncertainty in the scales of flux density used in the two sets of observations.*

A similar analysis has been made of the effect of source clustering having the various angular scales considered, and limits have again been determined for the maximum effect on the number–flux density relation. The flux density scales of the two sets of observations were normalized by relating each series to the intense sources for which special observations have been made (Elsmore, Ryle and Leslie 1959) and there is an additional uncertainty of 5 per cent in this scaling.

All the observations, corrected in these ways, are shown in Fig. 4; the limits of error shown include the uncertainty arising from all the effects considered, as well as the statistical uncertainty due to the finite number of sources.

For values of flux density $2 < S < 20 \times 10^{-26}$ w. (c/s)$^{-1}$ m^{-2} the observations are best fitted by a straight line having a slope of $-1{\cdot}80$; the limits of error would allow a slope lying in the range $-1{\cdot}68$ to $-1{\cdot}93$.

5. *Conclusion.*—The new observations have confirmed the earlier conclusions that there is an apparent excess of weak sources or deficit of intense ones. Previous suggestions that the effect might be caused by the presence of extended sources or by a strong clustering tendency have been investigated and it has been shown conclusively that neither effect would be sufficient to produce a number–flux density curve approaching that observed.

The high resolution survey has been further investigated using the statistical method of record analysis (Hewish 1961) in order to obtain information on the N–S relation for values of $S < 2 \times 10^{-26}$ w. (c/s)$^{-1}$ m^{-2}. The implications of the results obtained are considered in a separate paper (Ryle and Clarke 1961).

We should like to thank Dr Hewish and Miss Patricia Leslie for useful discussions, and Miss Ann Neville and Mr D. R. Marks for assistance in the reduction of the observations. One of us (P. F. S.) is indebted to the Royal Commission for the Exhibition of 1851 for a Senior Studentship.

Mullard Radio Astronomy Observatory,
Cavendish Laboratory,
Cambridge:
1961 *January.*

References

Bennett, A. S., and Smith, F. G., 1961, *M.N.*, **122**, 71.
Bolton, J. G., 1960, Reported at General Assembly of U.R.S.I., London.
Edge, D. O., Shakeshaft, J. R., McAdam, W. B., Baldwin, J. E., and Archer, S., 1959, *Mem. R.A.S.*, **67**, 37.
Elsmore, B., Ryle, M., and Leslie, P. R. R., 1959, *Mem. R.A.S.*, **67**, 61.
Hewish, A., 1961 (in preparation).
Leslie, P. R. R., 1961 a, *M.N.*, **122**, 51.
Leslie, P. R. R., 1961 b, *M.N.*, **122**, 371.
Mills, B. Y., Slee, O. B., and Hill, E. R., 1958, *Aust. J. Phys.*, **11**, 360.
Ryle, M., 1958, I.A.U. Symposium on Radio Astronomy, Paris, p. 475.
Ryle, M., 1960, *J.I.E.E.*, **6**, 14.
Ryle, M., and Clarke, R. W., 1961, *M.N.*, **122**, 349.
Scheuer, P. A. G., 1957, *Proc. Cam. Phil. Soc.*, **53**, 764.
Scott, F. F., Ryle, M., and Hewish, A., 1961, *M.N.*, **122**, 95.

AN ACCRETION HYPOTHESIS FOR THE ORIGIN OF THE SOLAR SYSTEM

R. A. Lyttleton

(Received 1961 January 31)

Summary

The possibility of direct accretion of interstellar matter by the Sun is considered as a source of material for a solar disk as the initial stage of planet formation. The existing mass and angular momentum require a size and density of the cloud in close agreement with observed values. The range of action of the Sun would require a relative speed of about 0·2 km sec^{-1}, and such a speed would have high probability of occurring at some time for any star over a period of several aeons. The amount of material falling directly into the Sun would probably be so small as to bring negligible angular momentum to it. The hypothesis would allow an origin for the planetary material quite separate from the Sun, and also would imply (assuming that a disk so formed would develop into planets) that a large proportion of old stars may have attendant planets. Besides resting on more secure hypotheses, a disk so formed would appear quite as suitable a source for planets as one relying on magnetic-coupling to the Sun for its formation.

---

1. *Introduction.*—The idea that planets could form directly from material released from a star appears gradually to have been abandoned, and instead modern theories mainly suppose that an intermediate stage is necessary in which a disk of dust and gas (mainly hydrogen) is first formed in orbital motion round the Sun. A number of processes for the formation of such a disk have been put forward, as for instance from a binary companion to the Sun by collision with another star, or by rotational break-up, or by a supernova explosion, and more recently through magnetic coupling of an equatorial disk shed from a rapidly rotating primitive Sun*. On the other hand vast tracts of interstellar dust, believed to have originated from supernovae, together with a far greater amount of hydrogen, already exist in space, and there arises the question whether such material could be captured by the Sun in a way leading to formation of a suitable planet-forming disk. Schmidt in particular has proposed the capture of such material as a result of a three-body encounter of the Sun, a second star, and a gas–dust cloud†. It is now a settled matter of celestial mechanics that a double system can form when three particles come together suitably from infinite separation, and there therefore seems little doubt by extension of the mechanism that part of an interstellar cloud could be captured by the Sun with requisite angular momentum. The process however would need special conditions of encounter, and to this extent would mean that planetary systems so originating would be correspondingly rare.

The alternative possibility remains whether any other process of a more direct kind can be effective in enabling the Sun (or any other star) to capture

* F. Hoyle, The Origin of the Solar Nebula, *Q.J.R.A.S.*, **1**, 28, 1960.
† O. Schmidt, *A Theory of the Earth's Origin*, Moscow 1958.

XUM

material on an adequate scale. It appears that the ordinary mechanism of accretion can accomplish this provided that the relative speed of Sun and cloud is sufficiently small, in fact of the order of $0{\cdot}2\ \mathrm{km\ sec^{-1}}$, and the object of the present paper is to examine this process in the present connection. As usual with cosmogonical hypotheses, it proves possible to carry this out only by means of order of magnitude comparisons, but striking agreement emerges with the main quantitative features of the planetary system.

2. *Nature of the relevant accretion process.*—The process of accretion has been satisfactorily studied from a mathematical point of view for two main cases. First, that of line-accretion with the star moving through the cloud and when all temperature effects can be ignored*. In this case, the scale of accretion is limited by the speed V of the star relative to the cloud, and the capture radius (for the Sun) is of order $2G\odot/V^2$. Second, that of spherically symmetrical accretion, in which the scale is limited by the thermal speed c in the gas at great distance. In this case the capture radius extends out to a distance of order $2G\odot/c^2$†.

The density of radiation in space within the galaxy remote from stars is such as would maintain a black-body temperature of $3{\cdot}18^\circ\,\mathrm{K}$‡. For a hydrogen cloud containing also dust, say to an amount of order 1 per cent by mass, so that it would be as cool as possible, then its minimum temperature would be equal to the black-body value. Also, the hydrogen in the presence of dust would take up molecular form, and this in turn would mean for the thermal speed $1{\cdot}965\times10^4\,\mathrm{cm\,sec^{-1}}$, or $c^2=3{\cdot}86\times10^8\,\mathrm{cm^2\,sec^{-2}}$. Now, as will appear later, this value of c is of the same order as the linear speed V appropriate to accretion on an adequate scale, and it is therefore necessary to regard the process as limited both by velocity and temperature. For the combined effect, Bondi has proposed the empirical formula

$$A=\frac{4\pi G\odot^2\rho}{(V^2+c^2)^{3/2}} \tag{1}$$

for the rate of accretion, since this reduces to the established formulae for the two cases $c=0$ of line-accretion, and $V=0$ of spherically symmetrical accretion. This corresponds to an effective capture radius

$$R=\frac{2G\odot}{V^2+c^2} \tag{2}$$

when line-accretion is modified by temperature effects. In any event, a length R so defined would give the order of magnitude of the distance within which capture occurred probably so long as V itself does not vanish. In the case we shall actually be concerned with, V and c turn out to be of the same order.

We have also to consider the angular momentum of the captured material arising from the extremely small angular velocity ω of the cloud as a whole. This can be taken, in order of magnitude, to be given by

$$\omega=10^{-15}\,\mathrm{sec^{-1}}. \tag{3}$$

If the Sun is regarded as capturing a cylinder of material of radius R and

* H. Bondi and F. Hoyle, *M.N.*, **104**, 273, 1944.
† H. Bondi, *M.N.*, **112**, 195, 1952.
‡ A. S. Eddington, *Internal Constitution of the Stars*, Cambridge, p. 371, 1930.

length L, where $L > R$, then if M is the total mass of material captured, the moment of inertia of it about an axis perpendicular to its length would be slightly in excess of $\frac{1}{3}ML^2$; the accurate form is $\frac{1}{4}MR^2 + \frac{1}{3}ML^2$, but the first term in this will be small compared with the second, and in any event we are concerned only with order of magnitude values. This way of calculating the angular momentum supposes ω more or less perpendicular to V, which would be the most representative case, and also regards the region of the cloud where the Sun enters to be at rest, so that the cloud as a whole is rotating about that point and V measured relative to this part of the cloud. This is justified since the time of passage turns out to be of order 10^6 years, during which time the cloud would have turned through only about 2°.

On the other hand, if ω is parallel to V, which would occur very rarely, the appropriate moment of inertia would be $\frac{1}{2}MR^2$. The resulting numerical values (arrived at in the next section) are not altered in order of magnitude, but L and R tend to be more nearly equal than in the more likely event of ω and V being inclined at a substantial angle.

3. *The mass and angular momentum requirements.*—The most important test of any hypothesis is whether both the mass and angular momentum of the planetary material can simultaneously be accounted for in order of magnitude. To set down relations for this we adopt the following notation:

M = mass of planetary material captured $= 3 \times 10^{30} m$ grams.

The figure 3×10^{30} g. is in round numbers the present mass of the planets, and the factor m is a numerical parameter (of order unity) introduced to allow for the possibility of escape of some of the material originally captured.

H = angular momentum of captured material $= 4 \times 10^{50} h$ c.g.s. units.

Here again the value 4×10^{50} represents the present value (in round numbers), and the factor h, again of order unity, enables account to be taken of the possibility of subsequent loss of angular momentum carried away by escaping material.

R = accretion capture radius, given by (2),
L = effective length of path of the Sun through the cloud,
V = velocity of the Sun relative to the cloud,
ρ = undisturbed density of cloud (assumed uniform),
ω = angular velocity of the cloud as a whole,
c = mean thermal speed of hydrogen molecules of the cloud,
G = constant of gravitation,
$T = L/V$ = time of passage through the cloud.

The quantity of captured material and its angular momentum then lead to the following:

$$M = 3 \times 10^{30} m = \pi R^2 L \rho, \tag{4}$$

$$H = 4 \times 10^{50} h = \tfrac{1}{3} M L^2 \omega. \tag{5}$$

Hence we have

$$H/M = \tfrac{4}{3} \times 10^{20} h/m = \tfrac{1}{3} L^2 \omega, \tag{6}$$

and for $\omega = 10^{-15}$, this leads at once to

$$L = 6{\cdot}33 \times 10^{17} h^{1/2} m^{-1/2} \text{ cm}. \tag{7}$$

Thus the effective path length through the cloud is of order 10^{18} cm (about one light-year) and is in general order of magnitude agreement with interstellar

distances. It would be expected that there would be a "cut-off" value limiting the range of action of a star because of the presence of adjacent stars.

It can readily be shown that accretion of mass equal to that of the planets will have negligible braking effect on the speed of the Sun through the cloud, so the time of passage through the cloud will be L/V, and the total mass captured, by (1), leads to the relation

$$3 \times 10^{30} m = \frac{4\pi G^2 \odot^2 \rho}{(V^2+c^2)^{3/2}} \cdot \frac{L}{V}. \tag{8}$$

If for the density we take $\rho = 10^{-23}\,\mathrm{g\,cm^{-3}}$ throughout, then inserting numerical values this gives

$$V(V^2+c^2)^{3/2} = 4{\cdot}71 \times 10^{17} h^{1/2} m^{-3/2}, \tag{9}$$

or, if $x = V/c$,

$$x(x^2+1)^{3/2} = 3{\cdot}16 h^{1/2} m^{-3/2}. \tag{10}$$

To proceed further, values have to be assigned to h and m. It seems reasonable to suppose that they will both exceed unity somewhat, but to determine the actual extent would require detailed analysis of the development of the planetary disk, and this in turn would require detailed knowledge of its initial composition and arrangement. However, it turns out that V, L, and R are not particularly sensitive to h and m, as the following examples show:

(i) $m = 1{\cdot}21$, $h = 1{\cdot}69$. Here $x = 1{\cdot}035$, and thence it is found that
$V = 2{\cdot}03 \times 10^4$ cm sec^{-1}.
$L = 7{\cdot}5 \times 10^{17}$ cm.
$R = 3{\cdot}9 \times 10^{17}$ cm.
$T = 1{\cdot}2 \times 10^6$ years.

(ii) $m = h = 1{\cdot}5$. Here $x = 0{\cdot}885$, and thence,
$V = 1{\cdot}74 \times 10^4$ cm sec^{-1}.
$L = 6{\cdot}3 \times 10^{17}$ cm.
$R = 3{\cdot}8 \times 10^{17}$ cm.
$T = 1{\cdot}1 \times 10^6$ years.

(iii) $m = 2{\cdot}25$, $h = 4$. Here $x = 0{\cdot}837$, and thence
$V = 1{\cdot}64 \times 10^4$ cm sec^{-1}.
$L = 8{\cdot}4 \times 10^{17}$ cm.
$R = 5{\cdot}0 \times 10^{17}$ cm.
$T = 1{\cdot}6 \times 10^6$ years.

In arriving at these values, both ω and ρ have been estimated simply in round numbers, but the interesting result emerges that R and L are both of interstellar order, and not differing from that by several powers of ten as usually happens for invalid hypotheses. Similarly the time of passage, about 10^6 years, is an entirely reasonable value.

4. *Likelihood of the small relative speed required.*—In each of the numerical cases considered above, the relative speed turns out to be of the order of $0{\cdot}2\,\mathrm{km\,sec^{-1}}$. The temperature limitation to accretion supposes adiabatic compression without loss of energy, but in fact the presence of dust and possibly molecules within the gas will enable it to cool below the adiabatic temperature,

and this would mean that the thermal limitation, represented by the presence of c in (1) and (2), is probably overestimated. To estimate the probability of a small relative speed occurring, if we suppose a Maxwellian distribution, then the absolute speed will be distributed in accordance with a law of the form

$$\frac{4}{\sqrt{\pi}v_0^3}\exp(-v^2/v_0^2)v^2\,dv. \qquad (11)$$

If we take $v_0 \sim 10\,\mathrm{km\,sec^{-1}}$, then the probability of a speed not exceeding $0{\cdot}2\,\mathrm{km\,sec^{-1}}$ is of the order 10^{-5}, while for other small speeds it increases in proportion to the cube of the speed.

In its whole history the Sun must certainly have passed through several hundred if not thousands of clouds (the existence of huge numbers of comets testify to this on the accretion theory of their origin), and since prior to the formation of the planets the Sun may have existed for a few times 10^9 years, a slow encounter at some stage would have a prior probability of order 10^{-3} anyway for the Sun. But there is of course no need to rely on any such consideration for a particular case, such as the Sun with its known solar system represents, for so long as the requisite low speed *can* occur, then its occurrence may be legitimately assumed as a postulate of the theory. On the other hand, since the probability is not by any means vanishingly small, it would follow that a proportion, of order 10^{-3} at least, of old stars will at some time have undergone sufficiently slow encounter with a cloud, and so have been enabled to capture material on a scale sufficient for planetary disk formation. It has also to be remembered that the accretion process in general involves a braking action on the star which, for large clouds, can substantially reduce the relative velocity, and the effect of this would certainly be to increase considerably the foregoing estimates of probability of suitable encounters.

5. *Angular momentum brought to the Sun.*—To estimate what proportion of the material would actually enter the Sun is difficult because of the complexities of the accretion process when disturbed by the slight rotation of the cloud. Since $R\omega \ll V$, it is reasonable to suppose as we have done that the motion is representable as a small deviation from symmetrical accretion. It is simple enough to find what proportion of the material has initially less angular momentum than would be needed to keep it clear of the Sun if in free particle motion. This upper limit corresponds to parabolic motion just grazing the solar surface, for which

$$h\ (\text{per unit mass}) = (2G\odot R_\odot)^{1/2} = 4{\cdot}3 \times 10^{18}\ \text{c.g.s. units.} \qquad (12)$$

Supposing ω to be more or less perpendicular to V, material having less angular momentum than this will be contained initially within a hemisphere of radius p centred at the Sun, where $p^2\omega$ is equal to the above numerical value (12). The total angular momentum of this is readily found to be $4\pi p^5\rho\omega/15$, which for the adopted numerical values is about 10^{46} c.g.s. units.

When ω is parallel to V, the corresponding amount is $(p/R)^4H$, and this comes to about 2×10^{46} c.g.s. units.

These values may be compared with the present angular momentum of the Sun, which various estimates agree is of the order of 2×10^{48} c.g.s. units. Accordingly in either case, if the Sun simply absorbed such material as had initially less than this parabolic angular momentum, the rotation thereby imparted to it would be far smaller than the present value.

The weakness of this comparison, especially in the case when ω is perpendicular to V, is that its basis fails to take account of how the process of absorption by the Sun might occur, and to remedy this would involve much fuller analysis of the modified accretion process than it seems possible to make. In the present instance, as we have assumed, the material would probably first converge to the axial line almost unaffected by the slight rotation of the cloud and form an inward flowing stream there. This stream must obviously have some finite width, in view of heating of the hydrogen gas, but just how wide it is not possible to say, and it would also possess the original angular momentum of the material about the Sun. In flowing towards the Sun it would be deviated from direct infall by its angular momentum, but it is not clear whether at first approach it would all pass to one side of the centre of the Sun, in which event the calculation (for the case of ω perpendicular to V) would perhaps be valid, or whether a secondary stage would occur in which the stream flowed past the Sun on all sides and converged symmetrically again on the far side of the Sun (as would certainly happen in the case ω parallel to V). Since the material all has elliptic speed because of the first stage of the accretion process, the radial extent of the second convergence to a line (more or less) will be substantially smaller than before, and the persisting almost unaltered angular momentum will lead to a greater degree of asymmetry. It would seem that the flow will oscillate from one side of the Sun to the other, but with diminishing range and ever increasing asymmetry owing to the angular momentum, until eventually the stream passes all to one side of the Sun, the material thereby going into orbit around it. Collisions within this material are regarded as capable of gradually bringing it to the required flattened disk form. The dust would presumably go into an extremely flat disk, but the hydrogen gas heated by the Sun would extend out above and below the plane of the disk.

A second possible way of estimating the angular momentum brought to the Sun might be to consider the material as first going to form a disk of uniform density per unit area and extending beyond the present orbit of Saturn, say to 2500 solar radii, as an underestimate in view of Uranus and Neptune, and assuming that the Sun absorbs the inner part within rather less than the present radius of the orbit of Mercury, say out to 50 solar radii. Since the angular momentum per radial step dr is proportional to $r^{3/2}\,dr$, the total out to r will vary as $r^{5/2}$, and so the amount absorbed by the Sun would be $(50/2500)^{5/2}$ of the whole, and with the value of this given by (3) this is about 5×10^{46} c.g.s. units.

The author is unable to see any reliable way of estimating the angular momentum brought to the Sun, but even though the bases of the foregoing estimates are open to question, it is of some interest that they suggest that only a negligible amount is communicated.

The corresponding mass added to the Sun will be $\frac{2}{3}\pi p^3\rho$ for the case when ω is perpendicular to V, which comes to about $3 \times 10^{-6}\odot$; while for ω parallel to V it is $(p/R)^2 M$, which is about $2 \times 10^{-5}\odot$. Containing as the material would, only a small proportion of heavy elements, neither of these additions of mass would be inconsistent with present knowledge of the composition of the Sun. For the disk method of estimating the angular momentum, the mass involved would be simply $(50/2500)^2$ of the whole, which gives as little as about $10^{-6}\odot$ for the mass added.

On the present hypothesis, the closeness of the Sun's rotation axis to the normal to the general plane of planetary motion (they differ by about 7°) would

appear at first sight to be pure coincidence. But it has to be remembered that the Sun may well have acquired further mass from outside since the time the planets were formed, and if this material were given systematic angular momentum as a result of planetary action the Sun's rotation axis may possibly have been brought to its present position from some entirely different direction. The present solar angular momentum could be produced by a mass of order 10^{30} g., as (12) shows. Also, the short period comets, which are almost all direct, suggest that the effect of Jupiter may be more likely to deflect material into direct motion than retrograde, and it is even possible that the absorption into the Sun of cometary material over a period of 5×10^9 years could have supplied the present solar angular momentum by a transfer from that originally possessed by planets.

6. *The accretion mechanism.*—At a speed of 2×10^4 cm sec^{-1}, the distance of the neutral point of the steady-state accretion stream from the Sun is about 4×10^{17} cm and in order of magnitude this is also the extent of the converging parts of the captured cloud. In the initial stages when the Sun first enters the cloud, the probability of collision for a particle in its path through other particles converging with it has been shown to be

$$24\rho GM_\odot/\sigma r V^2 \qquad (13)$$

where σ is the density and r the radius of the particles, supposed spherical†. If the particles are of very weak structure, perhaps of the character of snowflakes, σ may be much less than unity. If we take $\sigma = 0{\cdot}3$, and write $V = 10^5 v$ cm sec^{-1} then (13) reduces to

$$10^{18}\rho/rv^2. \qquad (14)$$

Supposing the dust to be about 1 per cent by mass of the cloud, then for $r = 10^{-4}$ cm, $\rho = 10^{-25}$ g cm^{-3}, and $v = 0{\cdot}2$ km sec^{-1}, this *initial* probability for collision solely of dust particles is as high as 0·025. Thus the collision process in the neighbourhood of the axial line is extremely effective, for when collisions occur they will tend to leave material near the axial line and thereby rapidly increase the probability of collision for later arriving particles. The presence also of hydrogen gas must increase the general tendency for material to be accumulated at and near the axial line, and there therefore seems good reason to accept the efficacy of the accretion process.

If interstellar dust particles have condensed from cool gases to form perhaps no more than mere smoke in space, they would be expected to have very weak structure; indeed, much of the material might even be "sticky", so that pretty well inelastic collisions would occur. This would not necessarily mean a complete loss of relative kinetic energy, because glancing collisions would be frequent. The stream would develop breadth as a result of small internal motions within the cloud over and above the systematic motion of streaming, and also from the general heating of the hydrogen gas as it became compressed towards the axial line before the presence of the dust could act to enable it to cool.

The total angular momentum of the captured material will define an invariable plane for the planet-forming material, and the general plane of the resulting disk will coincide with this. The disk form, with dust particles moving as nearly as possible in circular orbits (perturbations will not allow accurately circular orbits) is that in which collisions are reduced to a minimum, and this form will gradually

† Lyttleton, R. A., *The Comets and Their Origin*, pp 87, 88. Cambridge University Press, 1953.

come about through collisions in the manner hitherto described in presentation of disk theories*.

7. *Other considerations.*—Although the small masses of the inner planets may well be explicable on the disk hypothesis, it remains possible that the whole of the terrestrial group could have originated in a rotational break-up of a large primitive planet of which perhaps Jupiter survives as the larger component. (The similarity of the Moon to the four Galilean satellites suggests this.) The combined mass of the inner group is less than 1 per cent that of Jupiter, and so would represent an almost negligible set of intermediate droplets released in the break-up and escaping from both main pieces. The fact that the resulting initial orbits for them would pass near that of Jupiter seems no serious objection to the idea. The break-up could readily result in their having much the same orbital angular momentum as at present, and there would be at least the remains of the disk material within the orbit of Jupiter, especially uncollected hydrogen gas, to effect the rounding-up of their orbits. But also in some 5×10^9 years, other dissipative effects and even possibly purely dynamical action might suffice to round up the orbits.

There is also something to be said for the possibility of intersecting orbits at some stage of the solar system in connection with the formation of asteroids and meteorites. The break-up, presumably by direct collisions, to give these must be delayed till after the formation of planets from the disk had virtually been completed and till some massive iron- and rock-containing body or bodies had been formed. It is hard to see how the necessary collisions could ever come to occur if planets develop solely within a disk and from the outset have almost circular orbits that keep clear of each other. Although purely dynamical forces might allow eccentricities to grow to such values as to permit collisions, when regard is had to ever-present dissipative action it seems doubtful if almost circular orbits could ever become anything else. But it must be emphasized that this is pure speculation: we simply do not know how planetary orbits might change over periods of time comparable with the age of the planets.

In his "magnetic-coupling" theory, Hoyle is concerned to reduce the rotation of a primitive Sun undergoing Helmholtz contraction as the final stage of its formation by condensation within a cloud. This rotation according to the theory would be extremely rapid because of the intrinsic angular momentum supposed to be present in the material of the cloud from which the stars formed, and to effect the reduction a strong internal magnetic field for the Sun is further postulated. However, neither the original rapid rotation nor the internal field is actually established, and from this point of view the theory rests on assumptions having no observational basis but only indirect support, if theoretical interpretations, such as those relating to formation of stars, are accepted. That stars have condensed from a state of far greater extension, with the star having achieved its individuality from the moment of fragmentation of a cloud, is open to serious doubt in view of the existence of numerous close double-stars, for if these are thought of as expanded up again there simply would not be room for the components. This means that formation by contraction would have to be supplemented by some subsequent process reducing the separation, and the only mechanism capable of this without increasing the angular momentum per unit mass is large-scale accretion. But if this can substantially change the masses

* F. Hoyle, *M.N.*, **106**, 406, 1946.

of stars, there can be no reason to suppose that the whole mass of a star such as the Sun has been primitive to it.

The observational evidence is that all stars similar to the Sun rotate slowly, and it only leads to difficulty to suppose that they all must originally have rotated rapidly and been subsequently slowed. Once this is appreciated—and no mathematical working out of the process of formation of multiple stars as described by Hoyle has been given—the need to postulate a strong magnetic field for the Sun becomes equally doubtful quite apart from whether such a field would in fact operate in the way claimed at all.

On the other hand, a disk of dust and hydrogen gas, supplied by accretion to a Sun already in much its present state would seem adequately to fulfil the requirements later involved in Hoyle's theory. Moreover, there seems no need for any elaborate explanation for the removal of hydrogen from the inner parts of the disk (less than 3 a.u., say) in order that small planets should form from the dust only. For if now the Earth cannot retain hydrogen, there seems no reason to suppose that when its mass was less it could accumulate it from a cloud with temperature maintained by the Sun radiating much as at present. Thus small inner planets formed almost entirely from the dust component, and so having mass possibly of order 1 per cent of the great planets, might well result, as Hoyle suggests. Further out, where the hydrogen temperature would be lower, more massive planets, forming first from dust, could gather in hydrogen provided they were at sufficiently moderate distances at which hydrogen would still be retained by the Sun's attraction. This region corresponds to the positions of Jupiter and Saturn, and the argument suggests that these planets may have small metallic and rocky cores amounting perhaps to some few per cent of their entire masses.

Hoyle is further concerned with the details of composition of the Earth as evidenced by such knowledge as derives from the extreme outer layers. But the lunar surface, as directly observed, strongly suggests that much of the outer material, if not a great deal more, has been added by meteoritic impact. It would therefore seem dangerous to insist on a need to explain such details in terms of an Earth formed once for all and thereafter not added to from without. Mass for mass, asteroids and meteorites have far greater surface area than planets, and solar radiation of particles would be far more effective on them, mass for mass, than on the surface of the Earth.

St John's College,
Cambridge:
1961 *January.*

RADIAL PULSATIONS OF THE POLYTROPE $n=2$

C. Prasad and H. S. Gurm

(Received 1961 February 1)

Summary

The adiabatic radial oscillations of the polytrope, $n=2$, have been considered. The characteristic frequencies and the relative amplitudes, for the first four modes for three different values of the ratio of specific heats, have been obtained.

---

1. *Introduction.*—The pulsational properties of a star depend mainly on the density distribution in the star and the ratio of specific heats of the material of the star. Most of the stellar models can be roughly approximated in these respects to polytropic models by a suitable choice of the polytropic index n. It is, therefore, of interest to obtain the pulsational properties of the polytropic models for various values of n. The radial pulsations of the standard model have been considered by Eddington (1918) and Schwarzschild (1941), while those of polytropes, $n=1{\cdot}5$ and $n=1$, have been considered by Lucas (1956) and Chatterji (1951). Miller (1929) has considered the pulsations of the polytropes, $n=2$ and $n=4$, for the ratio of specific heats $\gamma=10/7$ ($\alpha=0{\cdot}2$). The low value of γ was taken in the belief, prevalent at that time that most of the thermal energy consisted of radiant energy.

The present paper considers the radial pulsations of the polytropic model of index 2. The characteristic frequencies and the relative amplitudes of the first four modes of oscillation are obtained for three different values of the ratio of specific heats of the material of the star (viz. $\alpha=0{\cdot}6$, $0{\cdot}5$ and $0{\cdot}4$)*. Care has been taken to ensure a five-figure accuracy. A feature of interest for the polytrope $n=2$ is that the periods for the fundamental mode and the first harmonic for $\alpha=0{\cdot}5$ are very nearly commensurable. This commensurability will have considerable effect on the anharmonic pulsations which are under consideration.

2. *Solution of the equation of pulsation.*—Using Emden variables ξ and θ, the equation of pulsation (Eddington 1918) for the polytrope, $n=2$, may be written as

$$\frac{d^2\eta}{d\xi^2}+\frac{1}{\xi}\left(4+\frac{3\xi}{\theta}\frac{d\theta}{d\xi}\right)\frac{d\eta}{d\xi}+\left(\frac{\omega^2}{\theta}+\frac{3\alpha}{\xi\theta}\frac{d\theta}{d\xi}\right)\eta=0, \tag{1}$$

where

$$\omega^2=\frac{\sigma^2R^2\rho_c}{\gamma\xi_R{}^2P_c}=\frac{3\sigma^2}{4\pi G\gamma\rho_c}. \tag{2}$$

Here η is the relative amplitude of displacement; $\alpha=3-4/\gamma$, γ being the ratio of specific heats; $\sigma=2n\nu$, where ν is the frequency of oscillation; G is the constant of gravitation, R is the radius of star while ξ_R is the radius of the star in Emden variables. Also P_c and ρ_c denote the equilibrium values of the pressure and density at the centre of the star.

* The values for the first three modes for the case $\alpha=0{\cdot}6$ were given by the first author in his D.Phil. thesis (Oxford, 1950).

XUM

Table II

The value of the amplitudes

ξ \ α / mode	0·6				0·5		0·4	
	1st	2nd	3rd	4th	1st	2nd	1st	2nd
0·0	0·42124	−0·12275	0·07282	−0·05308	0·48524	−0·12858	0·55966	−0·13473
·2	·42190	·12270	·07259	·05272	·48586	·12849	·56023	·13459
·4	·42388	·12253	·07187	·05162	·48775	·12820	·56196	·13417
·6	·42722	·12221	·07061	·04972	·49094	·12767	·56487	·13341
·8	·43198	·12165	·06872	·04696	·49575	·12682	·56900	·13224
1·0	0·43823	−0·12075	0·06606	−0·04322	0·50138	−0·12553	0·57440	−0·13052
·2	·44608	·11934	·06246	·03839	·50881	·12362	·58116	·12807
·4	·45567	·11719	·05768	·03234	·51785	·12085	·58935	·12463
·6	·46715	·11398	·05145	·02499	·52864	·11688	·59910	·11987
·8	·48073	·10927	·04344	·01635	·54135	·11127	·61053	·11330
2·0	0·49664	−0·10244	0·03331	−0·00659	0·55617	−0·10339	0·62380	−0·10431
·2	·51515	·09268	·02076	+0·00383	·57332	·09240	·63908	·09204
·4	·53657	·07886	+0·00561	·01395	·59306	·07718	·65658	·07537
·6	·56128	·05946	−0·01194	·02220	·61569	·05622	·67650	·05280
·8	·58969	−0·03243	·03106	·02614	·64154	−0·02748	·69910	−0·02232
3·0	0·62227	+0·00499	−0·04960	0·02263	0·67097	+0·01175	0·72466	+0·01871
·1	·64029	·02871	·05740	·01702	·68716	·03637	·73864	·04422
·2	·65955	·05651	·06316	+0·00841	·70441	·06505	·75347	·07376
·3	·68014	·08905	·06571	−0·00326	·72276	·09841	·76919	·10793
·4	·70214	·12707	·06348	·01764	·74228	·13719	·78584	·14743
3·5	0·72562	0·17147	−0·05441	−0·03366	0·76304	0·18221	0·80347	0·19304
·6	·75068	·22325	·03579	·04910	·78510	·23444	·82212	·24569
·7	·77741	·28355	−0·00411	·06004	·80852	·29496	·84184	·30640
·8	·80590	·35371	+0·04520	·05990	·83338	·36503	·86267	·37634
·9	·83627	·43523	·11797	−0·03827	·85975	·44606	·88466	·45685
4·0	0·86860	0·52985	0·22169	+0·02086	0·88769	0·53968	0·90785	0·54944
·1	·90300	·63953	·36585	·14145	·91728	·64772	·93229	·65583
·2	·93959	·76652	·56247	·35873	·94861	·77226	·95803	·77793
·3	·97847	·91336	·82669	·72366	·98173	·91566	·98512	·91792
4·35287	1·00000	1·00000	1·00000	1·00000	1·00000	1·00000	1·00000	1·00000

The equation (1) has singularities both at the centre and the surface and non-singular solutions exist for certain values of ω^2. To find the values of ω^2 corresponding to various modes of oscillation we proceed as follows.

With a trial value of ω^2, series solutions were developed near the singularities (i.e. $\xi=0$ and $\xi=\xi_R$). These provided values of η correct to six figures from $\xi=0$ to $\xi=0{\cdot}8$, and from $\xi=4{\cdot}15$ to $\xi=4{\cdot}35$, respectively. For the intervening values the integrations were carried out numerically with the help of the quadrature formulae (cf. Prasad 1950) outwards and inwards respectively. (The method is essentially the same as that used by Schwarzschild (1941), except that the correction terms for finite differences up to sixth order were taken in the present paper, while he neglected them altogether.) The interval, h, was taken as $0{\cdot}1$ for the outward integration and $0{\cdot}05$ for the inward integration.

For the comparison of the outward and the inward solutions, the ratio $\eta(3{\cdot}1)/\eta(3{\cdot}0)$ was calculated for both the solutions. The difference between the two values was compared with the difference for integrations with a different value of ω^2. From these, a better approximation to ω^2 was inferred by interpolation. A new integration with this value of ω^2 combined with the previous integrations gave a better estimate for ω^2. Often the process had to be repeated once more. As a check, the ratios $\eta(3{\cdot}0)/\eta(2{\cdot}9)$ were also compared in addition to $\eta(3{\cdot}1)/\eta(3{\cdot}0)$. In all, the integrations were carried out for about sixty values of ω^2. The values of ω^2 for the first four modes for three values of α ($0{\cdot}6$, $0{\cdot}5$, $0{\cdot}4$) are given in Table I. The error in ω^2 in the last place of decimals is expected to be less than a unit for the first mode and may be somewhat higher for other modes. The relative amplitudes, η's, for some of the modes are given in Table II. Complete tables have been deposited in the Society's library.

TABLE I

Values of ω^2

Mode / α	1st	2nd	3rd	4th
0·6	0·210 516	0·702 150	1·398 72	2·300 36
0·5	0·177 672	0·675 470	1·371 60	2·272 58
0·4	0·143 928	0·649 106	1·344 38	2·244 85

Department of Mathematics,
University of Roorkee,
Roorkee, India:
1961 *January.*

References

Chatterji, L. D., 1951, *Proc. Nat. Inst. Sci.* (India), **17**, 467.
Eddington, A S., 1918, *M.N.*, **79**, 2 (also *Internal Constitution of the Stars*, 1926, p. 186).
Lucas, D., 1956, *Bull. Soc. Roy. Sci. Liege*, **25**, 585.
Miller, J. C. P., 1929, *M.N.*, **90**, 59.
Prasad, C., 1950, D. Phil. thesis, Oxford, p. 16.
Schwarzchild, M., 1941, *Ap. J.*, **94**, 245.

PHOTOELECTRIC SPECTROPHOTOMETRY OF O-TYPE STARS

A. W. Rodgers

(Received 1961 February 2)

Summary

Observations are presented of 21 O stars in Cygnus and Cepheus made with a Cassegrain photoelectric scanner attached to the 60-inch and 100-inch telescopes on Mount Wilson. The wavelength interval observed is from 3400A to 6000A with a resolution of 20A. The observed fluxes are integrated over 100A bands. Reductions of the variously reddened O stars were separately made for Cygnus and Cepheus and show that the interstellar reddening curve is identical in these two regions. The observations further show that the differences between Cygnus and other galactic O stars in the $(U-B)$, $(B-V)$ plane are intrinsic in the Cygnus O stars in that they have an anomalously large Balmer discontinuity.

Introduction.—Photoelectric determinations of the form of the curve of interstellar absorption as a function of wave-length have been made by means of multi-colour wide band filter photometry, specifically the six-colour photometry and its extensions by Stebbins and Whitford (**1, 2**). In some instances it is desirable to have knowledge of the form of the space reddening law derived from narrow band photometry at points spaced less widely in wave-length than hitherto available, U, B, V photometry of galactic O stars by Johnson and Morgan (**3**) and Hiltner and Johnson (**4**) has shown that, with the exception of O stars in the region of Cygnus between galactic longitude 40°·0 and 48°·8 and latitude $-3°$ to $+5°$, there are only minor variations in the reddening path in the $U-B$, $B-V$ plane. This reddening line can be represented by the equation

$$U-B=-0{\cdot}91+0{\cdot}72(B-V)+0{\cdot}05(B-V)^2. \qquad (1)$$

The Cygnus Rift stars fall about a straight line in the two-colour diagram which has the equation

$$U-B=-0{\cdot}89+0{\cdot}83(B-V); \qquad (2)$$

Hiltner and Johnson (**4**) assumed for the purposes of their discussion that the cause of the difference between equations (1) and (2) was due to a difference in the reddening law in the Cygnus Rift from that found elsewhere. We note with Hiltner and Johnson that the two lines do not intersect in the region of intrinsic colour of the O stars but at around $B-V=-0{\cdot}1$ and $+1{\cdot}9$.

Greenberg (**5**) has pointed out that one of the criteria for deciding whether extinction by interstellar particles is due to a classical scattering process by large particles or by a quantum process in the smaller chemically unsaturated particles proposed by Platt (**6**), is whether there is a directional dependence of the form of the space reddening law. Thus Greenberg shows that for classical particles

XUM

TABLE I

O stars on scanner system,

λ in A	HD 191978	HD 193322	HD 216898	HD 192281	HD 229196	HD 190864	HD 193595	BD +40° 4227	BD +54° 2761	HD 210839
3450	8·44	8·47	9·12	9·09	9·57	8·45	9·29	10·11	8·87	8·30
3550	8·13	8·17	8·79	8·72	9·17	8·10	9·00	9·71	8·52	7·98
3650	7·97	8·00	8·56	8·49	8·91	7·84	8·74	9·48	8·33	7·79
3750	7·84	7·85	8·41	8·34	8·72	7·78	8·58	9·15	8·22	7·62
3850	7·69	7·70	8·21	8·19	8·47	7·62	8·37	8·89	8·06	7·50
3950	7·61	7·60	8·05	8·10	8·32	7·53	8·28	8·77	7·96	7·43
4050	7·56	7·55	7·95	8·02	8·17	7·49	8·21	8·54	7·88	7·36
4150	7·53	7·53	7·89	7·87	8·10	7·49	8·16	8·41	7·85	7·35
4250	7·56	7·53	7·87	7·95	8·05	7·47	8·15	8·31	7·83	7·36
4350	7·62	7·60	7·89	7·98	7·99	7·51	8·17	8·23	7·86	7·39
4450	7·63	7·60	7·84	7·99	7·95	7·53	8·18	8·17	7·87	7·41
4550	7·64	7·62	7·80	7·97	7·91	7·55	8·13	8·03	7·86	7·41
4650	...	...	...	...	...	...	...	...	...	...
4750	8·05	8·02	8·12	8·33	8·20	7·97	8·51	8·29	8·23	7·80
4850	8·09	8·10	8·19	8·37	8·18	8·01	8·57	8·23	8·27	7·84
4950	8·16	8·22	8·18	8·40	8·19	8·07	8·61	8·16	8·31	7·89
5050	8·13	8·25	8·21	8·46	8·20	8·13	8·66	8·13	8·37	7·98
5150	8·36	8·36	8·31	8·55	8·23	8·24	8·77	8·11	8·46	8·05
5250	8·55	8·55	8·43	8·74	8·37	8·45	8·95	8·21	8·63	8·26
5350	8·77	8·79	8·65	8·93	8·51	8·70	9·21	8·34	8·84	8·50
5450	9·06	9·06	8·90	9·22	8·74	8·97	9·45	8·52	9·09	8·78
5550	9·30	9·32	9·13	9·43	8·89	9·21	9·66	8·66	9·29	9·01
5650	9·55	9·57	9·39	9·67	9·09	9·47	9·85	8·84	9·49	9·26
5750	9·86	9·86	9·68	9·92	9·30	9·77	9·11	9·07	9·79	9·58
5850	10·38	10·35	10·09	10·37	9·72	10·33	9·55	9·49	10·32	10·09
5950	11·08	11·09	10·83	11·14	10·33	11·18	11·21	10·30	10·86	10·90

we would expect more ultra-violet extinction, for a given $E_{(B-V)}$, for light which traverses a cloud parallel to the galactic magnetic field than for that which passes perpendicularly across it. Such an effect could be masked by non-perfect alignment of the particles with respect to the field and by dispersion of the field vectors about the direction we take to be the axis of the spiral arm. However, 21 cm polarization and stellar distribution studies show that in the direction of the Cygnus Rift we are looking tangentially along a spiral arm. Thus if classical scattering is the mechanism by which interstellar extinction operates then we could expect an effect similar to the one observed in the $U-B$, $B-V$ plane by Hiltner and Johnson (4).

It was in order to test whether the reddening law *is* different in Cygnus to that elsewhere that the observations described below were carried out.

Observations and reductions.—With a photoelectric spectrum scanner attached to the Cassegrain foci of the 60-inch and 100-inch reflectors on Mount Wilson, 21 O stars in Cygnus and Cepheus ranging in type from O5 to O9·5 were observed.

arbitrary zeros, outside atmosphere.

HD 228854	HD 191423	HD 235673	BD +62° 2078	HD 214680	HD 216532	HD 228779	BD +53° 2843	BD +66° 1661	HD 24912	HD 194334
9·23	8·67	8·35	9·72	8·31	8·61	10·03	8·21	9·45	8·39	9·48
8·77	8·40	8·04	9·40	8·06	8·30	9·66	7·96	9·14	8·12	8·90
8·47	8·26	7·75	9·16	7·92	8·08	9·27	7·76	8·89	7·98	8·63
8·26	8·09	7·68	8·90	7·83	7·90	9·02	7·63	8·77	7·87	8·51
8·09	7·95	7·58	8·62	7·71	7·70	8·85	7·48	8·49	7·76	8·23
7·96	7·85	7·47	8·52	7·66	7·56	8·64	7·39	8·35	7·67	8·09
7·83	7·79	7·42	8·34	7·64	7·43	8·48	7·31	8·19	7·64	7·97
7·76	7·77	7·40	8·25	7·67	7·37	8·32	7·29	8·13	7·63	7·83
7·69	7·77	7·40	8·16	7·69	7·33	8·22	7·28	8·08	7·66	7·79
7·72	7·81	7·45	8·10	7·79	7·37	8·12	7·31	8·07	7·72	7·74
7·69	7·84	7·45	8·07	7·81	7·36	8·08	7·33	8·06	7·74	7·68
7·62	7·85	7·47	7·95	7·85	7·31	7·97	7·31	7·97	7·77	7·62
...	...	...	...	...	...	...	...	...	...	...
7·97	8·26	7·85	8·19	8·34	7·66	8·16	7·73	8·22	8·10	7·95
7·96	8·30	7·91	8·17	8·42	7·70	8·12	7·77	8·19	8·29	7·97
7·97	8·36	7·94	8·14	8·51	7·70	8·06	7·79	8·31	8·35	7·94
7·99	8·43	8·00	8·11	8·60	7·73	8·02	7·89	8·20	8·46	7·93
8·06	8·54	8·12	8·12	8·74	7·78	8·01	7·99	8·37	8·58	7·98
8·23	8·75	8·31	8·23	8·95	7·94	8·09	8·16	8·37	8·78	8·10
8·42	8·96	8·55	8·40	9·23	8·14	8·26	8·41	8·54	9·03	8·29
8·57	9·21	8·78	8·56	9·55	8·35	8·40	8·63	8·81	9·29	8·49
8·78	9·45	9·05	8·71	9·82	8·61	8·56	8·87	8·97	9·54	8·73
9·00	9·70	9·33	8·88	10·10	8·81	8·83	9·12	9·22	9·81	8·90
9·32	10·00	9·61	9·13	10·40	9·08	9·08	9·40	9·43	10·14	9·18
9·81	10·49	10·22	9·54	10·89	9·60	9·45	9·96	9·81	10·62	9·71
10·71	11·17	11·05	10·22	11·70	10·37	10·01	10·62	10·35	11·43	9·92

The scanner is identical with that described by Oke (**7**). The wave-length range covered is from 3400 A to 6000 A with a resolution of 20 A. Each star was scanned from red to blue and back to red; this process took 30 minutes and was regarded as a single observation. All stars were observed at least twice, some four times. Atmospheric extinction corrections were taken from a mean curve of extinction as a function of wave-length derived from a series of observations of α Lyrae extending over the period (3 months) of the observations described here. Several curves for individual nights were compared with this mean with excellent agreement. In no instance were observations of programme stars made through an atmosphere exceeding 1·25 air masses. While O stars are in general regarded as having an easily defined continuum, in this class of photometry, scans of even the brightest stars showed appreciable photon statistical noise particularly at wave-lengths greater than 5400 A and less than 3700 A where the response of the 1P21 photomultiplier is relatively low. For this reason the scans were reduced by integrating graphically under the tracing in bands 100 A

wide. Using a planimeter it was found possible to repeat this measurement to within 0·5 per cent. A measure of the internal accuracy of the photometry was made by comparing several stars, observed repeatedly on the two telescopes with a different photomultiplier, on different nights at different hour angles and related through observations of α Lyrae. The mean moduli of the residuals were

λ	3400–3700	3700–5400	5400–6000
$\overline{\lvert r \rvert}$	$0^{m}\cdot031$	$0^{m}\cdot012$	$0^{m}\cdot027$

The magnitudes were then reduced to a common instrumental system, again through the observations of α Lyrae, each star having an arbitrary zero point. These data are given in Table I.

It is worthwhile to compare the monochromatic colours with the *UBV* measures of Johnson and Hiltner and this has been done in Figs. 1 and 2 where the colour $m_{3600}-m_{4250}$ ($m_{3600}=m_{3550}+m_{3650}/2$) is plotted against $U-B$ and $m_{4250}-m_{5550}$ is plotted against $B-V$ respectively. Neither plot shows any systematic variation depending on whether Cygnus or Cepheus stars are considered suggesting that both the *UBV* and this photometry is homogeneous.

The reddening law was obtained by subtracting the continuum of a moderately reddened star from that of a highly reddened star of the same spectral type. The absorption curve as a function of wave-length was then normalized to a standard optical depth of 0·50 magnitudes between λλ4250 A and 5550 A, i.e. closely corresponding to an $E_{(B-V)}$ of the same amount. Separate mean values for the absorption curve, taken over the spectral types observed, were then formed for each region. The two interstellar absorption curves are shown plotted in Fig. 3, together with a portion of the curve derived from Stebbins and Whitford's (**1**) photometry.

Results.—Two main points are apparent in Fig. 3; first the close similarity of both Cygnus and Cepheus curves to that derived from the wide band photometry and secondly that, although there is a difference small enough to be accountable in terms of observational errors, between the Cygnus and Cepheus curves, it is in the *opposite* direction to that expected from the interpretation placed on the $(U-B)$, $(B-V)$ results by Johnson and Hiltner (**4**). Their view would suggest that the ultra-violet absorption in Cygnus is greater for a given $E_{(B-V)}$ than elsewhere. Fig. 3 shows that there is little or no difference between the absorption law in Cygnus and elsewhere and if anything it is less in the ultra-violet.

Returning to a consideration of the distribution of O stars in the $(U-B)$, $(B-V)$ plane, we note that the Cygnus stars fall about a straight line represented by equation (2). Now the curvature of the reddening line for normal galactic O stars as given by equation (1) had been predicted by Blanco (**8**) and explained as due to a shift of effective wave-length in the star–filter response curves of the *U*, *B*, *V* photometry as reddening increases. Thus we might ask why it is that the Cygnus stars are reddened, albeit by a different reddening law, along the linear path of equation (2). It can be shown easily that the curvature introduced into the reddening path by the absorption law as adopted by Blanco is for our purpose unchanged if we assume an absorption law, stronger in the ultra-violet, needed to explain the gross differences in the $U-B$, $B-V$ plane of equations (1) and (2).

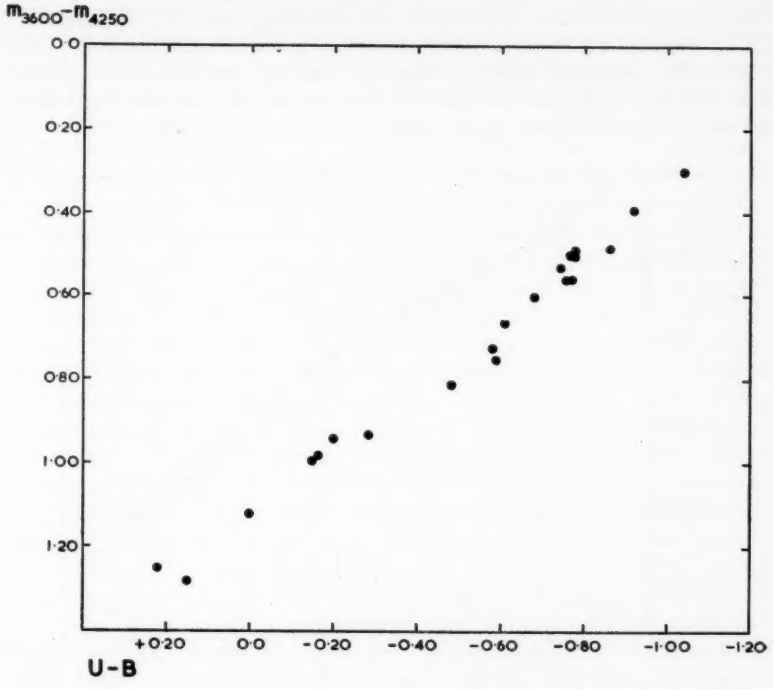

FIG. 1.—*The colour $m_{3600}-m_{4250}$ on the scanner instrumental system is plotted against U–B.*

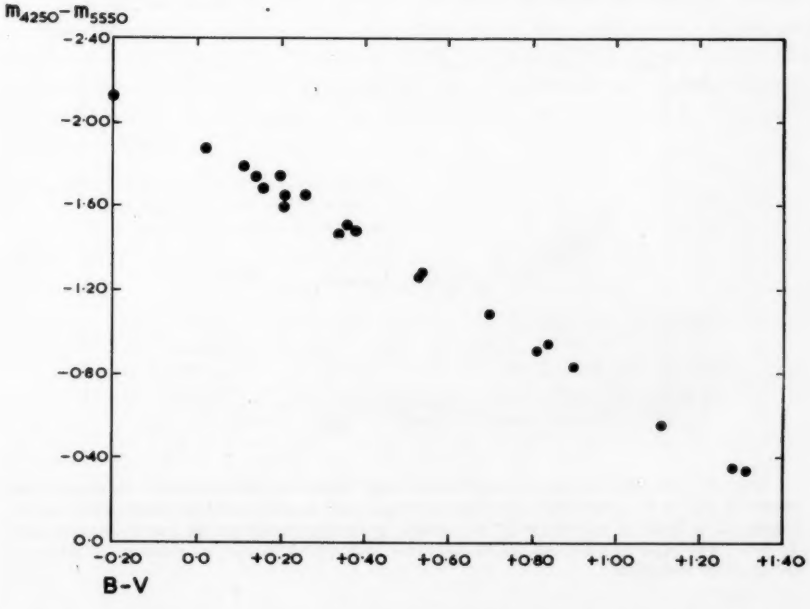

FIG. 2.—*The colour $m_{4250}-m_{5550}$ on the scanner instrumental system is plotted against B–V.*

Fig. 3, however, shows that the absorption law in Cygnus is nearly identical to that found elsewhere. Therefore the reddening line for the Cygnus stars has the same initial slope and curvature as that given in equation (1). Thus we are led to the conclusion that equation (2) does not represent a true reddening line for the Cygnus O stars but that it is the locus of the end points of reddening paths which are parallel to the reddening path of equation (1).

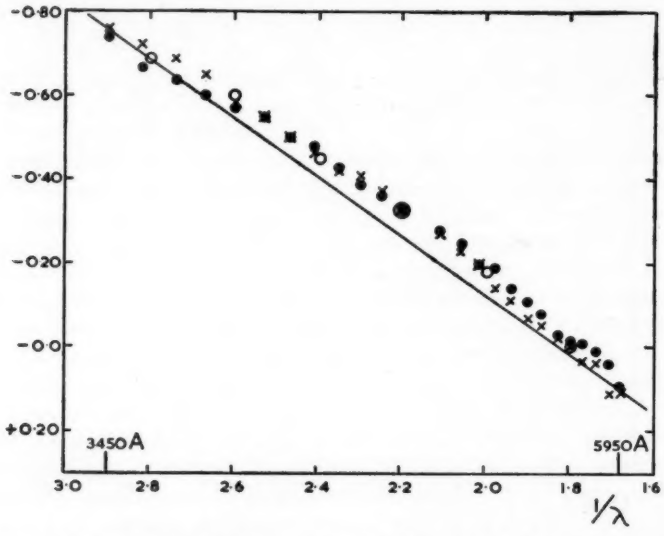

FIG. 3.—*The interstellar reddening curve plotted against* $1/\lambda$. *The curves for Cygnus and Cepheus are shown by filled circles and crosses respectively; the Whitford curve is shown by open circles. The curves are normalized so that* A^m *is* $+0^m{\cdot}50$ *between* λλ 4250A *and* 5550A.

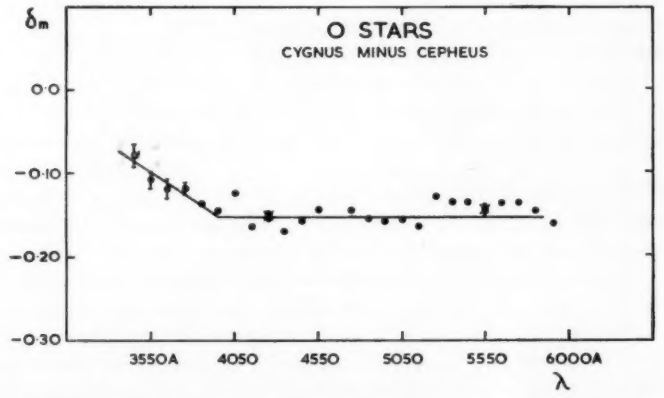

FIG. 4.—*The difference* δ_m, *between Cygnus and Cepheus O stars after both are corrected by means of Fig.* 3 *to a given apparent colour of* m_{4250}-m_{5550} *equal to* $-1^m{\cdot}43$ *plotted against wavelength. The limits of probable error are shown for the ultra-violet points and at* λλ4250A *and* 5550A. *The difference between* δ_m *at* λλ4250A *and* 5550A *is due to rounding-off errors of* $0^m{\cdot}01$ *in the reduction.*

This conclusion has two immediate implications one of which can be tested by further consideration of the scanner observations. From Fig. 3 the mean reddening curve was formed from the Cepheus and Cygnus curves. The continua of all stars were then corrected using this reddening law to an apparent $m_{4250} - m_{5550}$ colour of $-1^{m}\cdot43$, i.e. $B-V=+0^{m}\cdot40$. Differences were taken between the O5 stars in Cygnus and those in Cepheus and similarly for each spectral type through to O9. The mean curve of the differences taken over the five spectral types was then formed and plotted as a function of wave-length in Fig. 4. We are comparing in Fig. 4 two groups of stars which have been artificially made to suffer the same amount of interstellar reddening. If the Cygnus stars are intrinsically similar to those in Cepheus we would expect the differences in Fig. 4 to show no dependence on wave-length. From 6000 A down to 3900 A this is so, but in the region of the Balmer limit we find that the Cygnus stars are systematically fainter. The second implication of the linearity of equation (2) is that the Cygnus stars having the largest ultra-violet anomaly are those with $B-V$ colours around $+0^{m}\cdot60$. The ultra-violet deficiency shown in Fig. 4 is then only an average found over the range of colour excesses observed.

Conclusion.—The observations presented here demonstrate the close similarity of the space reddening law in Cygnus to that in Cepheus and to the mean law derived from the six-colour observations over a wide range of northern galactic longitude. Such a result has been also found by Mme Divan (**9**) in her spectrophotometric programmes. Theoretical studies of interstellar absorption based on the alignment of classically scattering particles in magnetic fields by Wilson (**10**) and Greenberg (**5**) suggest that there should be a directional dependence of the interstellar reddening curve. This is not confirmed by the present or previous spectrophotometric observations. The ultra-violet anomaly shown by the O stars of the Cygnus Rift is found to be intrinsic in these stars and not related to the properties of the interstellar medium.

Acknowledgments.—This work was done while the author was a Research Fellow of the Carnegie Institution of Washington and he is deeply indebted to the Director of the Mount Wilson and Palomar Observatories for making telescope time and research facilities available. I am very grateful to Dr J. B. Oke for his guidance in the use of the scanner.

Mount Wilson and Palomar Observatories,
Carnegie Institution of Washington,
California Institute of Technology:
1961 *February* 1.

References

(1) Stebbins, J., and Whitford, A. E., *Ap. J.*, **102**, 318, 1945.
(2) Whitford, A. E., *Ap. J.*, **107**, 102, 1948.
(3) Johnson, H. L., and Morgan, W. W., *Ap. J.*, **122**, 142, 1955.
(4) Hiltner, W. A., and Johnson, H. L., *Ap. J.*, **124**, 366, 1956.
(5) Greenberg, J. M., *Lowell Obs. Bulletins*, **4**, 105, 285, 1960.
(6) Platt, J. R., *Lowell Obs. Bulletins*, **4**, 105, 278, 1960.
(7) Oke, J. B., *Ap. J.*, **131**, 358, 1960.
(8) Blanco, V. M., *Ap. J.*, **123**, 64, 1955.
(9) Divan, L., *Ann. d'Astrophysique*, **17**, 456, 1954.
(10) Wilson, R., *M.N.*, **120**, 51, 1960.

ON THE FIGURE OF THE MOON

Harold Jeffreys

(Received 1961 February 6)

Summary

A rediscussion of the librations of the Moon's axis is carried out literally to orders e^2 and i^2 of the main terms, and a solar effect not evaluated by Hayn is taken into account. It appears that solar effects nearly cancel the corrections for e^2 and i^2. The observational data are rediscussed and it appears that

$$\beta = 0{\cdot}000\,627\,9 \pm 0{\cdot}000\,001\,5$$

if the discrepancies between the observational determinations can legitimately be treated as random, but if this is not true the uncertainty may well be multiplied by 4.

Recent discussions of the annual libration in longitude appear to give values of γ near to those given by the Yakovkin term. A method is proposed for dealing with the difficulty stated by Banachiewicz.

The data on the secular motions of the Moon's node and perigee show no serious discrepancy with the results on its figure.

1. On comparing various determinations of the constant β in the figure of the Moon from the inclination of the axis to the ecliptic I found that they were not wholly consistent, and that they showed a significant difference from the elementary formula obtained by neglect of all second-order terms, namely (e.g. Jeffreys 1955, p. 92):

$$P = \frac{3\beta \sin i}{(1+\kappa)(2\mu+\mu^2-3\beta)} \qquad (1)$$

where $\kappa = M/E$, $\mu = g/n$. The reference just given omits the term in μ^2. The standard solution for more accurate work is that of Hayn (1902, 1923) and the discrepancy was about 1 part in 100. Obvious corrections needed to the elementary formula are as follows. (*a*) Squares of the eccentricity and inclination need to be taken into account. (*b*) On account of solar perturbations the Moon's mean distance is 0·9991 of that calculated from

$$n^2a^3 = f(E+M) \qquad (2)$$

(Brown, 1899, p. 89). (*c*) The direct effect of the Sun is small but not quite negligible when calculations are taken to four figures, as is done by Hayn.

Hayn's elaborate theory, based on Euler's equations, is almost wholly numerical, and it is not easy to see where the difference comes from. But I could not find in his work any reference to the effect (*b*). In his 1902 paper he discussed (*c*) but decided that it is negligible. He evaluated it in his 1923 article. Jönsson (1917) uses a different method based on transformation theory but also appears to neglect (*b*).

A discussion more elaborate than that leading to (1) but less elaborate than those of Hayn and Jönsson seems desirable, so as to show the origin of the principal corrections, which is better displayed in a literal development. In addition, Hayn found a term of argument $2(\tilde{\omega} - \Omega)$ in the libration in longitude, and this term now seems to be of great importance (Jeffreys 1957). Jönsson

XUM

found the term with the opposite sign. Koziel (1949), working to higher accuracy, confirmed Hayn's sign. The calculation of this term requires long multiplications of series.

2. The method of my 1955 paper will be used, with a slight modification. The axes OX, OY, OZ are taken so that OZ is normal to the ecliptic, to the north, and OX, OY rotate uniformly about it with angular velocity ω equal to the Moon's mean motion, OX pointing nearly to the Earth. As the axes are right-handed OY is nearly opposite to the direction of motion. The displacements of the principal axes OA, OB, OC from OX, OY, OZ are small.

We take the matrix of direction cosines in the previous form

$$\begin{array}{c} \\ A \\ B \\ C \end{array}\!\!\begin{array}{c} \begin{array}{ccc} X & Y & Z \end{array} \\ \left[\begin{array}{ccc} 1-\frac{1}{2}\chi^2-\frac{1}{2}\xi^2 & \chi-\frac{1}{2}\chi\xi^2 & -\xi \\ -\chi+\xi\eta+\frac{1}{2}\eta^2\chi & 1-\frac{1}{2}\chi^2-\frac{1}{2}\eta^2+\chi\xi\eta & \eta-\frac{1}{2}\xi^2\eta \\ \xi+\chi\eta-\frac{1}{2}\xi(\chi^2+\eta^2) & -\eta+\chi\xi+\frac{1}{2}\eta\chi^2 & 1-\frac{1}{2}\xi^2-\frac{1}{2}\eta^2 \end{array}\right] \end{array}. \qquad (1)$$

Other forms were tried, including the simple one that makes the elements of the antisymmetrical part of the matrix $\pm\xi$, $\pm\eta$, $\pm\chi$, but all made either the kinetic energy or the work function, or both, more complicated. The angular velocity components are

$$\left.\begin{aligned} \omega_1 &= \dot\eta-(\omega+\dot\chi)\xi \\ \omega_2 &= \dot\xi+(\omega+\dot\chi)\eta \\ \omega_3 &= \omega+\dot\chi+\tfrac{1}{2}\chi^2\dot\chi-\tfrac{1}{2}(\omega+\dot\chi)(\xi^2+\eta^2)-\eta\dot\xi \end{aligned}\right\}. \qquad (2)$$

To the third order in ξ, η, χ

$$\begin{aligned} 2T = {} & A\dot\eta^2+B\dot\xi^2+C\dot\chi^2-2\omega A\xi\dot\eta-2\omega(C-B)\dot\xi\eta \\ & -(\omega^2+2\omega\dot\chi)\{(C-A)\xi^2+(C-B)\eta^2\} \\ & -2A\xi\dot\eta\dot\chi-2(C-B)\eta\dot\xi\dot\chi+\text{constant}+\frac{d}{dt}f(\xi,\eta,\chi). \end{aligned} \qquad (3)$$

(1) implies particular definitions of ξ, η, χ, and it appears that other definitions introduce χ explicitly into (3), otherwise than through the total differential, which does not affect the equations of motion.

The Moon is taken to move in an orbit at constant inclination i to the ecliptic, revolving at uniform speed $-g$. The motion of the perigee is c. We take temporarily axes X', Y', Z' opposite to XYZ. If Ω is the distance from X' to the rising node and θ the distance of the Moon from the node, the direction cosines of the Moon with respect to X', Y', Z' are

$$\left.\begin{aligned} l &= \cos\Omega\cos\theta-\sin\Omega\sin\theta\cos i \\ m &= \sin\Omega\cos\theta+\cos\Omega\sin\theta\cos i \\ n &= -\sin i\sin\theta \end{aligned}\right\}. \qquad (4)$$

These are also the direction cosines of the Earth with respect to X, Y, Z.

Then, the zero of t being suitably chosen,

$$\Omega = -(\omega+g)t, \qquad \theta = (\omega+g)t+w \qquad (5)$$

where w is the equation of the centre; and

$$\left.\begin{aligned} l &= \cos w\cos^2\tfrac{1}{2}i+\cos\{2(\omega+g)t+w\}\sin^2\tfrac{1}{2}i \\ m &= \sin w\sin^2\tfrac{1}{2}i-\sin\{2(\omega+g)t+w\}\cos^2\tfrac{1}{2}i \\ n &= -\sin i\sin\{(\omega+g)t+w\} \end{aligned}\right\}. \qquad (6)$$

If l', m', n' are direction cosines with respect to OA, OB, OC the work function due to the Earth is

$$W = \frac{1}{2}\frac{fE}{r^3}\{A+B+C-3(Al'^2+Bm'^2+Cn'^2)\}$$
$$= \frac{1}{2}\frac{fE}{r^3}\{B+C-2A-3(B-A)m'^2-3(C-A)n'^2\}. \quad (7)$$

Thus to get the part of W depending on ξ, η, χ to the third order we only need m' and n' to the second, except in terms whose leading terms are 1:

$$\left.\begin{aligned} m' &= l(-\chi+\xi\eta)+m(1-\tfrac{1}{2}\chi^2-\tfrac{1}{2}\eta^2+\xi\eta\chi)+n\eta \\ n' &= l(\xi+\chi\eta)+m(-\eta+\xi\chi)+n(1-\tfrac{1}{2}\xi^2-\tfrac{1}{2}\eta^2) \end{aligned}\right\} \quad (8)$$

and

$$\begin{aligned} W = -\frac{3}{2}\frac{fE}{r^3}[&(B-A)\{(l^2-m^2)\chi^2-2lm\chi+lm\chi^3-mn\chi^2\eta\} \\ &+(C-A)\{(l^2-n^2)\xi^2+2ln\xi+2mn\chi\xi-ln\xi^3+2lm\chi\xi^2\} \\ &+(C-B)\{(m^2-n^2)\eta^2-2mn\eta-2lm\xi\eta+2ln\chi\eta \\ &+2(l^2-m^2)\chi\xi\eta+mn\eta\xi^2-2lm\chi\eta^2\} \\ &+(2B-C-A)ln\xi\eta^2]. \end{aligned} \quad (9)$$

For elliptic motion, to order e^2, if a is the major semiaxis,

$$\left.\begin{aligned} w &= 2e\sin(\omega-c)t+\frac{5}{4}e^2\sin 2(\omega-c)t, \\ \left(\frac{a}{r}\right)^3 &= 1+\frac{3}{2}e^2+3e\cos(\omega-c)t+\frac{9}{2}e^2\cos 2(\omega-c)t \end{aligned}\right\}. \quad (10)$$

We develop the required coefficients to orders e^2 and i^3 in the terms of speed $\omega+g$, and those of long period and of speed near ω to order $e\sin i$:

$$\left.\begin{aligned} l^2 &= 1-2e^2-\tfrac{1}{2}\sin^2 i+2e^2\cos 2(\omega-c)t+\tfrac{1}{2}\sin^2 i\cos 2(\omega+g)t \\ m^2 &= 2e^2\{1-\cos 2(\omega-c)t\} \\ n^2 &= \tfrac{1}{2}\sin^2 i\{1-\cos 2(\omega+g)t\}, \\ lm &= -\tfrac{1}{4}\sin^2 i\sin 2(\omega+g)t+2e\sin(\omega-c)t, \\ ln &= -\sin i\{(1-2e^2-\tfrac{3}{2}\sin^2\tfrac{1}{2}i)\sin(\omega+g)t+e\sin(2\omega+g-c)t \\ &\qquad -e\sin(g+c)t\} \\ mn &= -\sin i\{(2e^2-\tfrac{1}{2}\sin^2\tfrac{1}{2}i)\cos(\omega+g)t+e\cos(g+c)t \\ &\qquad -e\cos(2\omega+g-c)t\} \\ ln(a/r)^3 &= -\sin i\{(1-\tfrac{1}{2}e^2-\tfrac{3}{2}\sin^2\tfrac{1}{2}i)\sin(\omega+g)t+\tfrac{1}{2}e\sin(g+c)t \\ &\qquad -O(e^2)\sin(\omega-g-2c)t\} \\ mn(a/r)^3 &= -\sin i\{(2e^2-\tfrac{1}{2}\sin^2\tfrac{1}{2}i)\cos(\omega+g)t+e\sin i\cos(g+c)t \\ &\qquad -e\cos(2\omega+g-c)t+e^2\cos(\omega-2c-g)t\} \end{aligned}\right\}. \quad (11)$$

The equations for ξ, η, to the first order, are*

$$B\ddot{\xi}+\omega(A+B-C)\dot{\eta}+\omega^2(C-A)\xi = \frac{\partial W}{\partial\xi}$$
$$= -\frac{3\omega^2\lambda(C-A)}{1+\kappa}[(1-\tfrac{1}{2}e^2-\sin^2 i)\xi-\sin i(1-\tfrac{1}{2}e^2-\tfrac{3}{2}\sin^2\tfrac{1}{2}i)\sin(\omega+g)t], \quad (12)$$

* There is a mistake in sign in the corresponding equations in my 1955 paper.

$$A\ddot{\eta}-\omega(A+B-C)\dot{\xi}+\omega^2(C-B)\eta=\frac{\partial W}{\partial\eta}$$

$$=-\frac{3\omega^2\lambda}{1+\kappa}(C-B)[(2e^2-\tfrac{1}{2}\sin^2 i)\eta+\sin i(2e^2-\tfrac{1}{2}\sin^2\tfrac{1}{2}i)\cos(\omega+g)t]. \quad (13)$$

We have put

$$\frac{fE}{a^3}=\frac{\lambda\omega^2}{1+\kappa}. \quad (14)$$

Apart from solar effects λ would be 1, but this is not quite correct on account of effect (*b*) mentioned above, which makes

$$\lambda=1{\cdot}0027. \quad (15)$$

For the direct effect of the Sun on the librations a rough approximation will be adequate. We take the direction cosines of the Sun with regard to OX, OY, OZ to be

$$\cos(\omega-\omega')t, \quad -\sin(\omega-\omega')t, \quad -(a/a')\sin i\sin(\omega-\omega'+g)t. \quad (16)$$

Then for the Sun

$$m'=-\chi\cos(\omega-\omega')t-\sin(\omega-\omega')t, \quad (17)$$

$$n'=\xi\cos(\omega-\omega')t+\eta\sin(\omega-\omega')t-(a/a')\sin i\sin(\omega-\omega'+g)t, \quad (18)$$

$$W_S=-\tfrac{3}{2}\omega'^2[(B-A)\{\chi\cos(\omega-\omega')t+\sin(\omega-\omega')t\}^2$$
$$+(C-A)\{\xi\cos(\omega-\omega')t+\eta\sin(\omega-\omega')t$$
$$-(a/a')\sin i\sin(\omega-\omega'+g)t\}^2]. \quad (19)$$

The terms in $(\chi,\xi,\eta)\sin(\omega-\omega'+g)t$ are smaller than the corresponding terms due to the Earth in the ratio $(a/a')(\omega'/\omega)^2$, which is about 1/45 000. They are therefore totally negligible. The term in $\chi\sin 2(\omega-\omega')t$ does not combine with any other term to give one of speed $\omega+g$ or $2(g+c)$. Thus we need consider only the average values of the coefficients and take

$$W_S=-\tfrac{3}{4}\omega'^2\{(B-A)\chi^2+(C-A)(\xi^2+\eta^2)\}. \quad (20)$$

The contributions to $\partial W/\partial\xi$, $\partial W/\partial\eta$ agree with Hayn (1923).

We are concerned mainly with corrections of orders e^2 and i^2 to the variations of ξ, η with speed $\omega+g$, which lead to displacements of the Moon's axis in space with speed g.

The terms of speed $g+c$ give the Poisson terms directly, but we shall not examine these further.

For the term in χ with speed $2(g+c)$, the importance of which has been emphasized by Banachiewicz and Koziel, we note that $\partial W/\partial\chi$ contains a term in lm, which can combine with a term in $(a/r)^3$ to give one of this speed. But also $\partial W/\partial\chi$ contains terms in $ln\eta$, $mn\xi$, and $\xi\eta$. Now the principal terms of ξ and η have speed $\omega+g$, and n contains terms of speeds $\omega+g$, $\omega+g\pm c$, $\omega+g\pm 2c$, while l is near 1. Thus the important parts of these terms, if any, will have speeds near c, $2c$, and $2(\omega+g)$, and only the last can combine with the e^2 term in $(a/r)^3$ to give speed $2(g+c)$. The $\xi\eta$ term is already of speed $2(\omega+g)$ and the same applies.

However ξ, η contain also the Poisson terms, and $\xi\eta$ can combine with the constant term in $(a/r)^3$.

l^2, m^2, n^2 depart from 1, 0, 0 by quantities of orders e^2 and i^2. The periodic parts can be neglected in a first approximation, and in a second they introduce terms of different speeds from those already calculated. Thus their neglect can only give errors of orders e^4 and i^4. For similar reasons we can neglect χ in the equations for ξ and η and conversely. Hence we need:

l^2, m^2, n^2: constant terms only.

ln and mn: terms in $(g+c)t$ and $(2\omega+g-c)t$.

lm: term in $2(\omega+g)t$.

$mn\xi$, $ln\eta$, $\xi\eta$ (main terms in ξ, η): term in $2(\omega+g)t$.

(Poisson terms): term in $2(g+c)t$.

It may be expected that in the terms affecting χ that in lm will be the most important, for if the amplitudes of the main and Poisson terms in ξ are P and P_1 the amplitudes of the term in $\sin 2(g+c)t$ will be of orders

$$e^2 \sin^2 i, \qquad e^2 P \sin i, \qquad e^2 P^2, \qquad e^2 P_1^2.$$

These are roughly in the ratios 1, 1/3, 1/10, 1/100.

Since the observations have still, apparently, left the existence of this term in some doubt, it seems that at present, at any rate, we need consider only the main term, while recognizing that it may need a correction of order 30 per cent.

$(mn)(a/r)^3$ and $ln(a/r)^3$ contain terms of speed $g+c$, which give the greater part of the Poisson terms. They also contain terms of speed $\omega-g-2c$, which are near resonance and will give long-period terms in the motion of the axis in space. However, it is easy to see that they are negligible, since, unlike the main libration, they contain the factor e^2, and they depart from the critical speed, close to ω, by about 6 times as much as the principal term does. Hence their effects may be expected to have amplitudes of the order of 1/2000 of the main libration.

3. *Numerical data.*—Brown gives (1905 a, p. 109) (with some further figures)

$$\omega = 17''{\cdot}3256 \times 10^6/\text{year}, \quad \omega' = 1''{\cdot}2960 \times 10^6/\text{year}, \quad e = 0{\cdot}054\,90.$$

Then $\omega'/\omega = 0{\cdot}074\,80$.

Some care is needed in the definition of i. In Brown's specification the latitude L is defined by

$$\sin L = n.$$

Then we find to our order, from Section 2 (6),

$$L = (1-e^2)(\sin i + \tfrac{1}{8}\sin^3 i)\sin(\omega+g)t + \text{terms of other speeds.}$$

Putting

$$\gamma = \sin \tfrac{1}{2} i$$

we have for the coefficient

$$2\gamma(1-e^2)$$

with no term in γ^3. This agrees to this order with an equation on p. 108 of Brown's memoir. Thus his definition of γ is consistent with the present one of i. The numerical value of the coefficient in L is $18\,461''{\cdot}480$, and leads to

$$\gamma = 0{\cdot}044\,887\,6,$$

agreeing with Brown to the fifth significant figure. Then

$$i = 5^\circ\,8'\,43'', \qquad \sin i = 0{\cdot}089\,682.$$

i is often given as $5°\,8'\,33''$, which is appreciably wrong. Hayn (1902, p. 876) adopts $i = 5°\,8'\,40''$.

We have also

$$g = 0''{\cdot}069\,679 \times 10^6/\text{year}, \qquad c = 0''{\cdot}146\,435 \times 10^6/\text{year}.$$

Hayn (1923) gives the expansion of $\sin L$, in which the coefficient of $\sin(\omega+g)t$ is $(1-e^2)\sin i$. He gives this coefficient as 0·089 42, whence $\sin i = 0{\cdot}089\,69$. The numerical data are therefore consistent.

4. *Solution for ξ, η.*—We put

$$\xi = P\sin(\omega+g)t, \qquad \eta = Q\cos(\omega+g)t. \tag{1}$$

The equations of motion reduce to, with $g/\omega = \mu$, $\omega'/\omega = m$, (2)

$$\{(1+\mu)^2-\beta\}P + (1+\mu)(1-\beta)Q = \frac{3\lambda}{1+\kappa}\beta\{(1-\tfrac{1}{2}e^2-\sin^2 i+\tfrac{1}{2}m^2)P - \sin i(1-\tfrac{1}{2}e^2-\tfrac{3}{2}\sin^2\tfrac{1}{2}i)\}, \tag{3}$$

$$\{(1+\mu)^2-\alpha\}Q + (1+\mu)(1-\alpha)P = \frac{3\lambda}{1+\kappa}\alpha\{(2e^2-\tfrac{1}{2}\sin^2 i)Q + (2e^2-\tfrac{1}{2}\sin^2\tfrac{1}{2}i)\sin i\} + \frac{3\lambda}{2(1+\kappa)}m^2\beta Q \tag{4}$$

$$\left.\begin{aligned} \mu &= 0{\cdot}004\,021\,7, \quad m = 0{\cdot}074\,80, \quad \kappa = 1/81{\cdot}3, \quad \lambda = 1{\cdot}0027,\\ 1-\tfrac{1}{2}e^2-\sin^2 i &= 0{\cdot}990\,450\\ 1-\tfrac{1}{2}e^2-\tfrac{3}{2}\sin^2\tfrac{1}{2}i &= 0{\cdot}995\,471\\ 2e^2-\tfrac{1}{2}\sin^2 i &= 0{\cdot}002\,006\\ 2e^2-\tfrac{1}{2}\sin^2\tfrac{1}{2}i &= 0{\cdot}005\,020 \end{aligned}\right\}. \tag{5}$$

We make four sets of solutions for $-P$ (Table I):

(1) e, i^2, $m=0$, $\lambda=1$; $\beta = 0{\cdot}000\,60$, $0{\cdot}000\,62$, $0{\cdot}000\,64$; $\alpha/\beta = 0{\cdot}5$, 1.

(2) Same with correct values of e and i.

(3) As (2) but with correct value of m.

(4) As (3) but with $\lambda = 1{\cdot}0027$.

TABLE I

β	(1)	(2)	(3)	(4)	(5)
0·00060	0·02538	0·02526(32)	0·02530(36)	0·02539(45)	0·02519
62	0·02647	0·02635(42)	0·02640(46)	0·02649(55)	0·02629
64	0·02759	0·02746(53)	0·02751(57)	0·02760(67)	0·02738

The values given first are for $\alpha/\beta = 0{\cdot}5$; the bracketed figures are the last two for $\alpha/\beta = 1$. In (1) the difference is only by 1 or 2 units in the last figure. $-Q/P$ is always 0·9960 to four places. (5) is Hayn's 1902 solution for $\alpha/\beta = 0{\cdot}6$, interpolated to the present values of β. He writes my P and Q as $-I-\delta$, $I-\delta$, and the values under (5) are his I. They are then very close to solution (2), which allows for e^2 and i^2 but not for the solar effects represented by m and λ. He remarks (1923) that the effect of m^2 is about $7''$; this corresponds to the difference between solutions (2) and (3).

In fact the corrections for λ and m have almost exactly cancelled the effects of e^2 and i^2, and the elementary solution (1) is very close.

The chief surviving errors of solution (4) are probably the neglect of the evection and variation of the Moon. These anomalies in longitude are about 0·2 and 0·1 of the eccentricity effect. The chief effects of any perturbation are due to disturbance of the alignment of the Moon's axis *OA* and the line of centres, and the corresponding changes in the distance. Since these enter through their squares it is likely that their effect will be to decrease the results by about 0·05 of the difference between solutions (1) and (2), which will only make a difference of 1 in the last figure. Thus there appears to be good reason to adopt solution (4). Converted into degree measure this gives Table II.

TABLE II

	$\alpha/\beta=0\cdot5$						$\alpha/\beta=1\cdot0$					
	$-P$			Q			$-P$			Q		
β	°	′	″	°	′	″	°	′	″	°	′	″
0·00060	1	27	17	1	26	57	1	27	30	1	27	9
61	1	29	10	1	28	48	1	29	23	1	29	2
62	1	31	4	1	30	42	1	31	17	1	30	55
63	1	32	59	1	32	36	1	33	11	1	33	50
64	1	34	54	1	34	31	1	35	8	1	34	45

The calculations were done on EDSAC by Dr D. W. Barron.

5. *Observations of the libration.*—The results of observation are usually given in terms of I, which is somewhat ambiguous, since the motion of the axis is not quite in a circular cone; $|P| \neq |Q|$. Recent reports of Commission 17 of the I.A.U. give the values in Table III.

TABLE III

1952	Belkovitch	1° 32′ 0″ ± 14″
	Nefediev	32′ 4″ ± 15″
	Yakovkin	33′ 48″ ± 17″
1955	Nefediev	32′ 10″ ± 18″
	Nefediev	33′ 26″ + 20″
	Yakovkin	32′ 49″ ± 12″
	Watts	33′ 50″ ± 12″
1958	Schrutka-Rechtenstamm	31′ 52″ ± 7″
	Habibulin	33′ 6″ ± 11″
	Habibulin	31′ 22″ ± 14″

It is obvious that the differences, even between different solutions by the same author, are far greater than the apparent uncertainties can explain. If we suppose that the estimates are derived from a single normal law they lead to

$$I = 1^\circ 32' 39'' \pm 17'',$$

standard deviation of one determination 52″. All but two of the determinations have stated standard errors less than that of the result of combining them?

On the other hand there is some reason to suppose that the best assumption to make about the probability rule for a suggested but not established discrepancy is the Cauchy law (Jeffreys 1948a, pp. 81, 244)

$$P(dx|\sigma\xi) = \frac{\sigma\, dx}{\pi\{\sigma^2 + (x-\xi)^2\}}. \qquad (1)$$

This does not yield sufficient statistics, but estimation by maximum likelihood is not difficult. We get the equations for ξ and σ

$$\frac{\partial \log L}{\partial \xi} = S \frac{2(x_r - \xi)}{\sigma^2 + (x_r - \xi)^2} = 0, \tag{2}$$

$$\frac{\partial \log L}{\partial \sigma} = S \frac{(x_r - \xi)^2 - \sigma^2}{\sigma\{\sigma^2 + (x_r - \xi)^2\}} = 0, \tag{3}$$

leading to

$$\sigma = 42'', \qquad \xi = 1^\circ 32' 30''.$$

Then the uncertainty of ξ comes from

$$s_\xi^{-2} = -\frac{\partial^2}{\partial \xi^2} \log L = 2S \frac{\sigma^2 - (x_r - \xi)^2}{\{\sigma^2 + (x_r - \xi)^2\}^2} \tag{4}$$

and $s_\xi = 28''$.

The distribution of the residuals favours the normal law in comparison with the Cauchy one, since no residual out of 10 reaches twice the standard error of one determination. On the other hand there may be a systematic bias, and if so one extreme determination may be better than any sort of weighted mean—and we do not know which extreme. The determinations are in fact nearly uniformly distributed over the whole range. What is conspicuous by its absence is a concentration of a set of values consistent with regard to their standard errors; if there was such a concentration we might regard these values as affected only by random errors. The errors are definitely not random.

Most of the methods depend mostly on N–S displacements of a crater near the centre of the disk, which are our coordinate ξ; hence their I is $-P$. Watts's method is exceptional, since he measures rotations in the plane of the disk, so that his I is Q. But Q is less than P by only 4 parts in 1000, and the difference is much less than the discrepancies, and in fact Watts's determination is the largest of the ten!

Tisserand (1891) effectively defines I^2 as $\frac{1}{2}(P^2 + Q^2)$. This is undesirable since P and Q are theoretically not quite equal and are measured in quite different ways. Hayn (1923) puts $-P = I + \rho$, $Q = I - \rho$. His 1902 values would lie between my $-P$ and Q on solution (2). Tisserand also omits the factor $1 + \kappa$ and yet takes the calculation to four figures. I have already commented on the fact that his values for the Poisson terms should be divided by 10 (Jeffreys 1955, p. 193).

Most recent determinations of the libration in longitude have given $\alpha/\beta = 0{\cdot}6$ to $0{\cdot}7$. Taking it as 2/3 I find from the above calculation that $P = 1^\circ 32' 39'' \pm 17''$ corresponds to $\beta = 0{\cdot}000\,627\,9 \pm 0{\cdot}000\,001\,5$. On the other hand the extreme determinations would give $\beta = 0{\cdot}000\,621\,2$ and $0{\cdot}000\,634\,0$. The main conclusion is that an optimist might say that β is determined with a standard error of about 1 part in 400; but if a pessimist should say that any uncertainty remotely corresponding to a standard error must be at least 1 part in 100 there is no decisive reply. If the observations are over different intervals of time and there is another term with speed near ω it could give rise to an apparent fluctuation of amplitude; but the only such term that has arisen here appears to be much too small.

Hayn's 1923 value for I was $1^\circ 32' 13''$, with $\beta = 0{\cdot}000\,630\,0$.

6. *The libration in longitude.*—2 (10) and (11) give, for the relevant terms,

$$lm\left(\frac{a}{r}\right)^3 = 2e\sin(\omega - c)t - \frac{9}{16}e^2\sin^2 i\sin 2(g+c)t.$$

The first coefficient is 0·11, agreeing closely with Koziel's value (1949, Table 5). The second is $-13{\cdot}4\times10^{-6}$. Koziel gives $-11{\cdot}65\times10^{-6}$. In the present treatment the term is essentially geometrical, arising from the projection of the Moon's orbit on to the ecliptic, and it does not appear that the terms neglected could alter this by more than 1 per cent. However Hansen's theory of the Moon's motion gives several periodic perturbations in and across the plane of the mean orbit, and I am indebted to Dr J. G. Porter for a discussion of these. It appears (Newcomb 1882; Brown 1905 b) that in longitude on the ecliptic there are contributions to the $2(g+c)t$ term arising from these perturbations amounting to about 1″; and other terms will arise when terms of other speeds are combined with $(a/r)^3$. It appears therefore that the agreement between the purely geometrical value and Koziel's is accidental, arising from the cancelling of several comparable terms.

Formerly values of the constant $f=\alpha/\beta$ were concentrated about 0·5 and 0·8, with none between. This situation is completely altered now. From the *Proceedings of the I.A.U.* for 1950–1958 I have collected the values of f determined from the annual term in χ. They give the distribution in Table IV. They

TABLE IV

0·50–0·54	0·55–0·59	0·60–0·64	0·65–0·70	0·70–0·74	0·75–0·79	>0·80
1	3	8	4	3	0	1

show a marked concentration (unlike the corresponding data for P). Omitting the outlying determination >0·80 and treating all as of equal weight we get

$$f = 0{\cdot}639 \pm 0{\cdot}014, \qquad s = 0{\cdot}058.$$

This is only a sketch of the data, because (*a*) some of the results are based on discussions of the same observations by different authors, and consequently are not independent, (*b*) some authors give alternative values and I have included both in the table. However, the uncertainty of one determination derived from comparison of the results is exceeded by three of those stated by the authors. At any rate the comparison is enough to show that $f=0{\cdot}67$ would not deviate by a prohibitive amount from the results based on the annual term.

It should be noted however that the annual term gives γ directly, and that f has been calculated from γ on the assumption of a standard value of β, usually, I think, that given by Hayn (1923)

$$\beta = 0{\cdot}000\,630\,0.$$

The critical value of γ, corresponding to agreement of the free speed with $2(g+c)$, is quoted from Hayn as corresponding to $f=0{\cdot}662$; this would be $\gamma=0{\cdot}000\,213\,1$. But they do not all appear to have used the same value of β, and the conversion to f has introduced some confusion. If we reconvert to γ with this value of β we get

$$\gamma = 0{\cdot}000\,227\,4 \pm 0{\cdot}000\,008\,8.$$

Yakovkin (1952) detected a term with approximately the speed $2(g+c)$, and interpreted it as a free vibration. If it is, it leads to

$$\gamma = 0{\cdot}000\,209\,8 \pm 0{\cdot}000\,002\,2.$$

I found however (Jeffreys 1957) that the phase was consistent with the term being the forced vibration with this speed, and if so

$$\gamma = 0{\cdot}000\,204\,9 \pm 0{\cdot}000\,000\,9.$$

The differences from the results from the annual term are just over twice the apparent standard error, and might cast some doubt on the reality of Yakovkin's term. On the other hand the standard error of the value based on the annual term may be too low, as the estimate is quite rough; and also there is always a possibility of some systematic error in an annual term, which may not have been completely excluded. In view of the doubts expressed above about the uncertainty of β it now seems at least possible that γ is better known than β. In any case as the measurements used in estimating β and γ are substantially independent it is much better not to use f, which combines the uncertainties.

7. *The Banachiewicz–Koziel paradox.*—Banachiewicz, followed by Koziel, has maintained that in an attempt to determine γ from observation by the method of least squares, when there is a possibility of resonance, the solution will always be ambiguous, since whatever value is taken as the trial value the corrected value found by least squares will be on the same side of the resonating frequency as the trial value. Several writers have verified this by starting with trial speeds of free vibration on opposite sides of $2(g+c)$ and finding corrected values nearer to this speed, but still on opposite sides of it. The point, and a way of avoiding it, may be illustrated by a simplified model.

As most other standard symbols for a speed are preoccupied I now use γ for the free speed, and suppose that the vibration x is given by

$$x = \frac{\alpha_1}{\gamma^2-\gamma_1^2}\cos\gamma_1 t + \frac{\alpha_2}{\gamma^2-\gamma_2^2}\cos\gamma_2 t \pm \sigma, \tag{1}$$

where in the present problem $\gamma_1 = 2(g+c)$, $\gamma_2 = 2\pi/\text{year}$; α_1 and α_2 are given and $|\alpha_2| \gg |\alpha_1|$. Then if there are n observations the likelihood is

$$L = \frac{1}{(2\pi)^{\frac{1}{2}n}\sigma^n}\exp\left\{\frac{-S}{2\sigma^2}\left(x_r - \frac{\alpha_1}{\gamma^2-\gamma_1^2}\cos\gamma_1 t_r - \frac{\alpha_2}{\gamma^2-\gamma^2}\cos\gamma_2 t_r\right)^2\right\}. \tag{2}$$

Suppose that the arrangement of the times of observation is well balanced, so that

$$S\cos^2\gamma_1 t_r = S\cos^2\gamma_2 t_r = \tfrac{1}{2}n, \qquad S\cos\gamma_1 t_r\cos\gamma_2 t_r = 0. \tag{3}$$

Put

$$Sx_r\cos\gamma_1 t_r = \tfrac{1}{2}na_1, \qquad Sx_r\cos\gamma_2 t_r = \tfrac{1}{2}na_2. \tag{4}$$

Then

$$L = \frac{1}{(2\pi)^{\frac{1}{2}n}\sigma^n}\exp\left[-\frac{n}{4\sigma^2}\left\{\left(\frac{\alpha_1}{\gamma^2-\gamma_1^2}-a_1\right)^2 + \left(\frac{\alpha_2}{\gamma^2-\gamma_2^2}-a_2\right)^2\right\} - \frac{Sx_r^2 - \frac{1}{2}n(a_1+a_2^2)}{2\sigma^2}\right]. \tag{5}$$

Put

$$Sx_r^2 - \tfrac{1}{2}n(a_1^2+a_2^2) = ns^2 \tag{6}$$

so that s is the mean square residual. Then the form of L is equivalent to two equations of condition for γ

$$f_1(\gamma) = \frac{\alpha_1}{\gamma^2-\gamma_1^2} - a_1 = 0 \pm \sigma\sqrt{\frac{2}{n}}; \qquad f_2(\gamma) = \frac{\alpha_2}{\gamma^2-\gamma_2^2} - a_2 = 0 \pm \sigma\sqrt{\frac{2}{n}}, \tag{7}$$

where we can take $\sigma = s$ if n is large. Further, if there is any doubt about the possibility of estimating γ_1 from a_1, $|a_1|$ will not be many times $\sigma/\sqrt{n}$, and ns^2 will not be very different from $Sx_r^2 - \frac{1}{2}na_2^2$.

Suppose then that $|a_2|$ is several times $s\sqrt{(2/n)}$. Then if $|\gamma^2 - \gamma_2^2|$ is large $f_2(\gamma)$ will be near $-a_2$, but will be small near where

$$\gamma^2 - \gamma_2^2 = \frac{\alpha_2}{a_2} = g^2 - \gamma_2^2,$$

say. In the same conditions $f_1(\gamma)$ will be near $-a_1$, and reference to (5) shows that L will be small except for γ in a range about g.

However, $L = 0$ when $\gamma = \gamma_1$, unless α_1 is exactly zero, and since $L \geqslant 0$ it must have two maxima, one on each side of $\gamma = \gamma_1$. If then search is made for a value of γ near a trial value the nearest maximum will be on the same side of γ_1 as the trial value. This is the result of Banachiewicz. But this difficulty does not appear insoluble; we consider two cases.

First, if a_1 is available, $f_1(\gamma)$ gives supplementary information; γ must be near the value that makes $f_1 = 0$, and in fact this information may determine γ more accurately than a_2 does.

Secondly, if a_1 is not available, we have in any case not completed the analysis. But the omission is due to the assumption that the γ_1 term is negligible and thus assumes also $\alpha_1 = 0$. If this is valid as an approximation we still have the f_2 equation, and the f_2 factor has only a single maximum, on whichever side of g γ_1 may lie.

This analysis assumes a balanced design, which will be possible only if the observations are fairly uniformly distributed over a range that is nearly a multiple of both periods. As it happens

$$2(g + c) = 0''{\cdot}432\,228 \times 10^6/\text{year}$$

and is almost exactly a third of the Sun's mean motion. Hence to get a satisfactory solution it is essential that the observations should extend over a multiple of 3 years. If longer intervals are available it would be desirable to make separate analyses for 3-year intervals to check the apparent uncertainties, and to combine them afterwards. The assumption of independence of the errors needs verification whenever such verification is possible.

8. *Secular motions of the Moon.*—A. H. Cook (1959) has given a very full discussion of recent data relevant to the figures of the Earth and Moon, with special reference to results from artificial satellites. In Section 6, dealing with the motions of the Moon, he quotes equations from a paper of mine (Jeffreys 1941). The uncertainties there given were estimates of probable errors, the larger part of which was based by de Sitter on E. W. Brown's estimate of the greatest possible outstanding errors of his calculation. I later (1948b) revised these; with the value $1{\cdot}625 \times 10^{-3}$ for J adopted by Cook, the equations for L' and K' become, with standard errors,

$$380L' - 1192K' = +0{\cdot}078 \pm 0{\cdot}056,$$
$$-460L' = -0{\cdot}251 \pm 0{\cdot}052.$$

Then*

$$L' = (5{\cdot}46 \pm 1{\cdot}13)10^{-4},$$
$$K' = (1{\cdot}07 \pm 0{\cdot}59)10^{-4},$$
$$K'/L' = 0{\cdot}20 \pm 0{\cdot}11,$$

* Cook's $K' = 1{\cdot}28 \times 10^{-4}$ seems to be a numerical error.

$$\beta = 0{\cdot}000\,628\,4,$$

$$L'/\beta = 0{\cdot}84 \pm 0{\cdot}18.$$

Now K'/L' should be equal to γ/β, which, according to my estimate, is very close to 0·33. The difference is just over the standard error. Also the value of L'/β for a homogeneous Moon would be 0·60, and the difference is 1·3 times the standard error. Cook does not give uncertainties for his values, and it does not appear that either discrepancy is serious.

It should be recalled, however, that the uncertainties above are not standard errors in the usual sense. The observational uncertainties are the smaller part of them. The larger part is based on Brown's estimate of the maximum uncertainty of the calculations (1904) and may be considerably reduced when the work of Eckert, now in progress, is completed. It seems that the remaining residuals are within Brown's maxima.

To put the matter in another way, assume a homogeneous Moon and estimate L' and K' from β and γ. We get, approximately,

$$L' = 0{\cdot}000\,377 \pm 0{\cdot}000\,002,$$

$$K' = 0{\cdot}000\,126 \pm 0{\cdot}000\,002,$$

whence

$$380L' - 1192K' = -0{\cdot}007 \pm 0{\cdot}002,$$

$$-460L' = -0{\cdot}173 \pm 0{\cdot}001,$$

leaving residuals of $+0{\cdot}085 \pm 0{\cdot}056$ and $-0{\cdot}078 \pm 0{\cdot}052$. Brown's limits of error (1904) were $\pm 0{\cdot}10$ and $\pm 0{\cdot}05$, which de Sitter considered to need no alteration as further corrections made by Brown were substantially independent. De Sitter also allows $\pm 0{\cdot}02$ in both estimates from uncertainties in the planetary masses adopted; and when the observational uncertainties $\pm 0{\cdot}006$ and $\pm 0{\cdot}012$ are considered it appears that both values are within the tolerable limits.

160 *Huntingdon Road,*
Cambridge:
1961 *January.*

References

Brown, E. W., 1899, *Mem. R.A.S.*, **53**, 39–116.
Brown, E. W., 1904, *M.N.*, **64**, 532.
Brown, E. W., 1905 a, *Mem. R.A.S.*, **57**, 51–145.
Brown, E. W., 1905 b, *M.N.*, **65**, 276–296.
Cook, A. H., 1959, *Geophys. J.*, **2**, 2,222–40.
Hayn, F., 1902, *Abh. sächs. Ges. Wiss.*, **27**, 861–921.
Hayn, F., 1923, *Enzycl. Math. Wiss.*, **VI 2**, 20a, 1020–1043.
Jeffreys, H., 1941, *M.N.*, **101**, 34–6.
Jeffreys, H., 1948a, *Theory of Probability*.
Jeffreys, H., 1948b, *M.N. Geophys. Suppl.*, **5**, 245.
Jeffreys, H., 1955, *Vistas in Astronomy*, **1**.
Jeffreys, H., 1957, *M.N.*, **117**, 475–7.
Jönsson, A., 1917, *Medd. Lund. Astr. Obs.* (2), No. 15.
Koziel, K., 1949, *Acta Astronomica a*, **4**, 61–193.
Newcomb, S., and Meier, J., 1882, *Astr. Pap. Am. Eph.* **1**, Part 2.
Tisserand, F., 1891. *Traité de Mécanique Céleste*, **2**, 444–475.
Yakovkin, A. A., 1952, *Trans. I.A.U.*, **8**, 231.

ANALYSIS OF RADIAL VELOCITIES OF STARS AND NEBULAE IN THE MAGELLANIC CLOUDS

M. W. Feast, A. D. Thackeray and A. J. Wesselink

(Received 1961 February 11)*

Summary

Radial velocities of 61 stars in the LMC are analysed together with Lick measures of nebular velocities.

It is pointed out that, in principle, instantaneous measures of radial velocity do not distinguish between the rotation and translation of a solid body. A least squares solution yields a vector 813 ± 65 km/s (corrected for solar motion and galactic rotation) which is held to be mainly due to solid-body rotation of the LMC. The corresponding gradient of radial velocities in the sky is 14·2 km/s/deg in p.a. 171° in which an uncertainty of $\pm 1{\cdot}7$ km/s/deg would be contributed by a translational velocity of 100 km/s.

Small departures from this solution in the outer parts indicate some differential rotation. Further analysis, on the basis of de Vaucouleurs' inclined plane model, yields a rotation curve which disagrees with de Vaucouleurs' but which is only slightly steeper than the corrected peak velocities derived from 21 cm profiles. The optical velocities are more symmetrical about the radio centre than about de Vaucouleurs' optical centre.

The mass of the LMC is derived from (*a*) a model of a uniform rotating ellipsoid, (*b*) a model of a non-uniform rotating ellipsoid (after Perek) and (*c*) Bottlinger's interpolation formula for differential rotation. The best estimate for the mass within 4°·5 of the centre is $1{\cdot}0 \times 10^{10} \odot$.

The velocity-dispersion appears to be slightly larger in the inner portions of the LMC and for the brightest stars compared with the faintest observed.

SMC stars with known velocities cover too small an area of the sky to deduce optical evidence of the rotation of the system. The velocity-dispersion in the SMC is of order 16 km/s, as in the LMC.

---

1. *Introduction.*—It was early noted that the radial velocities of nebulae in the Large Magellanic Cloud vary with their position in the sky. R. E. Wilson (**1**) suggested that rotation might be a possible explanation. Hertzsprung (**2**) remarked that the radial velocity field could be explained by assuming the various nebulae to move with equal and parallel velocities. He further suggested that the two Clouds also move together as the only radial velocity then known in the Small Cloud agreed with his formula for LMC. From 17 LMC and 1 SMC nebulae he deduced a common space velocity of 625 ± 80 km/s. In 1927 Oort (**3**) corrected the mean radial velocity of the Magellanic Clouds for galactic rotation. He suggested that the small residual velocities may mean that the Clouds are satellites of the Galaxy. In 1944 the subject was again taken up by R. E. Wilson (**4**) who considered the radial velocity field from Hertzsprung's standpoint but now taking galactic rotation into account.

Differential rotation of the outer parts of both Clouds, was first suggested by the radio observations of Kerr, Hindman and Robinson (**5**) in 1954. The

* Received in original form 1960 December 6.

XUM

first optical velocities relating to LMC stars were studied in a provisional way by Feast, Thackeray and Wesselink (**6**) in 1955 who found the same velocity gradient across the LMC for stars and nebulae and a direction of maximum velocity gradient which agreed very well with that of the radio observations and of the "major axis" determined from de Vaucouleurs's (**7**) isophotes of the faint outer parts of the LMC*. The gradient of the optical velocities was, however, much steeper than that of the radio observations for which velocities had been based on the *median* of the 21 cm profiles; when the *peaks* of the 21 cm profiles were used the gradients of optical and radio velocities agreed much better. This asymmetry of the 21 cm profiles can be understood in terms of differential rotation of the LMC which is also indicated by the trend of the velocities in the faint outer parts. Subsequently several papers by Kerr and de Vaucouleurs (**8, 9**) and by de Vaucouleurs (**10**) have appeared in which rotation of the LMC is considered the chief contributor to the velocity field.

In the present paper, the considerably richer Radcliffe material on optical velocities (**11**) than was available in 1955 is discussed in conjunction with the known data on nebulae.

2. *Indistinguishability of rotation and translation of a solid body.*—In previous work it does not seem to have always been realized that it is impossible, in principle, to distinguish between the rotation and translation of a solid body on the basis of instantaneous measures of radial velocity alone.

Radial velocities are concerned with the rate of change of distance from an observer. Consider any assemblage of stars not subject to differential rotation in which the stars preserve the same distances from one another; in other words, the assemblage can be regarded as a solid body. We can then choose a reference frame rigidly connected to the solid body. An external observer is moving relative to this frame and his motion is quite generally represented by the velocity vector **W**.

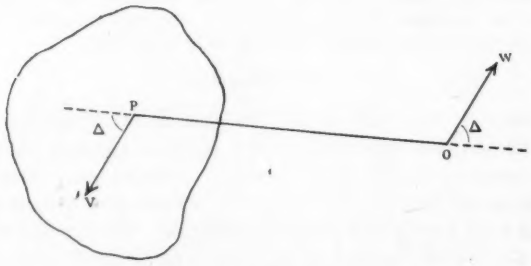

FIG. 1.—*Motion relative to a solid body.*

Fig. 1 shows the situation in a plane containing the observer O, the velocity vector **W** and a point P of the solid body. If Δ is the angle between **W** and the direction PO we have for the radial velocity of P

$$\rho = +w\cos\Delta \qquad (1)$$

where w is the absolute value of the vector **W**. This expression is derived without

* It may be pointed out that Kerr and de Vaucouleurs (**8**) reproduce small scale photographs of both Clouds with the axes of rotation and various centres marked. The optical and radio centres of the LMC which will be referred to in this paper are shown in (**8**) as C and C_R respectively, and the major axis shown there is close to the one derived in the present paper.

any assumption as to whether the solid body is rotating or only moving linearly with respect to an inertial frame.

If we consider the observer at rest and the motion of the point P to have a vector $\mathbf{V} = -\mathbf{W}$, the radial velocity of P relative to O is represented by

$$\rho = v \cos \Delta. \qquad (2)$$

It is to be noted that all other points in the solid body have equal and parallel velocity vectors V relative to O. It was the vector $\mathbf{V}$ that was determined by Hertzsprung from the nebular velocities. But no conclusion can be drawn with regard to the resolution of this vector into components due to translation $\mathbf{V}_T$ and rotation $\mathbf{V}_{rot}$ with respect to an inertial frame, so long as we are dealing with a solid body. The distinction can only be made if accelerations can be measured.

This ambiguity is of much greater importance in discussing radial velocities in the Magellanic Clouds than in other external systems. In the Large Cloud, for instance, the known stellar velocities change by about 85 km/s over 6° in the sky, and could be interpreted as due to a translation of 813 km/s as we shall see in the following section. For M31, on the other hand, supposing one's knowledge of radial velocities to be restricted to a constant velocity gradient within the nuclear regions (58 km/s per 2′ of arc according to early measures), we would have to postulate a translational velocity of 10^5 km/s in order to escape the conclusion that the system is rotating. Clearly one is safe here in assuming that the observed gradient is overwhelmingly due to rotation. The ambiguity could also occur in galactic clusters like the Hyades covering a sufficient area of the sky to reveal a gradient of velocities. But such clusters are so near that proper motions are available as well as radial velocities, so that space motions can be deduced.

Since our data in both Clouds refer almost entirely to the central portions of these systems which appear to behave to a first approximation as solid bodies (with a certain velocity dispersion superposed), we proceed in the first instance to analyse these velocities by Hertzsprung's method which is, in fact, the standard method of calculating a solar velocity from radial velocities (**34**). However, we shall regard the projection of the vector on the plane of the sky, corrected for solar motion and galactic rotation, as representing rotation of the LMC with some uncertainty due to the unknown translation of the Cloud. We are completely ignorant of the position angle of the vector representing relative translation of the LMC and Galaxy, but the amount is not likely to exceed 100 km/s. This feature of the translation will appear as the main contributor to the uncertainty of the rotation.

Large Cloud.

3. *Representation of observed radial velocities as solid body rotation.*—The LMC velocities actually used in our analysis are listed in three sections in Table I. ρ is the directly observed velocity, ρ' the velocity corrected for solar motion and galactic rotation according to equation (6) below. From the Radcliffe stellar velocities (**11**) we have excluded all stars with P Cyg or W characteristics, leaving 61 stars (with weight 2 to 53 stars with velocities of quality c or d, and weight 1 to 8 stars with e-quality velocities). In the second section we list the 17 Lick nebular velocities to which weight 3 was assigned because the dispersion of the nebular velocities appears to be smaller than that of the stellar velocities (including observational scatter). Finally, 5 Mt Stromlo nebular velocities by de Vaucouleurs (**10**) are listed (weight 1).

TABLE I

Radial velocities of LMC stars and nebulae analysed for rotation

(a) Stars

Radcliffe No.	x/100	y/100	ρ	ρ'	Weight (1)	Weight (2)	Outer zone
51	−14	+157	+306	+75	2	7	*
52	+ 8	75	266	+35	2	5	*
53	1	140	309	+77	2	7	*
54	16	78	250	+18	2	6	
56	2	174	312	+79	2	4	*
57	8	168	301	+69	2	8	*
58	18	104	271	+38	2	5	
59	22	86	258	+25	2	6	
61	12	175	286	+52	2	6	*
62	15	160	295	+62	2	16	*
65	29	85	258	+25	2	6	
67	43	53	244	+11	2	12	
68	25	213	313	+79	2	6	*
70	30	212	300	+65	2	7	*
71	56	13	192	−42	2	14	*
72	55	37	237	+ 3	2	5	*
73	42	171	305	+70	2	8	
74	47	161	299	+64	2	5	
75	48	180	297	+61	2	5	*
76	55	139	253	+18	2	15	
78	62	116	238	+ 2	2	7	
79	71	108	302	+66	2	5	
80	78	13	231	− 4	2	8	*
82	85	88	236	− 1	1	4	
85	98	92	292	+53	2	6	
89	103	78	285	+46	1	3	
92	103	218	322	+81	2	6	*
94	106	220	291	+50	2	3	
95	106	+220	329	+88	1	2	*
96	113	− 4	241	+ 4	2	7	*
97	106	+219	308	+67	2	4	*
98	106	216	308	+68	2	6	*
99	113	137	278	+38	2	5	
100	117	4	251	+14	2	6	*
101	126	10	251	+12	2	8	*
103	126	108	298	+58	2	8	
104	126	223	306	+53	2	8	*
105	132	97	268	+27	1	2	
107	138	155	336	+93	2	5	
108	139	165	318	+75	1	2	
111	140	83	260	+20	2	5	
112	139	28	237	− 3	2	10	*
113	141	28	244	+ 4	1	2	*
117	145	150	317	+74	2	8	
118	152	174	342	+99	2	14	

TABLE I (*cont.*)

Radcliffe No.	x/100	y/100	ρ	ρ'	Weight (1)	Weight (2)	Outer zone
119	+153	+176	+312	+69	1	2	•
120	154	162	288	+45	2	5	
121	154	162	319	+76	2	6	
122	155	155	257	+13	2	3	
123	154	78	267	+26	2	6	
125	157	158	292	+49	2	4	
126	158	89	258	+16	2	8	
128	158	84	268	+26	2	4	
129	162	105	273	+29	2	4	
131	163	98	269	+25	2	6	
143	165	97	263	+19	2	6	
150	169	78	241	− 1	2	10	
152	173	73	258	+15	2	9	•
153	186	101	253	+ 8	2	6	•
154	196	63	242	− 3	1	3	•
155	202	53	248	+ 3	2	6	•

(*b*) *Lick nebulae*

NGC	x/100	y/100	ρ	ρ'	Weight
1714	− 2	+167	+309	+77	3
1722	+ 17	78	265	+33	3
1743	22	86	260	+28	3
1748	23	87	256	+24	3
1763	17	189	296	+62	3
1935	110	140	299	+48	3
1936	110	139	292	+52	3
1949	121	122	260	+19	3
2029	156	155	297	+53	3
2070	165	99	275	+32	3
2077	167	79	259	+16	3
2079	167	74	255	+12	3
2080	168	79	251	+ 8	3
2086	170	78	271	+28	3
Anon	170	77	264	+21	3
2105	7	84	293	+62	3
2115	17	189	292	+58	3

(*c*) *Mt Stromlo nebulae*

N55A	146	195	323	+80	1
N63A	158	211	312	+67	1
N72	186	200	334	+88	1
N206A	141	28	218	−22	1
N213A	162	42	185	−57	1

The last five entries in the Table refer to observations by de Vaucouleurs (10). These velocities were used in the analysis of Section 5 but not Section 3.

For convenience, the Harvard coordinates x, y (smoothed to the nearest 100″ of arc) are tabulated as they are not listed in (**11**), although we preferred to use α, δ in our solutions. The last two columns contain information required later in Section 7.

In a system of rectangular coordinates with the usual notation (x, y towards $\alpha = 0, 90°$ respectively, in the equator, z towards the north pole), we write X, Y, Z for the corresponding components of the vector **V**. Then equation (2) can be written

$$\begin{aligned}\rho &= v\cos\Delta \\ &= X\cos\alpha\cos\delta + Y\sin\alpha\cos\delta + Z\sin\delta \end{aligned} \qquad (3)$$

where α, δ are the (1975) coordinates of a Cloud star or nebula.

TABLE II

Solid body solutions for LMC stars and nebulae

	Solution	X	Y	Z	v
I	61 Stars	$+80\pm89$	$+899\pm84$	$+54\pm32$	904 ± 85
II	17 Nebulae	$+174\pm90$	$+753\pm164$	$+3\pm60$	773 ± 160
III	61 Stars 17 Nebulae	$+113\pm59$	$+875\pm65$	$+47\pm25$	883 ± 65

Various least-squares solutions for X, Y, Z and v are tabulated in Table II with their standard errors. We list first a solution based on the 61 stars of Table I *a*. Secondly we give the solution for the 17 nebulae of Table I (*b*), i.e. omitting the one SMC nebula with a Lick velocity; the inclusion of this one nebula by Hertzsprung brought down his standard error in v to ± 80 km/s because of the much larger extent of the area covered by his objects. But since we now know of differential rotation in parts of the LMC it is clear that the two Clouds must be treated separately.

We note that the separate solutions for stars and nebulae do not differ significantly from each other, in accordance with our previous findings by a different approach (**6**). We therefore combine stars and nebulae in a third solution which may be regarded as our final one for the LMC regarded as a solid body.

In spite of the fact that the standard errors of X, Y and Z are always quite large, the uncertainty in a computed velocity in the Cloud according to (3) is quite small. This is because of the correlation between errors of the components of v. For instance we find the computed velocity for de Vaucouleurs' optical centre (**12**) of the LMC ($5^h\,24^m - 69°{\cdot}8$) to be

$$\rho = +260 \pm 2 \text{ km/s}.$$

No allowance has been made as yet for the effect of galactic rotation and solar motion. We have used the same data as employed by Kerr and de Vaucouleurs (**8**) viz:

Galactic rotation: 270 km/s towards $l = 57°$, $b = 0$
Solar motion: 20 km/s towards $\alpha = 18^h\,00$,
$\delta = +30°{\cdot}0$ (1900).

We then find that any object with coordinates α, δ will have a radial velocity (km/s) due to solar motion of

$$S = +17{\cdot}3\sin\alpha\cos\delta - 10{\cdot}0\sin\delta \qquad (4)$$

and due to galactic rotation of

$$G = -130{\cdot}0\cos\alpha\cos\delta + 125{\cdot}5\sin\alpha\cos\delta - 200{\cdot}6\sin\delta. \quad (5)$$

The combined effect due to solar motion and galactic rotation is the sum of (4) and (5), or

$$S + G = -130{\cdot}0\cos\alpha\cos\delta + 142{\cdot}8\sin\alpha\cos\delta - 210{\cdot}6\sin\delta. \quad (6)$$

Hence the vector solution (3) for an observer at our position in the Galaxy but freed from galactic rotation and solar motion is found by subtracting (6) from (3), adopting Solution III of Table II. If accents denote quantities corrected for galactic rotation and solar motion, we have

$$\rho' = +243\cos\alpha\cos\delta + 732\sin\alpha\cos\delta + 258\sin\delta \quad (7)$$

with standard errors somewhat larger than those of Table I as a consequence of the additional uncertainty in the corrections for galactic rotation and solar motion.

In Table III the data relevant to these vectors are summarized. They are resolved for a point near the centre of the Cloud into components in the plane of the sky and in a radial direction. $G+S$ predominates in the radial direction, but makes a relatively small contribution to the total vector **V** in the plane of the sky.

TABLE III

Vectors in analysis of LMC radial velocities

Vector	Total km/s	Apex	Δ	Component in plane of sky: Amount km/s	p.a.	Radial component km/s	km/s/deg
		h m	°				
$G+S$	286	8 49 −48°	33·2	156	74·9	+239	2·7
V	883	5 31 + 3°	72·8	844	1·7	+260	14·7
V'	813	4 47 +18°	88·5	813	351·1	+ 21	14·2
V_{rot}	813	4 46 +21°	90	813	351	0	14·2
V_T	120	—	—	100	?	+ 21	

S = reflex of solar motion; formula (4)
G = reflex of galactic rotation; formula (5)
V = solid-body motion: formula (3)
$V' = V - (S+G)$, solid body motion corrected for solar motion and galactic rotation
V_{rot} = solid-body rotation
V_T = translational velocity of LMC centre relative to centre of galaxy.
Adopted centre of LMC = $5^h\ 24^m - 69°{\cdot}8$.

The radial component of the translation vector $\mathbf{V}_T$ is equal to the radial component of $\mathbf{V}'$ at the centre of the Cloud (since by definition the vector $\mathbf{V}_{rot}$, representing the rotational motion of the Clouds, is in the plane of the sky at the centre). For the optical centre (see Section 4) it has the small value of 21 km/s. The component of $\mathbf{V}_T$ in the plane of the sky is unknown but is unlikely to exceed the radial component by a large factor.

The situation is shown diagrammatically in Fig. 2 where the components of the vectors in the plane of the sky are plotted. With the end of the vector $\mathbf{V}'$ as centre we draw a circle with radius 100 km/s, representing the uncertainty of the

component $\mathbf{V}_T$ in the plane of the sky. The end of the vector $\mathbf{V}_{rot}$ must lie somewhere within this circle.

It is of interest that since the apex of $\mathbf{V}'$ lies nearly 90° from the Large Cloud, the lines of equal velocity across the Cloud are nearly straight in the sky.

We may sum up this section by saying that the variation in stellar radial velocities across the Large Cloud corrected for galactic rotation and solar motion is characterized by a vector 813 ± 65 km/s in position angle $171 \pm 4°.6$.

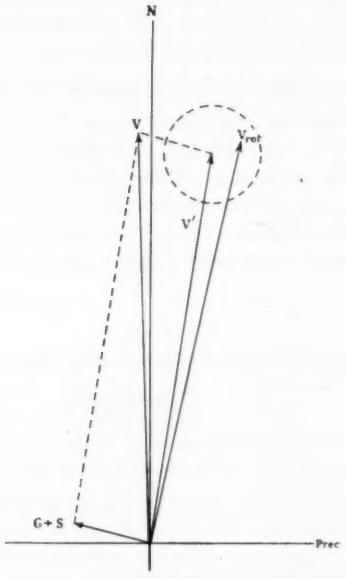

FIG. 2.—*Vector diagram for LMC.*

Our grounds for believing that this corresponds mainly to rotation of the system of stars rather than to translation are:

(*a*) there is evidence of differential rotation, both from the radio and optical observations (see following section);

(*b*) a translational velocity of the Cloud (régarded either as a companion to the Galaxy or as a completely independent system) relative to the centre of the Galaxy is unlikely to exceed 100 km/s;

(*c*) the position angle of our derived rotational axis agrees well with that found from the 21 cm observations and from de Vaucouleurs' (7) discussion of the outer isophotes.

4. *Deviation from solid-body rotation.*—In Fig. 3 we plot the radial velocities of our stars and of the Lick nebulae (crosses) corrected for galactic rotation and solar motion, against the projected angular distance (with arbitrary zero) along the direction (p.a. 171°) of the maximum gradient of velocity. Since this direction is so closely north–south, examination of Table I will show the effect of rotation in the correlation of ρ' and $y/100$.

The slope of the straight line corresponds to a gradient of $14{\cdot}2$ km/s/deg $\pm 1{\cdot}1$. The uncertainty in this figure, due solely to an uncertainty of, say, 100 km/s in the translation, is $1{\cdot}7$ km/s/deg.

There appears to be some tendency for the points to deviate from a straight line in the outermost parts in a manner that suggests differential rotation. (The point with the large residual of −45 km/s in the bottom left corner refers to the peculiar emission object R71.) The points of Fig. 3 were grouped into means of roughly equal weight and are replotted (filled circles), referred to the radio centre, in

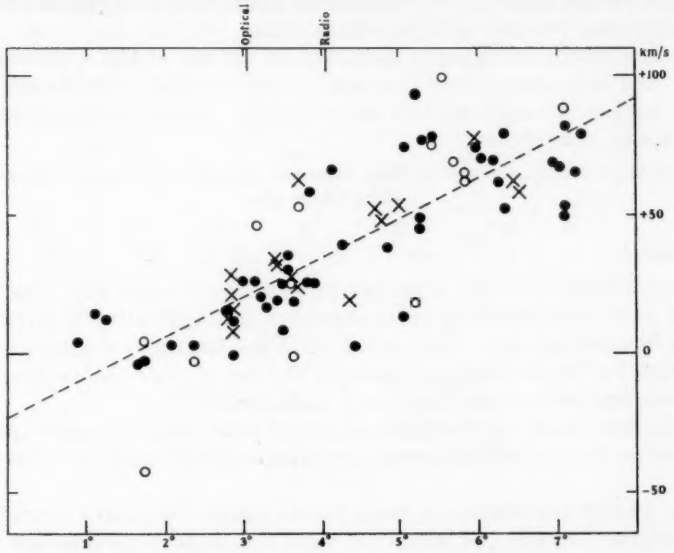

FIG. 3.—*Radial velocities in LMC (corrected for solar motion and galactic rotation) plotted against angular distance along p.a. 171°.*
×, Lick nebulae; ○, measures of low weight and emission stars; ●, stars weight 1.
Abscissae corresponding to the optical and radio centres are marked by long lines at the top.

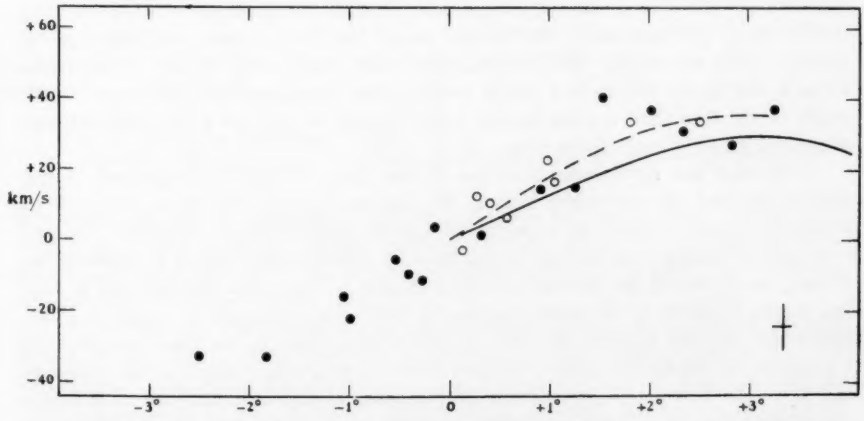

FIG. 4.—*Fig. 3 repeated with measures grouped into means of equal weight. Open circles: left-hand points reflected in radio centre. Dashed curve: drawn free-hand through open and closed circles. Full curve: 21 cm curve from corrected velocities (9).*
The standard error of the means is indicated in the bottom right corner.

Fig. 4. In this figure curvature is apparent at both ends. It is of special interest that the curve is much more symmetrical about the *radio centre* ($5^h\,20^m - 68°{\cdot}8$; 1950), the point about which the 21 cm rotation curve is symmetrical, than about de Vaucouleurs' *optical centre* ($5^h\,24^m - 69°{\cdot}8$). This is the first optical evidence that the dynamical centre of the Large Cloud is associated with the radio centre which, as already noted by de Vaucouleurs and others, is displaced a full degree in the sky from the main axial bar of the Cloud.

We have therefore reflected the points on the left of Fig. 4 about the radio centre, and they reappear on the right as open circles. The dashed curve is drawn freehand through the two sets of points. Values corresponding to this curve are tabulated below.

Mean optical velocities referred to radio centre as function of projected angular distance along major axis.

$r^{(0)}$	0	0·5	1·0	1·5	2·0	2·5	3·0	3·5
V (km/s)	0	8	17	25	31	34	35	35

For comparison in Fig. 4 the full curve shows the similarly reflected curve for the 21 cm peak velocities (after correction for bandwidth) as given by Kerr and de Vaucouleurs (**9**). The optical curve still lies above the radio curve, but correction for bandwidth, and especially the use of peak- rather than median-velocities, has reduced the discrepancy considerably.

It can now be claimed that both optical and radio velocities begin to show signs of departure from solid-body rotation at distances greater than 2° from the radio centre.

Fig. 5 shows the positions in the sky of the stars we have used (circles) and the Lick nebulae (squares), in which the signs and sizes of the residuals from our solid-body solutions are indicated by different symbols (see legend). This form of plotting the data does not indicate differential rotation as clearly as Figs. 3 and 4, but is of interest in that any local signs of ordered stream motion, if marked, should show up. The figure also shows the positions of the optical and radio centres with lines in p.a. 171 and 81° through them. It is at once apparent that our stars (which include as many as possible from the outer regions of the Clouds) are far more symmetrically distributed about the radio centre than the optical centre. The elongated distribution about the major axis is also of interest. Finally, the figure shows how much better is the distribution of our stars for the study of rotation than are the earlier Lick nebulae or the few additional nebulae observed by de Vaucouleurs (**10**).

Now that the differential rotation of the Cloud must be recognised in the region covered by our observations, we can no longer represent the lines of constant velocity exactly by straight lines as in the solid-body solution. Moreover it is no longer true that the radial velocity will be independent of *depth* in the Cloud, as it would be for solid-body rotation. The error introduced in our treatment is likely to be small compared with observational or cosmic scatter. However, for the further analysis of differential rotation we have adopted de Vaucouleurs' model of a plane system inclined at a small angle to the plane of the sky. In this model, treatment of the stars as confined strictly to a plane recaptures the simplifying circumstance that to each position in the sky there corresponds a unique predicted radial velocity.

5. *Differential rotation in an inclined plane system.*—It is necessary to adopt values for certain parameters in this model. In the first instance we have followed

de Vaucouleurs (**10**) very closely so that the results of analysing our more extensive material may be fairly compared with his.

(i) *Centre of rotation.*—de Vaucouleurs adopted the optical centre ($5^h\,24^m$, $-69°{\cdot}8$) which he defined as the centre of symmetry of the faint outer structure. Our analysis has been performed twice, once for the optical centre and again for the radio centre ($5^h\,20^m$, $-68°{\cdot}8$).

(ii) *Major axis.*—Instead of the position angle 165° used by de Vaucouleurs we have adopted our value of 170°·6. The change is trivial and affects the derived rotation curves only slightly.

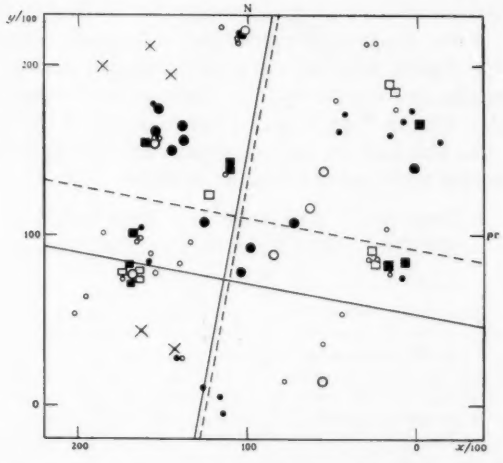

FIG. 5.—*Distribution of observed velocities (LMC) in plane of sky. The coordinates are the Harvard x, y system. A photograph of the LMC ruled in these coordinates is given in H.A.* **60**, *Plate II.*

The residuals ξ from solid-body rotation are indicated as below:

		Residual (km/s)
Stars:	○	$\xi < -20$
	◦	$-20 < \xi < 0$
	•	$0 < \xi < +20$
	●	$\xi > +20$
Lick nebulae:	□	$\xi < 0$
	■	$\xi > 0$
de Vaucouleurs' nebulae:	×	

Dashed lines in p.a. 171° and 81° pass through the radio centre, full lines through the optical centre.

(iii) *Solar and galactic rotation.*—We have adopted the values used in Section 3 which only differ slightly from de Vaucouleurs' value of 300 km/s for G and S in direction $l^{II}=55°$ $b^{I}=0$. The difference is not sufficient to affect the analysis appreciably.

(iv) *Inclination* (i).—We adopt $i=27°$ as the inclination to the plane of the sky with de Vaucouleurs (who, however, prefers to use the complement of this, the "tilt angle", with the same designation, i, in violation of the usual convention in double star orbits). Uncertainty in this angle seriously affects an analysis of this sort.

(v) *Systemic velocity* (V_s).—Our value from equation (7) for the optical centre is +21 km/s, whereas de Vaucouleurs used +10 km/s. For the radio centre, equation (7) gives +35 km/sec.

The rotational curve can be determined on the above assumptions. If r_0, θ_0, V_0 are the observed polar coordinates and radial velocity of a star the corresponding polar coordinates, r, θ and rotational velocity V_r in the plane of the system are given by (**8**)

$$\tan\theta = \tan\theta_0 \sec i$$
$$r = r_0 \sec\theta / \sec\theta_0$$
$$V_r = (V_0 - V_s)/\cos\theta \sin i = (V_0 - V_s)f.$$

The observed stellar velocities were weighted as in the previous discussion (viz. either 1 or 2) and the Lick nebular velocities were given weight 3. The five Mt Stromlo nebular velocities were given weight 1. Following de Vaucouleurs, if w represents these assigned weights the calculated values of V_r were weighted w/f. All objects with $w/f < 0{\cdot}1$ were rejected and in Figs. 6 and 7 objects of low weight ($0{\cdot}1 < w/f < 0{\cdot}5$) are distinguished from objects of high weight ($w/f > 0{\cdot}5$). Also in Figs. 6 and 7 points south of the minor axis have been reflected in this axis and the various objects are distinguished.

The accompanying table summarizes the available data:

Object		Total no. available	Low weight $0{\cdot}1 < w/f < 0{\cdot}5$	High weight $w/f > 0{\cdot}5$	
Mt Stromlo nebulae	(**10**)	5	5	0	Optical centre
			5	0	Radio centre
Lick nebulae	(**1**)	16	6	7	Optical centre
			5	11	Radio centre
Radcliffe stars	(**11**)	61	23	34	Optical centre
			29	29	Radio centre

In the case of the 30 Dor nebula (NGC 2070) the velocity from (**13**) is used in preference to the Lick velocity.

(*a*) *Optical centre* (*Fig.* 6)

The curve corresponds to de Vaucouleurs' composite spheroid model (after Perek) (**10**) determined with this centre from the nebular velocities alone. Fig. 6 shows that our stellar material extends further from the optical centre than de Vaucouleurs' nebular material besides adding very considerable weight to the plot at $r = 4^\circ{\cdot}0$. It must be stressed that owing to projection factors the present treatment increases the scatter of the points compared with the more direct plot in Fig. 3. Moreover this treatment increases the apparent range in distance from the centre since this range is also dependent on projection factors and the maximum distance reached depends too on the adopted centre. This last point is of importance in the present case since the optical centre lies away from the centre of gravity of our group of stars (cf. Fig. 5).

We have determined a mean rotation curve for stars and nebulae by dividing the objects into four groups: $r \leqslant 1{\cdot}5$, $1{\cdot}5 < r \leqslant 2{\cdot}5$, $2{\cdot}5 < r \leqslant 3{\cdot}5$, $r > 3{\cdot}5$. The vertical lines in Fig. 6 are centred on these points, the lengths of the lines being twice the standard errors of the means. In our view these points show no significant deviation from a straight line of slope 31 km/s/deg and do not support the rotation curve derived by de Vaucouleurs. It may be noted that with $\mathrm{cosec}\, i = 2{\cdot}2$ the slope of 31 km/s/deg corresponds to a gradient of 14·1 km/sec/deg in the plane of the sky (cf. the value of 14·2 km/s/deg in Fig. 3).

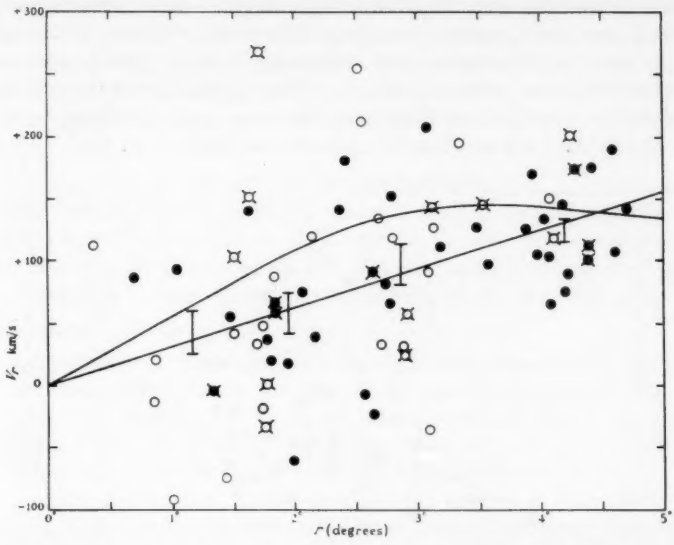

FIG. 6.—*Rotation curve about optical centre; LMC inclined plane model. Filled circles, high weight ($w/f > 0{\cdot}5$). Open circles, low weight ($0{\cdot}1 < w/f < 0{\cdot}5$). Crossed circles represent nebulae, the other points stars. The vertical bars are centred about weighted means of the points divided into four groups. The lengths of the bars are twice the standard errors of these means. The straight line is the best fit to the weighted means (slope 31 km/s/deg). The curved line is the rotation curve according to the composite spheroid model deduced by de Vaucouleurs from the nebulae above* (10). *One star of low weight at $r = 2^\circ{\cdot}38$, $V_r = -162$ km/s lies outside the area of the figure.*

(*b*) *Radio centre* (*Fig.* 7)

The same data as used above but now analysed with respect to the radio centre is shown plotted in Fig. 7. Since both the radio and optical rotation curves suggest rotational symmetry about this point, Fig. 7 should represent a more realistic approach to the rotation problem. The symbols have the same significance as in Fig. 6. The best straight line through the mean points has a slope of 30 km/s/deg in good agreement with the slope derived in the previous section. However there is a clear indication of deviation from a straight line, i.e. from solid body rotation. A good fit to the points may be obtained using Bottlinger's interpolation formula

$$V^2 = \frac{ar^2}{1 + br^3}. \tag{8}$$

A least square solution to the mean points gives

$$b = 0{\cdot}030\,(\text{deg})^{-3}$$

$$a = 2{\cdot}1 \times 10^3\,(\text{km/s})^2(\text{deg})^{-2}$$

and the resulting curve is shown in Fig. 7. It may be noted that again de Vaucouleurs' rotation curve is not a good representation of the mean points.

We thus find confirming evidence from this model that differential rotation is present in the Large Cloud out to $3^\circ{\cdot}5$ from the centre. The interpretation of this differential rotation is discussed in the next section on the mass of the Large Cloud.

It is not surprising that the model of an inclined plane system has yielded qualitatively the same results regarding differential rotation as the previous analysis in terms of deviations from solid-body rotation (which does not postulate concentration of stars in a plane). The residuals from the two solutions are quite similar and do not allow one, on these grounds alone, to conclude whether or not the stars are closely confined to a plane.

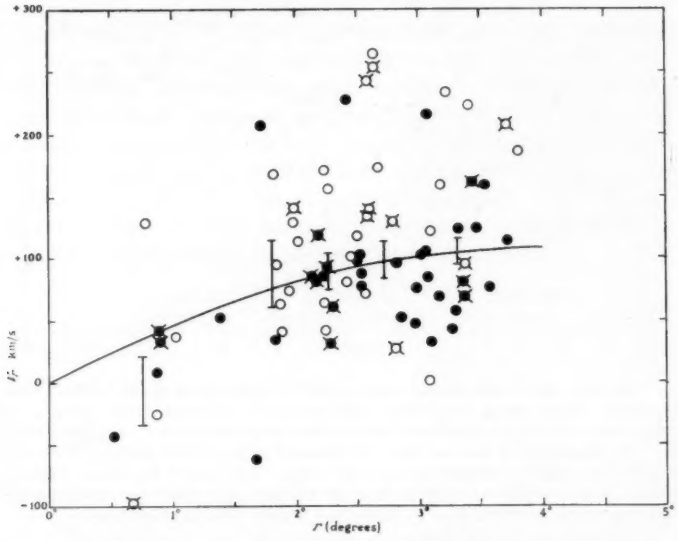

FIG. 7.—*Rotation curve about radio centre; LMC inclined plane model. The symbols have the same significance as in Fig.* 6 *but here the objects have been grouped in five mean points. The curve is the best fit to these mean points using the Bottlinger interpolation formula discussed in the text. Three points of low weight fall outside the area of the figure. They are* $r=0°.75$, $1°.24$ *and* $2°.14$, $V_r=-286$, -249 *and* -103 *km/s.*

6. *The mass of the LMC.*—The rotation curves presented in Figs. 6 and 7 may be used to estimate a mass for the LMC. Because of the uncertainty as to the centre we discuss both cases (optical and radio centres).

(*a*) *Optical Centre.*

Fig. 6 indicates no significant deviations of the rotation curve from a straight line, i.e. from solid body rotation over the range covered by the observations. The simplest model which will produce a such rotation curve is that of a rotating ellipsoid of uniform density. The equation used to determined the mass of the ellipsoid is (cf. **14**)

$$M=\frac{a^3\omega^2}{G\alpha}$$

where

$$\alpha=\frac{3}{2}\frac{a^2}{a^2-c^2}\left[\frac{a}{\sqrt{(a^2-c^2)}}\cos^{-1}\frac{c}{a}-\frac{c}{a}\right]$$

$2a$ = length of major axis of ellipsoid

$2c$ = length of minor axis of ellipsoid

ω = angular velocity of ellipsoid

G = gravitational constant.

Kerr and de Vaucouleurs (**9**) adopt $c/a = 1/5$ by analogy with the ratio estimated for NGC 55. We also adopt this ratio; fortunately a change in the value of c/a from 1/3 to 1/15 (a factor of 5) only changes α by a factor of 1·5 (cf. **15**). As previously (**11**) we adopt 55 kpc for the distance of the LMC. Then $a = 4°{\cdot}5 = 4{\cdot}3$ kpc = the greatest value of r in Fig. 6, and $\omega = 31$ km/s/deg = 32 km/s/kpc. We then obtain

$$M_{4\cdot5} = 1{\cdot}0 \times 10^{10} \text{ solar masses}$$

for the mass within 4°·5 of the centre. The density of the ellipsoid is 0·15 solar masses/pc^3 (1×10^{-23} gm/cm^3). It is of interest to note that recent studies by Hill (**16**) and Woolley (**17**) which are also discussed by Oort (**18**) lead to a density of just this amount in our Galaxy at $z = 0$ in the solar neighbourhood.

(*b*) *Radio centre*

Though in this case there appears to be significant deviation from solid body rotation we may make a rough estimate of the mass by fitting a linear rotation curve. The best straight-line fit to the mean points of Fig. 7 has a slope of 30 km/s/deg which is insignificantly different from that found using the optical centre. However since the results only extend out to about $r = 3{\cdot}5$ kpc (due to the radio centre being more nearly central with respect to our group of stars than the optical centre) the size of the ellipsoid is reduced by a factor $(4{\cdot}5/3{\cdot}5)^3 = 2{\cdot}1$. Thus the mass determined is reduced in this ratio, and we find

$$M_{3\cdot5} = 0{\cdot}5 \times 10^{10} \odot$$

for the mass within 3°·5 of the centre. The density however remains the same as in the previous case viz. 0·15 solar masses/pc^3.

Whilst deviation from solid body rotation seems established in the case under discussion the effect is not large enough or over sufficiently large angular distance in the LMC to warrant a very elaborate treatment. Models consisting of non-homogeneous ellipsoids have been discussed by Perek (**19**) (**20**) and attempts have been made to fit them to the LMC (**9**) (**10**). A sufficiently good fit may be made to the present mean points with a non-homogeneous ellipsoid having a density law of the form

$$\rho = \rho_c(1 - m^2)$$

where

$$m^2 = \frac{x^2 + y^2}{a^2} + \frac{z^2}{c^2}$$

and taking the radius a as 3°·5 and the axial ratio c/a as 1/5 as above. We then obtain a mass of $0{\cdot}5 \times 10^{10}$ solar masses and a central density (ρ_c) of 0·41 $\odot$pc^{-3}. The rotation curve corresponding to this model is not shown in Fig. 7 but is quite closely similar to the Bottlinger curve plotted. It will be noted that the mass does not differ from the uniform ellipsoidal model. It will be clear that in both these cases, since we limit considerations to within 3°·5 of the centre where the observations were made, the mass determined will be a lower limit.

It was shown above that a sufficiently good representation of the mean points can be obtained with a Bottlinger formula (eqn. (8) above) with $b = 0{\cdot}030$ (deg)$^{-3}$ $a = 2{\cdot}1 \times 10^{-3}$ (km/s)^2(deg)$^{-2}$ (see the curve shown in Fig. 7). In this case an estimate of the *total* mass of the system can be made from the equation (**21**)

$$M_B = a/bG.$$

This of course presupposes that the Bottlinger formula is also followed in the unobserved regions with $r > 3°{\cdot}5$. The above results yield

$$M_B = 1{\cdot}6 \times 10^{10} \text{ solar masses.}$$

The present observations therefore yield masses ranging from $0{\cdot}5 \times 10^{10}$ solar masses (minimum mass only) to $1{\cdot}6 \times 10^{10}$ solar masses. We adopt $1{\cdot}0 \times 10^{10}$ solar masses as the best estimate that can be made of the mass of the LMC at the present time. In view of the considerable extent of H I around the LMC it is likely that this is a minimum value and in the following we adopt the view that it probably represents matter within about $4^\circ{\cdot}5$ of the centre.

In the following table are given the mass derived by de Vaucouleurs from limited optical data (**10**) and by Kerr and de Vaucouleurs (**9**) from the 21 cm observation. For comparison, in the right hand column of the table, all masses are reduced to 55 kpc for the distance of the LMC.

Mass determinations (solar masses)

	Published	Reduced to 55 kpc
21 cm (9)	$0{\cdot}3 \times 10^{10}$	$0{\cdot}36 \times 10^{10}$
Optical (10)	$2{\cdot}5 \times 10^{10}$	$2{\cdot}2 \times 10^{10}$
Radcliffe	$1{\cdot}0 \times 10^{10}$	$1{\cdot}0 \times 10^{10}$

Though we have shown in Section 5 that our more extensive observations do not substantiate the rotation curve on which de Vaucouleurs based his mass estimate, we cannot entirely rule out the possibility that the total mass of the system may be as high as he gives. However, the radio result is below any of our values although it is based on observations extending over a much larger area of the LMC and hence might be expected to give a value greater than our result. Possible explanations of this discrepancy, which is probably connected with the complexity of the 21 cm profiles, have been discussed by de Vaucouleurs (**10**).

The total visual luminosity of the LMC is, according to de Vaucouleurs (**22**) $3{\cdot}66 \times 10^9$ solar units at the uncorrected modulus of $19^m{\cdot}2$.

Taking $1{\cdot}0 \times 10^{10}$ solar masses as a minimum mass we find $M/L \geqslant 2{\cdot}7$ solar units, or $M/L \geqslant 2{\cdot}2$ if correction is made for self-absorption in the system (**10**). We may estimate roughly from de Vaucouleurs (**22**) the fraction of the total light within $4^\circ{\cdot}5$ of the centre as about 0·65 so that a better estimate of M/L is probably 4·2 solar units (3·4 if correction for absorption in the system is made). These values are similar to those found in the solar neighbourhood (**18**).

Kerr and de Vaucouleurs (**9**) estimated from 21 cm intensities that the total mass of neutral hydrogen within $7^\circ{\cdot}3$ of the centre is $0{\cdot}57 \times 10^9$ solar masses for an adopted distance of 46 kpc. At our adopted distance of 55 kpc this corresponds to $0{\cdot}82 \times 10^9$ solar masses. We thus find (H I)/total mass $(4^\circ{\cdot}5) \leqslant 8$ per cent.

According to Kerr and de Vaucouleurs (**9**) an area of radius $4^\circ{\cdot}5$ near the centre contains about 0·72 of the total mass of neutral hydrogen so that a better estimate of (H I)/total mass $(4^\circ{\cdot}5)$ is 6 per cent. This is of the same order as that found in other galaxies as can be seen in Table IV where the present results are collected.

7. *Velocity dispersion.*—Superposed on the mean variation in radial velocity across the Large Cloud we observe a certain dispersion in velocities. It is of interest to enquire whether this velocity dispersion is associated with any physical properties of the stars, their positions in the Clouds etc. Since the observations are necessarily restricted to supergiant stars or to the gas, the velocity dispersion of course refers only to Population I.

TABLE IV

Comparison of LMC and Galaxy (based on distance 55 kpc and cosec $i = 2{\cdot}2$ for LMC.)

	LMC	Galaxy etc.
Mass	$\geqslant 1{\cdot}0 \times 10^{10}$ solar masses	$7{\cdot}0 \times 10^{10}$ solar masses (23)
Mean density (uniform ellipsoid)	$0{\cdot}15\ \odot pc^{-3}$	$0{\cdot}15\ \odot pc^{-3}$ in plane near Sun (18)
Central density (Perek)	$0{\cdot}41\ \odot pc^{-3}$	
Period of rotation (uniform ellipsoid)	$1{\cdot}9 \times 10^{8}$ years	$\sim 1{\cdot}8 \times 10^{8}$ years at Sun
Mass light ratio (corrected for self-absorption)	$\geqslant 2{\cdot}2$ solar units Best estimate 3·4 solar units	2·4 near Sun (18) 4·2 in cylinder $\perp$ to galactic plane at Sun (18)
(H I)/total mass	$\leqslant 8$ per cent Best estimate 6 per cent	2 per cent Galaxy (24) 1·3 per cent M31 (25) 5·5 per cent M33 (26)

Investigations into this point have shown that while there is no correlation of velocity dispersion with spectral type of our supergiants, there are two apparently significant correlations:

(i) If the stars are divided into two equal groups, an outer and an inner zone, centred on $x = 9800$, $y = 11500$, the stars in the outer zone show a significantly smaller velocity dispersion than the inner. Stars in the "outer" zone are asterisked in Table I.

(ii) Some of the largest residuals are shown by the brightest stars (with best determined velocities). There is no tendency for these residuals to have systematically one sign (an effect which could be attributed to P Cyg contours in the lines used for radial velocities). A comparison of the visually brightest stars with the less bright stars shows that indeed there is a significantly greater velocity dispersion for the brightest stars.

TABLE V

Corrected velocity-dispersions in Large Cloud (relative to curve of Fig. 4)

	σ_1 (km/s)	σ_2 (km/s)	Number of stars
Inner zone	$18{\cdot}3 \pm 3{\cdot}3$	$18{\cdot}9 \pm 3{\cdot}1$	29
Outer zone	$6{\cdot}9 \pm 3{\cdot}0$	$11{\cdot}0 \pm 3{\cdot}2$	29
Inner-outer	$+11{\cdot}4 \pm 4{\cdot}5$	$+\ 7{\cdot}9 \pm 4{\cdot}5$	
Brighter	$15{\cdot}5 \pm 3{\cdot}0$	$18{\cdot}2 \pm 2{\cdot}5$	26
Fainter	$12{\cdot}4 \pm 3{\cdot}0$	$12{\cdot}8 \pm 2{\cdot}7$	32
Brighter-fainter	$+\ 3{\cdot}1 \pm 4{\cdot}2$	$+\ 5{\cdot}4 \pm 3{\cdot}7$	
All stars	$13{\cdot}4 \pm 2{\cdot}1$	$15{\cdot}1 \pm 1{\cdot}9$	61

Before correction for observational scatter the computed dispersion for all stars is 17·5 km/s.

Details of these two results are shown in the accompanying Table V. The calculations of velocity dispersion have been based on the following system of weighting according to the camera used for each measure of velocity (see notes to Table II of (11)): c = weight 4, d or c: = weight 2, d: = weight 1. The actual weights assigned in this system appear in the second column of weights of Table I. From 88 stars (and 240 plates) in the two Clouds with more than one plate each, the observational error per unit weight was found to be $23{\cdot}6 \pm 1{\cdot}4$ km/s.

The columns headed σ_1 and σ_2 give the dispersions calculated according to the commonly used expressions for observations of different weight (**27**) and a second approximation due to Wesselink (**28**) respectively; in the latter refinement, weights are applied which take account of the varying accuracies as well as the number of the observations.

There is a slight tendency for the fainter stars to be found in our outer zone, as defined, but the difference in mean magnitude of our actual samples of "outer" and "inner" stars is scarcely significant. If therefore the differences in velocity dispersions shown in the Table are accepted as real it appears that we must search for two separate causes. We consider first the greater velocity dispersion of the "inner" stars. There are at least three ways to explain this.

(*a*) *Spherical System* held together by gravitational forces neglecting stellar encounters. Many years ago Eddington (**29**) showed that in such a system with the velocity-distribution obeying Schwarzschild's ellipsoidal law, the major axis of the ellipsoid would remain constant throughout the system (and directed towards the centre) while the prolateness of the ellipsoid would increase radially outwards from the centre. If we regard the LMC as such a spherical system characterized by a velocity ellipsoid with semi-axes a, b, b, then the velocity dispersion in the innermost parts should be approximately a, and that in the outermost parts should be b. Since we have necessarily chosen rather coarse inner and outer zones, the data of Table V give a maximum value of b/a; the values of σ_2 suggest $b/a < 0{\cdot}58$.

(*b*) *Flattened System*, slightly inclined to plane of sky, as suggested by de Vaucouleurs for the LMC. Suppose such a system to be characterized by a velocity-ellipsoid as before. If b decreases outwards as in Eddington's case, then, even if there is no inclination of the system to the plane of the sky (in which case a would make no contribution to the dispersion in radial velocities) we would expect a larger velocity dispersion in the inner than the outer parts following on the variation in b; thus $b_{\text{outer}}/b_{\text{inner}} = 0{\cdot}58$. The greater the inclination of the system to the plane of the sky the more will the major-axis of the velocity ellipsoid become of importance, *particularly at the ends of the apparent minor axis* of the system in the sky. Our meagre data shows no significantly greater velocity dispersion at the ends of the "minor axis" of the LMC (p.a. 81°) than at the ends of the "major axis" but the possibility that more extensive and accurate velocities might show such an effect cannot, of course, be ruled out.

(*c*) *Spherical System* subject to expansion. If all the stars in the LMC were subject to an expansion from some central point or region, then it is obvious that we would observe a greater dispersion in radial velocities in the direction of that central point or region than at the periphery of the system. This would also be true to a modified extent if the LMC contained many independent centres of expansion.

This model would predict systematically positive velocities for stars on the far side of the Cloud, negative velocities for those on the near side. Unfortunately we have no certain means at present of locating stars in depth within the Cloud. If the cloud dust were distributed sufficiently uniformly then we would expect the stars on the far side to be systematically reddened compared with those on the near side. However, the dust clouds are clearly distributed with great irregularity, and it was not surprising that when our observed colour excesses were compared with individual velocity-residuals, no significant correlation of the type predicted by this model could be found.

We are therefore forced to conclude that there is at present no means of surely distinguishing between these three alternative explanations for the apparently greater velocity dispersion of supergiants in the central regions of the LMC.

As regards the second indication of Table V, that the brightest stars show an apparently large velocity dispersion, we can perhaps draw a useful analogy with the known galactic O-type stars with high velocity. About 10 per cent of galactic O stars have random radial velocities exceeding 50 km/s (**30**) and Blaauw (**31**) finds that the proportion of such high velocity stars diminishes as one proceeds to later types although the numbers known per unit volume remain fairly constant in each spectral class. According to evolutionary theory the O stars should evolve quickly into B or A supergiants. Thus it is possible that our brightest Cloud B – A supergiants with large residuals have evolved from stars which correspond closely with the known O stars in the Galaxy. Supergiants of type late B or early A as bright as our brightest Cloud stars are difficult to find, and we cannot at present rule out the possibility that a large proportion of such stars have high velocities.

Small Cloud.

8. *Representation of observed radial velocities in SMC as solid-body rotation.*— A Hertzsprung analysis of the radial velocities of SMC stars has been carried out in the same manner as for the LMC stars in Section 3. 40 stars have been used in the solution with the same system of weighting as before. One star (R42, HD 7099) has such a high velocity (+247 km/s, giving a residual of +81 km/s from our final solution) that it was omitted from the analysis.

The solution gives for the radial velocity ρ within the SMC, uncorrected for solar motion and galactic rotation,

$$\rho = -39\cos\alpha\cos\delta + 196\sin\alpha\cos\delta - 169\sin\delta$$
$$\pm 271 \qquad \pm 279 \qquad \pm 93$$

After correction for solar motion and galactic rotation according to (4) and (5), we have for the SMC

$$\rho' = +91\cos\alpha\cos\delta + 52\sin\alpha\cos\delta + 42\sin\delta \qquad (9)$$

corresponding to (7) for the LMC.

The total velocity corresponding to (9) is $v' = 113$ km/s, whereas without correction for solar motion and galactic rotation $v = 262 \pm 178$ km/s.

The maximum velocity gradient is ~2 km/s/deg in p.a. ~12°, both figures being quite uncertain, whereas Kerr and de Vaucouleurs (**8**) give ~6 km/s/deg in p.a. 40°.

The standard errors quoted above indicate the very great uncertainty in the results. This might have been expected if the stellar velocities conform even approximately to the 21 cm observations, since our stars cover a range of only about 2° along the major axis. Indeed the results are quite as well represented by the simple assumption of random scatter about a weighted mean velocity

$$\rho = 166 \pm 3 \text{ (s.e.) km/s.}$$

The residuals do not show any noticeable dependence on position in the sky.

The velocity dispersion relative to the solution (eqn. (9)) has been calculated according to the usual method (**27**), and the second approximation σ_2 as for the LMC. The result is

$$\sigma_1 = 15{\cdot}4 \pm 3{\cdot}5$$
$$\sigma_2 = 15{\cdot}4 \pm 2{\cdot}9.$$

Similar values are obtained if the dispersion is calculated about the weighted mean velocity.

22 of our stars are in or close to the loose grouping NGC 371. Treated separately these stars give a mean velocity of +166 km/s and $\sigma_1 = 18{\cdot}9 \pm 5{\cdot}1$ (or $14{\cdot}5 \pm 5{\cdot}1$ if one strongly deviating velocity is omitted). The dispersion of this group does not differ significantly from the mean.

Previously the only optical velocity determined in the SMC was that of IC 1644 (Lick) so that the above is the first estimate of the cosmic scatter in SMC velocities. The 21 cm observations may be used in principle to obtain a velocity dispersion, but the treatment is not straight-forward due to the complexity of the line profiles, and no determination was attempted by Kerr and de Vaucouleurs.

9. *Random motions in the Clouds and mass determinations.*—We have found the same value of about 16 km/s for the dispersion of stellar velocities in the two Clouds. De Vaucouleurs (**32**) found 7 km/s for the dispersion of the Lick nebular velocities: this value seems rather uncertain in view of the small number of nebulae, despite the small probable error given to it by de Vaucouleurs. The velocity dispersion of the nebulae appears to be similar to that found for B type stars in the Galaxy ($\sigma_z \sim 5$ km/s, $\sigma_x = \sigma_y \sim 10$ km/s). The group of stars that we have studied in both Clouds seems to give a significantly higher dispersion. We may note that no similar group of galactic supergiants has been studied for comparison. Indeed it is not clear that our group is comparable with the group of galactic B stars since the latter are mainly main-sequence objects presumably considerably less massive than our Cloud stars. Without further study we cannot say whether or not our velocity dispersion applies to main sequence B stars in the Magellanic Clouds. The lower velocity dispersion found for the gaseous nebulae in the LMC would appear to indicate that not all the young LMC objects have quite such a high velocity dispersion as our supergiants (cf. last paragraph of Section 7).

In Section 6 a minimum mass of the LMC was derived from the observed rotation curve. This derivation assumes that the random motions are small compared with the rotational velocities. A complete solution taking into account both random motions and rotation cannot be made at the present time since it would require more observational data than we possess. Kerr and de Vaucouleurs made a first order approximation to the problem by treating the rotational and random motions separately and summing the derived masses. However, in their case the effects of random motions were more important than in ours since the mass derived from the rotation was considerably lower than our value.

A mass determination from random motions alone may be made using the virial theorem if the velocity dispersion is isotropic. In the LMC, a radial velocity dispersion of 16 km/s and radius of $4^\circ{\cdot}5$ yields a mass of $1{\cdot}5 \times 10^9$ solar masses according to the virial theorem in the form given by Chandrasekhar (**33**) for a non-rotating system. This is only about 10 per cent of the mass obtained from the rotational velocity. Clearly therefore we are justified in neglecting the random motions in our determination of the mass of the LMC.

It also follows that *unless* the axis about which the LMC rotates (the z-axis) is orientated at a large angle to the line of sight (the angle is only 27° according to de Vaucouleurs), the velocity dispersion in the z coordinate must be of the same order as the observed radial velocity dispersion. Thus in this case σ_z is much less than the average velocity of rotation at right angles to the z-axis; it

follows that the subsystem studied will be flattened in agreement with de Vaucouleurs's model for the LMC.

Applying the virial theorem to the SMC with a radial velocity dispersion of 16 km/s and a radius of 2° (an overestimate for the area covered by the optical observations but in any case of the right order of magnitude), we obtain a mass of $0{\cdot}7 \times 10^9$ solar masses. Published mass estimates for the SMC must be considered quite uncertain. Kerr and de Vaucouleurs suggested that the mass should be about $1{\cdot}3 \times 10^9$ solar masses, from an analogy with the LMC. More recently de Vaucouleurs (**10**) has increased this to $5\text{–}15 \times 10^9$ solar masses. In any case it would appear likely that the mass is considerably greater than that deduced from the above calculation and this of course is to be expected if the SMC is actually in rotation.

Radcliffe Observatory,
Pretoria,
South Africa:
1960 *November.*

References

(1) R. E. Wilson, *Lick. Obs Pub.*, **13**, 187, 1917.
(2) E. Hertzsprung, *M.N.*, **80**, 782, 1920.
(3) J. H. Oort, *B.A.N.*, **4**, 88, 1927.
(4) R. E. Wilson, *P.A.S.P.*, **56**, 102, 1944.
(5) F. J. Kerr, J. F. Hindman and B. J. Robinson, *Aust. J. Phys.*, **7**, 297, 1954.
(6) M. W. Feast, A. D. Thackeray and A. J. Wesselink, *Observatory*, **75**, 216, 1955.
(7) G. de Vaucouleurs, *Observatory*, **74**, 158, 1954.
(8) F. J. Kerr and G. de Vaucouleurs, *Aust. J. Phys.*, **8**, 508, 1955.
(9) F. J. Kerr and G. de Vaucouleurs, *Aust. J. Phys.*, **9**, 90, 1956.
(10) G. de Vaucouleurs, *Ap. J.*, **131**, 265, 1960.
(11) M. W. Feast, A. D. Thackeray and A. J. Wesselink, *M.N.*, **121**, 337, 1961.
(12) G. de Vaucouleurs, *A.J.*, **62**, 69, 1957.
(13) M. W. Feast, *M.N.*, **122**, 1, 1961.
(14) E. M. Burbidge, G. R. Burbidge and K. H. Prendergast, *Ap. J.*, **130**, 26, 1959.
(15) E. M. and G. R. Burbidge, *Ap. J.*, **132**, 30, 1960.
(16) E. R. Hill, *B.A.N.*, **15**, 1, 1960.
(17) R. v. d. R. Woolley, *M.N.*, **117**, 198, 1957.
(18) J. H. Oort, *B.A.N.*, **15**, 45, 1960.
(19) L. Perek, *Contr. Astr. Inst. Masaryk U.*, **1**, No. 6, 1948.
(20) L. Perek, *Bull. Ast. Inst. Czech.*, **2**, 75, 1950.
(21) W. Lohmann, *Z. f. Ap.*, **35**, 159, 1954.
(22) G. de Vaucouleurs, *Ap. J.*, **131**, 574, 1960.
(23) M. Schmidt, *B.A.N.*, **13**, 15, 1956.
(24) F. J. Kerr and J. V. Hindman, *P.A.S.P.*, **69**, 558, 1957.
(25) H. C. v. d. Hulst, E. Raimond & H. v. Woerden, *B.A.N.*, **14**, 1, 1957.
(26) L. Volders, *B.A.N.*, **14**, 323, 1959.
(27) R. J. Trumpler and H. F. Weaver, *Statistical Astronomy* (University of California Press 1953) p. 126.
(28) A. J. Wesselink (to be published).
(29) A. S. Eddington, *M.N.*, **75**, 366, 1915.
(30) J. H. Oort, *B.A.N.*, **12**, 177, 1954.
(31) A. Blaauw, *P.A.S.P.*, **68**, 495, 1956.
(32) G. de Vaucouleurs, *P.A.S.P.*, **67**, 397, 1955.
(33) S. Chandrasekhar, *Principles of Stellar Dynamics* (University of Chicago Press, 1942) p. 200.
(34) See, for example, W. M. Smart, *Stellar Dynamics*, (Cambridge, 1938) p. 12, eqn. (5).

XUM

THE GRAVITATIONAL INSTABILITY OF AN INFINITE HOMOGENEOUS ROTATING VISCOUS MEDIUM IN THE PRESENCE OF A MAGNETIC FIELD

G. Stephenson

(Received 1961 February 21)*

Summary

It is shown that the Jeans criterion for the gravitational instability of an infinite homogeneous medium is unaffected by the combined action of a Coriolis force, a magnetic field and a viscous force. The necessary and sufficient conditions for stability are also discussed.

---

1. *Introduction.*—It has been shown by Chandrasekhar and Fermi (1) and Chandrasekhar (2) that the Jeans criterion for the gravitational instability of an infinite homogeneous non-viscous medium with infinite electrical conductivity remains unaffected both when a magnetic field is present and when a Coriolis force is acting. In a later paper (3), Chandrasekhar showed that the combined action of a magnetic field and a Coriolis force also left the Jeans criterion unchanged. We now extend the work of this later paper to the case when the medium has a coefficient of viscosity ν.

2. *Basic equations.*—Using Chandrasekhar's notation (3) the basic equations of the system are now

$$\left.\begin{aligned} \rho\frac{d\mathbf{u}}{dt} &= \frac{1}{4\pi}\operatorname{curl}\mathbf{h}\wedge\mathbf{H}+2\rho\mathbf{u}\wedge\boldsymbol{\Omega}-\operatorname{grad}\delta p+\rho\operatorname{grad}\delta V+\nu\nabla^2\mathbf{u}, \\ \frac{\partial\mathbf{h}}{\partial t} &= \operatorname{curl}(\mathbf{u}\wedge\mathbf{H}), \qquad \operatorname{div}\mathbf{h}=0, \\ \frac{\partial}{\partial t}\delta\rho &= -\rho\operatorname{div}\mathbf{u}, \qquad \nabla^2\delta V=-4\pi G\delta\rho, \end{aligned}\right\} \tag{1}$$

where $\delta p=c^2\delta\rho$ and $c=\sqrt{\gamma p/\rho}$, c being the velocity of sound. In these equations $\mathbf{H}$ is a uniform magnetic field, $\boldsymbol{\Omega}$ the angular velocity of the medium, ν the coefficient of viscosity and $\delta\rho$, δp, δV and $\mathbf{h}$ the changes in density, pressure, gravitational potential and magnetic field, respectively.

As with Chandrasekhar, we now suppose that the coordinate axes are chosen such that

$$\mathbf{H}=(0, H_y, H_z), \qquad \boldsymbol{\Omega}=(\Omega_x, \Omega_y, \Omega_z), \tag{2}$$

and that solutions of (1) will be sought corresponding to the propagation of waves in the z-direction. Since $\partial/\partial z$ is the only non-vanishing component of

* Received in original form 1961 January 2.

XUM

gradient, the equation div $\mathbf{h}=0$ gives $h_z=0$. Equations (1) now become

$$\left.\begin{aligned}
\frac{\partial h_x}{\partial t}-H_z\frac{\partial u_x}{\partial z}&=0,\\
\frac{\partial h_y}{\partial t}+H_y\frac{\partial u_z}{\partial z}-H_z\frac{\partial u_y}{\partial z}&=0,\\
\frac{\partial u_x}{\partial t}-\frac{H_z}{4\pi\rho}\frac{\partial h_x}{\partial z}+2(u_z\Omega_y-u_y\Omega_z)-\frac{\nu}{\rho}\frac{\partial^2 u_x}{\partial z^2}&=0,\\
\frac{\partial u_y}{\partial t}-\frac{H_z}{4\pi\rho}\frac{\partial h_y}{\partial z}+2(u_x\Omega_z-u_z\Omega_x)-\frac{\nu}{\rho}\frac{\partial^2 u_y}{\partial z^2}&=0,\\
\frac{\partial u_z}{\partial t}+\frac{H_y}{4\pi\rho}\frac{\partial h_y}{\partial z}+\frac{c^2}{\rho}\frac{\partial}{\partial z}\delta\rho-\frac{\partial}{\partial z}\delta V+2(u_y\Omega_x-u_x\Omega_y)-\frac{\nu}{\rho}\frac{\partial^2 u_z}{\partial z^2}&=0,\\
\frac{\partial}{\partial t}\delta\rho+\rho\frac{\partial u_z}{\partial z}&=0,\\
\frac{\partial^2\delta V}{\partial z^2}+4\pi G\delta\rho&=0.
\end{aligned}\right\}\qquad(3)$$

Corresponding to a wave-motion in the z-direction we now put

$$\frac{\partial}{\partial t}=i\omega,\qquad \frac{\partial}{\partial z}=-ik,\qquad(4)$$

where ω is the wave-frequency and k the wave-number. Using (4), equations (3) become in matrix form

$$\begin{bmatrix}
\omega & 0 & kH_z & 0 & 0 & 0 & 0\\
0 & \omega & 0 & kH_z & -kH_y & 0 & 0\\
\frac{kH_z}{4\pi\rho} & 0 & \omega-i\frac{\nu k^2}{\rho} & 2i\Omega_z & -2i\Omega_y & 0 & 0\\
0 & \frac{kH_z}{4\pi\rho} & -2i\Omega_z & \omega-i\frac{\nu k^2}{\rho} & 2i\Omega_x & 0 & 0\\
0 & -\frac{kH_y}{4\pi\rho} & 2i\Omega_y & -2i\Omega_x & \omega-i\frac{\nu k^2}{\rho} & -\frac{c^2k}{\rho} & k\\
0 & 0 & 0 & 0 & -\rho k & \omega & 0\\
0 & 0 & 0 & 0 & 0 & 4\pi G & -k^2
\end{bmatrix}\begin{bmatrix} h_x\\ h_y\\ u_x\\ u_y\\ u_z\\ \delta\rho\\ \delta V\end{bmatrix}=0.\qquad(5)$$

The condition that these equations possess a non-trivial solution is that the determinant of the (7×7) matrix should be zero. This condition leads, on expansion, to the equation

$$\begin{aligned}
&\omega^3\left(\omega-i\frac{\nu k^2}{\rho}\right)^3-4\omega^3\left(\omega-i\frac{\nu k^2}{\rho}\right)\Omega^2-\omega^2\left(\omega-i\frac{\nu k^2}{\rho}\right)^2(2\Omega_A^2+\Omega_B^2+\Omega_J^2)\\
&\quad+\omega^2\{4\Omega_A^2\Omega_x^2+4\Omega_z^2\Omega_J^2+4(\Omega_y\Omega_A-\Omega_z\Omega_B)^2\}\\
&\quad+\omega\left(\omega-i\frac{\nu k^2}{\rho}\right)(2\Omega_A^2\Omega_J^2+\Omega_A^4+\Omega_A^2\Omega_B^2)-\Omega_A^4\Omega_J^2=0,\qquad(6)
\end{aligned}$$

where

$$\Omega_A^2 = \frac{k^2 H_z^2}{4\pi\rho}, \qquad \Omega_B^2 = \frac{k^2 H_y^2}{4\pi\rho}, \qquad \Omega_J^2 = c^2k^2 - 4\pi G\rho, \qquad \Omega^2 = |\boldsymbol{\Omega}|^2. \tag{7}$$

When $\nu = 0$, equation (6) reduces to Chandrasekhar's equation (**3**, eqn. (7)). On rewriting (6) we find

$$\omega^6 - 3i\frac{\nu k^2}{\rho}\omega^5 - \omega^4\left(A + B + 3\frac{\nu^2k^4}{\rho^2}\right) + i\omega^3\left(\frac{\nu^3k^6}{\rho^3} + 2\frac{\nu k^2}{\rho}B + \frac{\nu k^2}{\rho}A\right) + \omega^2\left(\frac{\nu^2k^4}{\rho^2}B + C + D\right) - i\omega\frac{\nu k^2}{\rho}D - E = 0, \tag{8}$$

where

$$\left.\begin{aligned} A &= 4\Omega^2, \\ B &= 2\Omega_A^2 + \Omega_B^2 + \Omega_J^2, \\ C &= 4\{\Omega_A^2\Omega_x^2 + \Omega_z^2\Omega_J^2 + (\Omega_y\Omega_A - \Omega_z\Omega_B)^2\}, \\ D &= 2\Omega_A^2\Omega_J^2 + \Omega_A^4 + \Omega_A^2\Omega_B^2, \\ E &= \Omega_A^4\Omega_J^2. \end{aligned}\right\} \tag{9}$$

The condition for stability is that the imaginary part of ω (all roots) should be positive, since this ensures that the amplitude of the wave-form does not grow with time. We now put $\omega = -iz$ so that (8) becomes a polynomial of degree six in z with real coefficients, namely

$$z^6 + 3Fz^5 + z^4(A + B + 3F^2) + z^3(F^3 + 2FB + FA) + z^2(F^2B + C + D) + zFD + E = 0, \tag{10}$$

where

$$F = \frac{\nu k^2}{\rho}. \tag{11}$$

The stability condition is now that the real part of z (all roots) should be negative. The necessary and sufficient conditions for this to be so are given by the Routh–Hurwitz criteria which require for a polynomial

$$a_0z^n + a_1z^{n-1} + a_2z^{n-2} + \ldots + a_{n-1}z + a_n = 0,$$

(where $a_0, a_1, a_2 \ldots a_{n-1}, a_n$ are real constants), that

$$D_1 = a_1 > 0, \qquad D_2 = \begin{vmatrix} a_1 & a_0 \\ a_3 & a_2 \end{vmatrix} > 0,$$

$$D_3 = \begin{vmatrix} a_1 & a_0 & 0 \\ a_3 & a_2 & a_1 \\ a_5 & a_4 & a_3 \end{vmatrix} > 0, \quad \ldots$$

$$\ldots D_n = \begin{vmatrix} a_1 & a_0 & 0 & 0 & \ldots \\ a_3 & a_2 & a_1 & a_0 & \ldots \\ a_5 & a_4 & a_3 & a_2 & \ldots \\ . & . & . & . & \\ . & . & . & . & \\ . & . & . & . & \\ a_{2n-1} & a_{2n-2} & . & . & a_n \end{vmatrix} > 0,$$

where $a_m = 0$ for $m > n$ (n being the degree of the polynomial). Now, since in the nth determinant, the terms of the bottom row are all zero except the last we have

$$D_n = a_n D_{n-1}. \tag{12}$$

Consequently, since both D_n and D_{n-1} must be positive for stability, a necessary condition for stability is that $a_n > 0$. Applying this condition to equation (10) we require therefore that

$$a_6 = E = \Omega_A^4 \Omega_J^2 > 0. \tag{13}$$

Hence $\Omega_J^2 > 0$ is a necessary condition for stability. However, this condition is not sufficient and in addition we must have $D_1 > 0$, $D_2 > 0$, $D_3 > 0$, $D_4 > 0$ and $D_5 > 0$. We note, however, that since F is a positive quantity (see (11)), the condition $D_1 = 3F > 0$ is automatically satisfied. The other four conditions give rise to complicated relations between the quantities A, B, C, D, E and F. In special cases, as we shall see in the next section, these conditions simplify to some extent. If, however, $a_6 < 0$ so that

$$\Omega_J^2 = c^2k^2 - 4\pi G\rho < 0, \tag{14}$$

then the system is gravitationally unstable. This is precisely the Jeans criterion which remains unaffected therefore by the combined action of a Coriolis force, a magnetic field *and* a viscous force.

3. *Necessary and sufficient conditions for stability in special cases.*—We now discuss the necessary and sufficient conditions for stability in two special cases.

Case I: No magnetic field and no rotation

Here, from (9), $A = 0$, $B = \Omega_J^2$, $C = D = E = 0$. Consequently (10) becomes

$$z^4 + 3Fz^3 + z^2(\Omega_J^2 + 3F^2) + z(F^3 + 2F\Omega_J^2) + F^2\Omega_J^2 = 0. \tag{15}$$

In this case we can proceed without the Routh–Hurwitz criteria since (15) factorizes into

$$(z + F)^2(z^2 + Fz + \Omega_J^2) = 0, \tag{16}$$

whence it follows that if $\Omega_J^2 > 0$ the roots are either all negative or have negative real parts. Hence $\Omega_J^2 > 0$ is a necessary and sufficient condition for stability.

Case II: Rotation, but no magnetic field

Here, from (9), $A = 4\Omega^2$, $B = \Omega_J^2$, $C = 4\Omega_z^2\Omega_J^2$, $D = E = 0$. In this case (10) becomes

$$z^4 + 3Fz^3 + z^2(4\Omega^2 + \Omega_J^2 + 3F^2) + z(F^3 + 2F\Omega_J^2 + 4F\Omega^2) + (F^2 + 4\Omega_z^2)\Omega_J^2 = 0. \tag{17}$$

Hence for stability we must have (using the Routh–Hurwitz criteria)

$$D_1 = 3F > 0, \qquad D_2 = \begin{vmatrix} 3F & 1 \\ F^3 + 2F\Omega_J^2 + 4F\Omega^2 & 4\Omega^2 + \Omega_J^2 + 3F^2 \end{vmatrix} > 0,$$

$$D_3 = \begin{vmatrix} 3F & 1 & 0 \\ F^3 + 2F\Omega_J^2 + 4F\Omega^2 & 4\Omega^2 + \Omega_J^2 + 3F^2 & 3F \\ 0 & (F^2 + 4\Omega_z^2)\Omega_J^2 & F^3 + 2F\Omega_J^2 + 4F\Omega^2 \end{vmatrix} > 0,$$

and

$$D_4 = \Omega_J^2(F^2 + 4\Omega_z^2)D_3 > 0.$$

On expanding D_2 and D_3 the conditions $D_2 > 0$ and $D_3 > 0$ become respectively

$$F(8\Omega^2 + \Omega_J^2 + 8F^2) > 0 \tag{18}$$

and

$$F^2\{8F^4+40F^2\Omega^2+8F^2\Omega_J^2+2\Omega_J^4+32\Omega^4+20\Omega^2\Omega_J^2-36\Omega_J^2\Omega_z^2\}>0. \quad (19)$$

Now $D_1>0$ since F is positive and, from (18), $D_2>0$ if $\Omega_J^2>0$. Furthermore, the left-hand side of (19) will be positive if $\Omega_J^2>0$ and if

$$2\Omega_J^4+32\Omega^4+20\Omega^2\Omega_J^2-36\Omega_J^2\Omega_z^2\geqslant 0. \quad (20)$$

However, since $\Omega_z^2\leqslant\Omega^2$, the left-hand side of (20) is such that

$$2\Omega_J^4+32\Omega^4+20\Omega^2\Omega_J^2-36\Omega_J^2\Omega_z^2\geqslant 2\Omega_J^4+32\Omega^4-16\Omega_J^2\Omega^2=2(\Omega_J^2-4\Omega^2)^2\geqslant 0. \quad (21)$$

Hence, if $\Omega_J^2>0$, then $D_3>0$. Finally, if $\Omega_J^2>0$ then $D_4>0$ also. In this case, therefore, $\Omega_J^2>0$ is both a necessary and sufficient condition for stability.

4. *Conclusions.*—We have shown in this paper that even when a viscous force is acting (in addition to a Coriolis force and a magnetic field) the Jeans criterion for gravitational instability is unaffected and the medium is gravitationally unstable if

$$\Omega_J^2=c^2k^2-4G\rho<0.$$

For stability, $\Omega_J^2>0$ is shown to be a necessary condition. In the general case of the simultaneous action of a magnetic field and a Coriolis force the necessary and sufficient conditions for stability (the positivity of the Routh–Hurwitz determinants) lead to complicated relations between the quantities defined in (9). However, in the two special cases of (*a*) no rotation and no magnetic field, and (*b*) rotation but no magnetic field, the Routh–Hurwitz determinants simplify considerably, and $\Omega_J^2>0$ is shown to be both a necessary and sufficient condition for stability.

Acknowledgment.—The author is grateful to the referee for comments which have substantially improved this paper.

Dept. of Mathematics,
Imperial College,
London, S.W.7:
1961 *February* 20.

References

(1) S. Chandrasekhar and E. Fermi, *Ap. J.*, **118**, 116, 1953.
(2) S. Chandrasekhar, *Vistas in Astronomy* (London, Pergamon), 1954.
(3) S. Chandrasekhar, *Ap. J.*, **119**, 7, 1954.